Faisabilité technique d'un bois lamellé-collé composé d'espèces feuillues du nord-est de l'Amérique du Nord

Mémoire

ALEXANDRE MORIN-BERNARD

MAÎTRISE EN GÉNIE DU BOIS ET DES MATÉRIAUX BIOSOURCÉS
Maître ès sciences (M.Sc.)

Québec, Canada

Résumé

Dans un contexte où l'on cherche à limiter l'empreinte écologique milieu bâti et à valoriser les ressources locales, le bois s'est imposé comme un matériau incontournable dans le secteur de la construction. Parmi les produits de bois d'ingénierie, le bois lamellé-collé est l'un des plus fréquemment utilisés. Les produits actuellement offerts sont presque exclusivement composés d'espèces résineuses. Toutefois, un regain d'intérêt pour les espèces feuillues est aujourd'hui manifeste, en raison de leurs propriétés mécaniques impressionnantes ainsi que de leur apparence noble et distinctive. L'objectif de ce projet était d'évaluer la faisabilité technique d'un bois lamellé-collé structural composé d'espèces feuillues du nord-est de l'Amérique du Nord. Le chapitre consacré à l'identification des propriétés indicatrices pertinentes à la prédiction de la résistance en traction des espèces étudiées a permis de conclure qu'il est possible de classer ces dernières selon leur résistance à partir de propriétés mesurables en contexte industriel. Le chapitre consacré à l'évaluation de la résistance au cisaillement d'assemblages composés de différentes espèces feuillues et adhésifs structuraux a permis d'identifier les combinaisons les plus appropriées pour un produit d'ingénierie structural composé de ce type. Le troisième et dernier chapitre a permis de sélectionner un profil de joint à entures multiples qui convient aux espèces étudiées et de mettre à l'essai des poutres pleine grandeur. Les résultats ont confirmé que la rupture de l'élément se produit consécutivement à la rupture d'un joint situé dans la lamelle inférieure de la poutre. Une optimisation plus poussée des paramètres d'aboutage permettrait d'augmenter considérablement la résistance du produit. Les poutres fabriquées et mises à l'essai ont atteint une résistance de 47,0 MPa pour le frêne d'Amérique et de 41,6 MPa pour le bouleau jaune, pour des modules d'élasticité respectifs de 15 078 et 16 712 MPa. La rigidité supérieure constitue un atout majeur du produit.

Abstract

The current growing demand for engineered wood products in the construction sector is largely attributable to their outstanding ecological performance. Aware of the market opportunities as well as of the lack of high value-added opportunities for some wood species, industry and policy-makers from several jurisdictions have recently joined forces to develop products made from non-conventional species, especially with hardwoods. In addition to the possibility of creating products with a noble and distinctive appearance, the high mechanical properties of some hardwood species offer the opportunity to create engineered products of outstanding strength. The objective of this study was to assess the technical feasibility of a glued-laminated timber made from northeastern North American hardwood species. Work presented in the first chapter confirmed that it is feasible, using a modelling approach, to predict the UTS of white ash and yellow birch lumber from the density, dynamic modulus of elasticity, sinus of the maximum local grain deviation (SGD_{max}) and Knot Area Index (KAI). Work presented in chapter 2 has shown that acceptable wood failure levels can be achieved in bondline shear strength tests with commercially available structural adhesives. Tensile tests on finger-jointed lamellae presented in chapter 3, allowed to select the 15 mm finger joint as the most appropriate for the jointing of the investigated species. Bending tests conducted on full-size hardwood glued-laminated timber beams, also presented in chapter 3, confirmed the possibility to achieve a bending strength up to 47.0 MPa for white ash and 41.6 MPa for yellow birch, with a corresponding modulus of elasticity of respectively 15 078 and 16 712 MPa. Since the failure of the beams initiated at the finger joints, further study and optimization of the finger-jointing parameters would lead to a superior bending strength.

Table des matières

Liste des tableaux

Liste des figures

Liste des abréviations, sigles, acronymes

Abréviations

AAC	Annual allowable cut
AIC	Akaike information criterion
BLC	Bois lamellé-collé
EPI	Émulsion d'isocyanate et de polymères
EPS	Épinette-pin-sapin
FPC	Factory production control
GLT	Glued-laminated timber
ITT	Initial type testing
KAR	Knot Area Ratio [%]
MC	Moisture content [%]
MF	Mélamine-formaldéhyde
MOE_{app}	Module d'élasticité apparent [MPa]
MOE_{dyn}	Module d'élasticité dynamique [MPa]
MOE_{mean}	Module d'élasticité moyen [MPa]
MOE_{stat}	Module d'élasticité statique [MPa]
MOR	Module de rupture [MPa]
MPa	Mégapascal [N/mm^2]
MSR	Machine stress-rated lumber
MUF	Mélamine-urée-formaldéhyde
PRF	Phénol-résorcinol-formaldéhyde
PUR	Polyuréthane
SD	Standard deviation
SE	Standard error
SPF	Spruce-Pine-Fir
TH	Teneur en humidité [%]
UTS	Ultimate tensile strength [MPa]
WF	Wood failure level [%]

Lettres latines

a	Distance par rapport à l'axe neutre [mm]
A	Aire [mm^2]
b	Largeur [mm]
d	Profondeur [mm]
E	Module d'élasticité [N/mm^2] [MPa]
$(EI)_{ef}$	Effective bending stiffness [Nmm^2]
F	Force [N]
f_b	Résistance en flexion [MPa]
$f_{m,g,k}$	Résistance caractéristique en flexion du bois lamellé-collé [MPa]
$f_{m,j,k}$	Résistance caractéristique en flexion des joints à entures multiples [MPa]
f_t	Résistance en traction [MPa]
$f_{t,0,l,k}$	Résistance caractéristique en traction parallèle au fil [MPa]
f_v	Résistance au cisaillement [MPa]
I	Second moment of area [mm^4]
l	Longueur [mm]
m	Paramètre de forme de la distribution de Weibull
n	Nombre d'échantillons
N	Newtons
p	Pas des entures du joint [mm] / Probabilité
P	Contrainte appliquée [N]
P_{max}	Contrainte à la rupture [N]
s	Angle des entures du joint [°]
t	Largeur des pointes du joint à entures multiples [mm]
V	Vitesse de l'onde acoustique [km/s]
w_i	Poids d'Akaike

Lettres grecques

Δ	Increment of deflection of the specimen [mm]
ρ	Masse volumique [kg/m^3]
σ	Contraintes normales [MPa]
τ	Contrainte de cisaillement [MPa]
λ	Paramètre d'échelle de la distribution de Weibull
γ	Facteur d'efficacité de connexion

À Patrick, Lucie, Alain et Florence pour leur appui inconditionnel tout au long de cette grande étape.

Remerciements

La réalisation du projet de recherche ici présenté est le fruit d'un travail considérable qui n'aurait été possible sans la contribution de plusieurs collaborateurs dévoués.

Je tiens d'entrée de jeu à remercier sincèrement mon directeur de recherche, M. Pierre Blanchet, pour sa confiance dès les débuts du projet et pour l'occasion de réaliser un projet qui ralliait mes intérêts et m'offrait l'occasion de travailler en étroite collaboration avec un partenaire de l'industrie. Ce projet constituait un défi d'envergure et j'ai fortement apprécié le relever au sein de ton équipe. Merci à Christian Dagenais dont l'expertise et les conseils m'ont gardé sur le droit chemin tout au long de ma maîtrise. La réalisation d'un diplôme de deuxième cycle dans une discipline différente du baccalauréat peut engendrer certains défis et je suis reconnaissant des efforts que tu as consacrés au projet et à répondre à mes questions. À Alexis Achim, je tiens à adresser des remerciements tout particuliers. J'ai certainement abusé de ta disponibilité, mais nos nombreuses discussions ont été des moments clés qui ont assuré l'avancement de mon projet et le maintien de ma confiance dans ce cheminement parfois semé d'embûches. Tu m'as permis de me développer en tant que chercheur et d'acquérir la motivation nécessaire à l'une des plus grandes décisions de ma vie; poursuivre mes études au troisième cycle!

La réalisation de ce programme de recherche ambitieux n'aurait pas non plus été possible sans la précieuse assistance de plusieurs. À Luc Girompaire, je tiens à adresser toute ma reconnaissance pour le travail réalisé, pour ton efficacité et pour ta rigueur qui m'ont permis d'être en confiance même lorsque j'étais à l'extérieur du pays. Tes qualités et ton expertise ont été indispensables au succès de ce projet. Je tiens également à faire part de ma reconnaissance envers mes collègues Christine Bombardier-Cauffopé, Clément Fleury, Baptiste Giorgio et Clément Blanquet Du Chayla. Vous avez été mes yeux et mes mains alors que la distance m'empêchait d'avancer le projet et j'ai été impressionné par votre rigueur et votre efficacité.

Je suis également privilégié d'avoir pu compter sur l'aide du personnel du Centre de recherche sur les matériaux renouvelables de l'Université Laval. Je tiens à faire part de ma reconnaissance pour le travail et les conseils de Luc Germain, Jean Ouellet, Daniel Bourgault et David Lagueux et pour la coordination réalisée par Benoît St-Pierre. Vous avez contribué à faire de ma maîtrise un succès et j'ai grandement apprécié tout le temps que j'ai passé avec vous dans les ateliers et les laboratoires. Je souhaite également adresser mes remerciements les plus sincères à l'équipe d'Art Massif qui a été impliquée tout au long du projet et qui a permis de le concrétiser, tout particulièrement à Steve, Guillaume, Ghislain, Richard, Tristan et à tous les autres qui nous ont prêté main forte. Je tiens également à souligner la contribution de Roger Poirier de chez Conception RP pour ses conseils sur l'usinage des joints à entures multiples et sur les configurations des joints à utiliser.

Finalement, ce projet n'aurait pu être réalisé sans la contribution financière de nombreux partenaires. Les travaux réalisés ont été financés par la chaire industrielle de recherche du CRSNG sur la construction écoresponsable en bois (CIRCERB), grâce aux octrois par l'intermédiaire des programmes IRC et CRD (IRCPJ 461745-18 et RDCPJ 524504-18) du Conseil national de recherche en sciences et génie du Canada (CRNSG) et du soutien des partenaires industriels. L'obtention d'une bourse d'études supérieures du Canada à la maîtrise du CRSNG et d'une bourse de maîtrise en recherche octroyée par le Fonds de recherche du Québec – Nature et technologies (FRQNT) ont également contribué au financement du projet. Le programme des Bourses canadiennes du jubilé de diamant de la reine Elizabeth II (BRE) et le Bureau international de l'Université Laval (BI) ont également contribué en me permettant de réaliser un stage à l'Edinburgh Napier University à l'automne 2019.

Avant-propos

Le contenu du présent mémoire est divisé en trois chapitres, comprenant chacun un article scientifique rédigé en anglais et présentant les résultats des différentes phases expérimentales du projet. Au moment du dépôt du mémoire, l'un des articles était accepté et sous presse, un autre avait été soumis et un troisième était prêt à être soumis. Les détails relatifs au statut de publication ainsi qu'aux rôles respectifs des co-auteurs sont décrits ci-dessous.

Chapitre 1:
Morin-Bernard, A., Blanchet, P., Dagenais, C., & Achim, A. (2020). Strength grading of northern hardwood species for structural engineered wood products: Identification of the relevant indicating properties.

Cet article sera soumis dans les semaines suivant le dépôt du présent mémoire à la revue *BioResources*. À titre de premier auteur de cet article, j'ai réalisé l'ensemble des manipulations expérimentales, ainsi que le développement des modèles et le processus de sélection de modèles. J'ai également dégagé les principales conclusions à partir des résultats et défini le plan d'expérience. Les co-auteurs de cet article sont Pierre Blanchet, directeur de mes travaux de maîtrise, Christian Dagenais, co-directeur de recherche ainsi qu'Alexis Achim, co-directeur de recherche. Cet article est présenté tel qu'il sera soumis pour publication, à l'exception des numéros de figures, de tableaux et d'équations qui ont été modifiés.

Chapitre 2:
Morin-Bernard, A., Blanchet, P., Dagenais, C., & Achim, A. (2020). Use of northern hardwoods in glued-laminated timber: A study of bondline shear strength and resistance to moisture. *European Journal of Wood and Wood Products*. Sous presse.

Cet article a été accepté avec révisions mineures dans l'*European Journal of Wood and Wood Products* le 26 décembre 2019. La version finale, telle que présentée dans ce mémoire, sera publiée au courant du mois de juillet 2020. À titre de premier auteur de cet article, j'ai réalisé l'ensemble des manipulations expérimentales, comprenant la préparation des échantillons et les essais mécaniques. J'ai également réalisé les analyses statistiques, l'interprétation des résultats, le dégagement des conclusions principales ainsi que la rédaction complète de l'article. Le plan d'expérimentation a été élaboré en collaboration avec le directeur de recherche et l'ensemble des co-auteurs est intervenu de façon ponctuelle dans la démarche expérimentale ainsi que lors de la révision du manuscrit. Les co-auteurs de cet article sont Pierre Blanchet, directeur de mes travaux de maîtrise, Christian Dagenais, co-directeur de recherche ainsi qu'Alexis Achim, co-directeur de recherche. Cet article est présenté tel qu'il a été accepté pour publication, à l'exception des numéros de figures, de tableaux et d'équations qui ont été modifiés.

Chapitre 3:
Morin-Bernard, A., Blanchet, P., Dagenais, C., & Achim, A. (2020). Glued-laminated timber from northern hardwoods: effect of finger-joint profile on lamellae tensile strength and study of the bending properties from full-size beams.

Cet article a été soumis à la revue *Construction and Building Materials* le 29 juin 2020. À titre de premier auteur de cet article, j'ai réalisé l'ensemble des manipulations expérimentales, parfois avec l'aide d'un auxiliaire de recherche et de collègues. J'ai aussi réalisé les analyses statistiques, avec l'assistance du service de consultation statistique pour l'une des analyses réalisées, l'interprétation des résultats, le dégagement des conclusions principales ainsi que la rédaction complète de l'article. Les co-auteurs de cet article sont Pierre Blanchet, directeur de mes travaux de maîtrise, Christian Dagenais, co-directeur de recherche ainsi qu'Alexis Achim, co-directeur de recherche. Cet article est présenté tel qu'il a été soumis pour publication, à l'exception des numéros de figures, de tableaux et d'équations qui ont été modifiés.

Introduction

Dans un contexte où l'on cherche à limiter l'empreinte écologique milieu bâti et à valoriser les ressources locales, le bois s'est imposé comme un matériau incontournable dans le secteur de la construction. L'usage du bois est d'autre part stimulé par les avantages écologiques du recours à ce matériau. Les produits d'ingénierie permettent d'utiliser de façon plus efficace cette ressource naturelle renouvelable en générant des produits à forte valeur ajoutée qui disposent des caractéristiques requises pour se substituer à des matériaux dont l'impact environnemental est plus important. Un usage accru du bois permet ainsi de diminuer l'empreinte écologique du milieu bâti (Thormark, 2006), élément identifié dès 2007 par le Groupe d'experts intergouvernemental sur l'évolution du climat (GIEC) comme incontournable dans le cadre d'une stratégie intégrée de lutte aux changements climatiques (Nabuurs *et al.*, 2007).

Au Québec, l'utilisation du bois dans la construction de bâtiments commerciaux, industriels et multifamiliaux de quatre étages ou moins a plus que doublé entre 2007 et 2018, passant de 15 % à 31 % (Cecobois, 2019). Le marché pour ces produits est d'ailleurs appelé à poursuivre sa croissance au cours des prochaines années. Selon l'APA – The Engineered Wood Association (2015), la croissance de la demande nord-américaine pour ces produits est évaluée à 20 à 25 % pour la période 2015-2020 alors qu'une société d'études de marché l'évalue à 24,8 % pour la période 2016-2022 (Allied Market Research, 2016).

On désigne sous l'appellation de produits du bois d'ingénierie structuraux les produits fabriqués à partir de bois réduit en pièces de petite taille ou encore à partir de bois de sciage abouté dans le but d'en éliminer les défauts et d'obtenir un produit d'une résistance et d'une dimension supérieures à celles du bois de sciage conventionnel (Cecobois, 2015).

Le bois lamellé-collé

Bien que le premier brevet pour le bois lamellé-collé ait été émis en 1906 (Hetzer, 1906), le bois lamellé-collé n'a connu son véritable essor que plusieurs décennies après son invention. Le bois lamellé-collé est fabriqué à partir de lamelles classées selon leur résistance et leur rigidité et aboutées par joints à entures multiples pour former des lamelles possédant la longueur totale souhaitée, tel que présenté à la figure 1. Ces lamelles sont ensuite rabotées et assemblées en couches successives grâce à des adhésifs structuraux hydrofuges (Cecobois, 2015). Le recours au bois lamellé-collé est aujourd'hui de plus en plus fréquent, tant dans les systèmes à poutres et poteaux que pour la construction à ossature légère. La production de bois lamellé-collé connaît d'ailleurs une croissance soutenue en Amérique du Nord, avec une augmentation estimée à 463 000 m^3 entre 2010 et 2018 (UNECE/FAO, 2018).

Figure 1. Étapes simplifiées de fabrication du bois lamellé-collé.

Au Canada, la fabrication de bois lamellé-collé à usage structural est régie par une série de normes et de standards présentant des exigences en lien avec le produit (CSA O122, 2016), les adhésifs (CSA O112.9/10, 2010) et les installations industrielles (CSA O177, 2006). Il est toutefois possible de mettre en marché un produit qui ne répond pas spécifiquement aux exigences de ces normes, mais qui possède les propriétés mécaniques requises pour s'y substituer. On désigne un produit de ce type sous l'appellation de bois lamellé-collé propriétaire. Une évaluation indépendante réalisée par le Centre canadien des matériaux de construction (CCMC) est toutefois requise avant qu'il puisse être reconnu comme produit structural pouvant être utilisé dans la construction de bâtiments (Cecobois, 2015).

Les contraintes mécaniques au sein d'une poutre en bois lamellé-collé

Au sein d'une charpente en bois lamellé-collé, les poutres sont sollicitées en flexion, ce qui entraîne l'apparition de contraintes dans la section transversale. Les lamelles situées du côté où la charge est appliquée subiront une contrainte de compression alors que celles situées sur la face opposée de la poutre subiront une contrainte de traction. La grandeur des contraintes normales (σ), comme présentée à la figure 2, suit un gradient croissant partant de la surface de la poutre jusqu'à son centre, les lamelles centrales n'étant que très peu sollicitées. Ces lamelles subissent toutefois la plus grande contrainte de cisaillement (τ) puisque la valeur de celle-ci suit un gradient décroissant partant de l'axe neutre de la poutre jusqu'à sa surface (Thelandersson & Larsen, 2003).

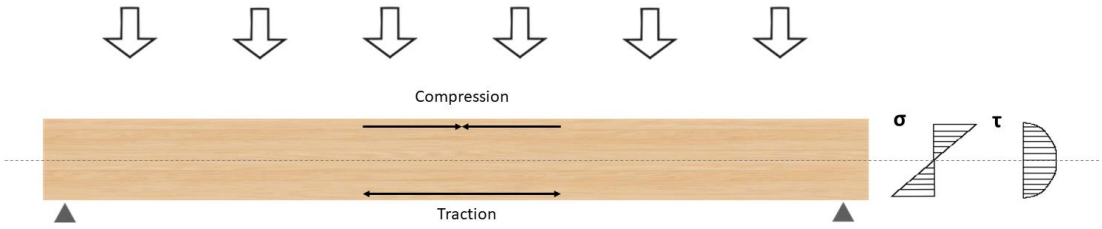

Figure 2. Contraintes normales (σ) et de cisaillement (τ) dans une poutre sollicitée en flexion.

Un élément en bois lamellé-collé peut comporter une section homogène ou encore être composé de différentes zones de rigidité. Un bois lamellé-collé homogène est fabriqué à partir de lamelles d'une même classe de qualité, dont les propriétés mécaniques sont équivalentes et qui peuvent être positionnées indifféremment dans la section transversale. Une poutre composée nécessite quant à elle l'utilisation de lamelles de différentes classes de qualité, qui seront positionnées dans la section transversale en fonction de leur rigidité et de leur résistance estimée (CSA, 2016; Ross, 2010).

Les lamelles les plus rigides et les plus résistantes seront positionnées à l'extérieur de la poutre, là où les contraintes normales sont les plus élevées. Le recours à une section comportant différentes zones de rigidité permet d'utiliser plus rationnellement la matière première, en incluant par exemple des lamelles de moins bonne qualité dans la partie centrale de la poutre et en conservant les lamelles de qualité supérieure pour la portion externe de la section transversale. On évalue la rigidité des lamelles par leur module d'élasticité (MOE), dont la valeur est liée au rapport entre la charge appliquée et la déformation subie par la pièce. Plus le module d'élasticité est important, moins la flèche de l'élément en flexion sera prononcée, indicateur d'une plus grande rigidité (Ross, 2010).

La figure 3 présente un exemple d'une poutre à section composée dans laquelle le module d'élasticité des lamelles extérieures (A) est plus élevé que celui des lamelles suivantes (B) qui ont elles-mêmes un module d'élasticité supérieur aux lamelles centrales (C). La présence de différentes zones de rigidité engendre aussi des modifications dans la distribution des contraintes normales au sein de la section transversale, telle qu'illustrée à la figure 3.

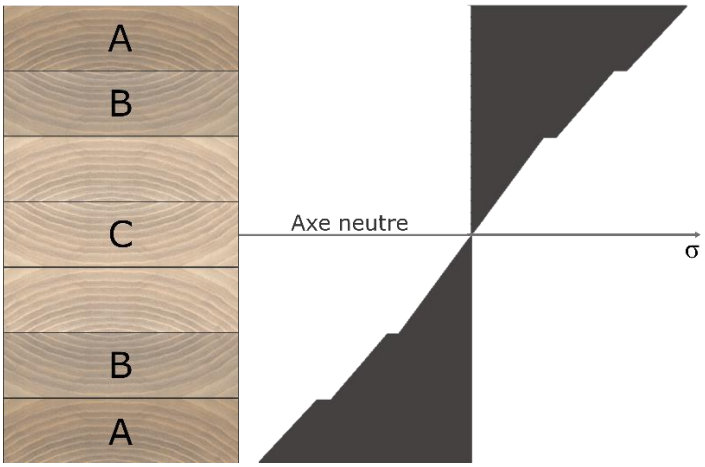

Figure 3. Zones de rigidité et distribution des contraintes normales (σ) au sein d'une poutre en bois lamellé-collé composée.

Au Canada, la norme CSA O122 (2016) régit l'agencement des lamelles et fournit des plans d'assemblages permettant d'atteindre les classes de résistances spécifiées par la norme. Les lamelles peuvent être disposées de façon symétrique (EX) ou pas (E) par rapport à l'axe neutre de la poutre, en fonction de l'usage prévu de l'élément.

Les propriétés mécaniques déclarées dans les différentes normes régissant la fabrication du bois lamellé-collé reposent sur différentes méthodes de calcul et permettent de tenir compte de la variabilité naturelle du matériau bois, ainsi que d'autres facteurs liés à la fonction et au confort des bâtiments. Ces propriétés qui sont considérées dans les calculs de conception des structures permettent de garantir la sécurité et la fonction des constructions. Elles sont basées des dimensions et sur une teneur en humidité qui sont définies dans les normes et varient en fonction de la durée d'application de la charge. Par exemple, ces valeurs doivent être ajustées pour être comparées à des essais mécaniques réalisés en laboratoire, ou la durée d'application de la charge sera ponctuelle.

L'une des pratiques les plus répandues aujourd'hui consiste à présenter la valeur du 5^{e} centile inférieure à partir de la distribution normale des propriétés mécaniques du produit. Ces valeurs sont aussi appelées propriétés caractéristiques. Les normes européenne EN 14080 (2013) et canadienne CSA O86 (2014) dédiées aux produits en bois lamellé-collé reposent notamment sur cette pratique. La valeur utilisée pour la conception de structures est obtenue en ajoutant des facteurs d'ajustement considérant le produit utilisé, la durée d'application de la charge et la teneur en humidité (EN 1995-1-1:2004+A2:2014). Les valeurs présentées dans la norme sont pour une durée normale d'application de la charge.

Aux États-Unis, c'est plutôt la résistance admissible qui est présentée dans les normes et standards dédiés au bois lamellé-collé. Les valeurs obtenues par cette méthode sont plus faibles que les propriétés caractéristiques, car elles incluent déjà des facteurs de sécurité et considèrent également une durée d'application normale de la charge (AITC, 1996).

Au Canada, la norme régissant la fabrication du bois lamellé-collé exprime les propriétés mécaniques par la résistance prévue. Les valeurs de résistance prévues sont également inférieures aux valeurs du 5e centile, car elles comprennent des facteurs de normalisation, qui considèrent notamment le coefficient de variation des propriétés du produit, un facteur de résistance nominal ainsi qu'un facteur de fiabilité. Ces valeurs sont également pour une durée d'application normale de la charge. Les classes de résistance prévues par la norme canadienne de bois lamellé-collé sont 20f-E(X), correspondant à une résistance prévue en flexion (f_b) de 25,6 MPa selon la méthode de calcul aux états limites et 24f-E(X), correspondant à une résistance prévue de 30,6 MPa. Les résistances caractéristiques pour une durée d'application de charge ponctuelle de ces produits seraient respectivement de 26,67 MPa et de 31,88 MPa (CSA O86, 2014).

Utilisation d'espèces feuillues pour la fabrication de bois lamellé-collé structural

Les produits en bois lamellé-collé actuellement offerts sont presque exclusivement composés d'espèces résineuses, mais un regain d'intérêt pour les espèces feuillues est aujourd'hui manifeste. En plus de leurs propriétés mécaniques impressionnantes, certaines espèces feuillues sont abondantes et leur utilisation pour la fabrication de produits d'ingénierie structuraux pourrait permettre d'offrir des débouchés à certaines de ces espèces qui sont actuellement sous-valorisées (Franke *et al.*, 2014; Ross, 2010). En plus de constituer une ressource dont la disponibilité est parfois importante, le bois de ces espèces possède des qualités esthétiques indéniables, ce qui permet de concevoir un produit noble, distinctif et qui se démarque du bois lamellé-collé traditionnel. En effet, de récentes études (Markström *et al.*, 2018; Gosselin *et al.*, 2016; Laguarda Mallo & Espinoza, 2015; Gaston, 2014) ont permis d'identifier l'aspect esthétique des produits du bois comme l'un des facteurs principaux conduisant les concepteurs de bâtiments à choisir le bois comme matériau de structure principal. Une offre accrue de tels produits est susceptible de fournir de nouveaux débouchés pour les produits d'ingénierie destinés à la construction en répondant à des exigences particulières des concepteurs de bâtiments et de leurs clients.

Au cours des dernières décennies, plusieurs efforts de mobilisation ont été mis en place et de nouveaux produits structuraux composés d'espèces feuillues ont fait leur apparition. En Europe, un partenariat d'envergure baptisé «Wood Wisdom – Net EU – Hardwoods» a été mis en place entre plusieurs pays, dont l'Autriche, l'Allemagne, la France et de nombreux partenaires industriels, avec comme objectif d'assurer la reconnaissance du bois des espèces feuillues comme matériau de construction et d'en augmenter les parts de marché (FCBA, 2017). L'Europe demeure à ce jour la région où les efforts de développement de produits d'ingénierie structuraux à partir d'essences feuillues sont les plus avancés. Dès le milieu des années 60, les travaux de Egner et Kolb (1966) ont démontré la possibilité d'utiliser le bois du hêtre européen (*Fagus sylvatica* L.) pour la production de bois lamellé-collé structural. Depuis, de nombreux travaux ont étudié les propriétés mécaniques de tels produits (Aicher *et al.*, 2018; 2014; Aicher & Stapf 2014; Tran *et al.*, 2014; Frese & Blaß, 2007) ou ont évalué l'influence de différents paramètres sur la résistance des produits (Franke *et al.*, 2014; Aicher & Ohnesorge, 2011; Ohnesorge *et al.*, 2010). En 2009 l'Institut allemand des techniques de construction (DIBt) a émis une homologation pour un produit lamellé-collé structural entièrement composé de hêtre ainsi que pour un hybride hêtre-épinette (DIBt, 2009). Le bois des chênes européens (*Quercus robur* L., *Quercus petraea* (Matt.) Liebl.) s'est

également révélé être une matière première valable pour la production de bois lamellé-collé structural, plusieurs travaux en ayant démontré l'intérêt (Aicher *et al.*, 2018; 2014; Tran *et al.*, 2016; Aicher & Stapf, 2014). Au courant de la dernière décennie, deux homologations techniques (DIBt, 2013; 2012) pour des produits en bois lamellé-collé composés de ces espèces ont été émises. D'autres espèces, dont le châtaignier (*Castanea sativa* Mill.) et le meranti (*Shorea sp.)* ont également fait l'objet d'homologations (ETA-13/0646, 2013; DIBt, 2004). Plus récemment, certains auteurs se sont intéressés au développement de bois lamellé-collé à partir de frêne européen (*Fraxinus excelsior* L.) avec des résultats prometteurs (Clerc *et al.*, 2018; Ammann *et al.*, 2016; Knorz, 2014; Knorz *et al.*, 2014). Les produits actuellement disponibles peuvent atteindre une résistance caractéristique de 33 MPa pour les chênes et 48 MPa dans le cas du hêtre, avec des modules d'élasticité respectifs moyens de 14 400 MPa et 15 100 MPa.

Aux États-Unis, la pertinence de valoriser le bois d'essences feuillues notamment dans les produits structuraux est reconnue depuis longtemps (Ross & Erickson, 2020; Cumbo *et al.*, 2003). Dès les années 1990, plusieurs travaux ont étudié les propriétés mécaniques et la disponibilité de certaines essences feuillues (Janowiak, 1997; Green, 1993; Janowiak *et al.*, 1992) ainsi que la performance de produits lamellés-collés structuraux en étant composés (Manbeck *et al.*, 1999; Shedlauskas *et al.*, 1996; Janowiak *et al.*, 1995; 1994; Moody *et al.*, 1993). Depuis 1985, l'American Institute of Timber Construction (AITC) a d'ailleurs adopté une norme permettant la fabrication de bois lamellé-collé structural à partir d'espèces feuillues variées (AITC, 1996). Cette norme permet la fabrication d'éléments en bois lamellé-collé jusqu'à une résistance admissible de 30,60 MPa. La résistance caractéristique équivalente, pour une durée d'application de la charge ponctuelle, serait de 34,75 MPa. Les éléments lamellés-collés ainsi produits sont principalement utilisés pour la construction de ponts routiers (Manbeck *et al.*, 1996; Ritter *et al.*, 1994).

Particularités inhérentes aux espèces feuillues

Tant chez les espèces feuillues que chez les espèces résineuses, le type de cellules, leur proportion et la quantité relative de leurs composants chimiques sont hautement variables en fonction de l'espèce, mais également entre les individus d'une même espèce et au sein d'un individu donné (Ridley-Ellis *et al.*, 2016; Panshin & Zeeuw, 1970). Les espèces feuillues constituent un groupe plus hétérogène que les résineux. Leur structure anatomique et leurs propriétés mécaniques sont encore plus complexes et variables que dans le cas des espèces conifériennes et la nature des défauts y est également différente (Schlotzhauer *et al.*, 2019; Bollmus *et al.*, 2017; Panshin & Zeeuw, 1970). Leur masse volumique est en moyenne plus élevée et présente une plus grande variabilité (Sellers *et al.*, 1988). Les espèces feuillues commerciales de l'est du Canada présentent des valeurs de masse volumique allant de 430 kg/m^3 à 820 kg/m^3 alors que l'étendue de la masse volumique des essences résineuses varie de 340 kg/m^3 à 500 kg/m^3 (Jessome, 1977). Cette masse volumique supérieure, liée à une structure anatomique particulière, confère à ces bois une résistance mécanique plus élevée, puisqu'ils contiennent davantage de matériel par unité de volume (Ross, 2010). Ils sont donc, a priori, de bons candidats pour un usage structural.

L'utilisation de nouvelles espèces pour la fabrication de bois lamellé-collé introduit toutefois une incertitude quant aux propriétés et à la performance du produit fini. La résistance d'un élément en bois lamellé-collé dépend de la résistance des lamelles individuelles, de la résistance des joints à entures multiples ainsi que de la qualité du collage garantissant l'intégrité de la section transversale (Dietch & Tannert, 2015; Brandner & Schickhofer, 2008). Dans le cadre d'un processus de développement de produit composé d'espèces feuillues, il est donc essentiel d'étudier avec attention ces différents paramètres. Les sections suivantes

présentent, pour chacun des éléments influençant la résistance des produits en bois lamellé-collé, les plus récentes avancées ainsi que les éléments spécifiques aux espèces feuillues dont il faut tenir compte.

Classement des bois d'espèces feuillues basé sur la résistance

Puisque les propriétés mécaniques des lamelles utilisées influenceront la résistance du produit fini, il est essentiel de pouvoir compter sur des méthodes de classement permettant de les estimer sans endommager les pièces de bois. Dans le cas des éléments à section composée, le classement permet également d'assigner aux lamelles une position dans la section transversale en fonction de leurs propriétés.

Le classement du bois basé sur la résistance permet de séparer la matière première en groupes pour lesquels des propriétés relativement uniformes peuvent être assignées. Il s'agit d'un procédé qui est basé sur la mesure de propriétés indicatrices qui sont reconnues pour leur influence sur la résistance du bois et qui peuvent être mesurées de façon non destructive (Ross & Erickson, 2020; Schlotzhauer *et al.*, 2019). Les approches de classement peuvent être basées sur des propriétés mesurées visuellement ou à partir d'équipements spécialisés. Le classement visuel se base notamment la position et la dimension des nœuds, ainsi que sur l'angle formé par les fibres du bois par apport à l'axe longitudinal d'une planche ainsi que sur la détection de défauts indésirables comme les fissures, le bois de réaction ou la présence de pourriture. Ces méthodes visuelles étaient les seules disponibles jusque dans les années 1960 et sont basées, depuis les années 1990, sur des essais mécaniques à grande échelle (Galligan & McDonald, 2000). Le classement visuel n'est pas réputé être la méthode permettant l'utilisation la plus rationnelle de la matière première, puisqu'une marge de sécurité considérable doit être ajoutée pour tenir compte de la précision limitée de l'évaluation humaine et de la corrélation limitée entre certains indicateurs et les propriétés mécaniques.

Le classement utilisant des équipements de mesure spécialisés est appelé classement mécanique. Le classement mécanique est aujourd'hui bien établi et permet de mesurer des caractéristiques qui peuvent ou non être mesurées visuellement, notamment le module d'élasticité, la masse volumique, ainsi que l'angle des fibres du bois et la présence de nœuds (Galligan & McDonald, 2000). De nos jours, la plupart des méthodes de classement reposent sur une combinaison d'approches visuelles et mécaniques (Ehrhart *et al.*, 2016a; Niemz & Mannes, 2012). Par exemple, le bois MSR (Machine Stress Rated Lumber) fait l'objet d'un classement mécanique, qui est par la suite complété par une inspection visuelle permettant de rejeter certains spécimens. En effet, l'introduction de critères visuels relatifs aux nœuds améliore significativement la précision de la résistance prédite (Bendtsen & Youngs, 1981).

En raison des particularités inhérentes aux espèces feuillues, le classement de ces espèces basé sur la résistance est assez peu développé comparativement aux procédures disponibles pour les espèces résineuses (Kovryga *et al.*, 2019a; Weidenhiller *et al.*, 2019). Au Canada, l'usage dominant des feuillus dans les produits d'apparence a défini le type de classement qui est utilisé pour ces espèces. Les normes de classement actuelles dédiées à ces espèces se basent sur l'apparence et la possibilité de fabriquer certains produits plutôt que sur leur résistance mécanique (NHLA, 2019). Toutefois, les travaux de Green, Ross et McDonald (1994) ont montré que la procédure de classement par contrainte mécanique du bois MSR pouvait prédire adéquatement la résistance des espèces feuillues, bien que cela induise une incertitude. La distribution et la nature des défauts sont différentes chez les feuillus (Aicher *et al.,* 2001) et le coefficient de détermination de la relation liant la rigidité et la résistance de ces bois est

généralement plus faible que pour les espèces résineuses (Ross & Erickson, 2020). La corrélation plus faible entre le module d'élasticité (MOE) et le module de rupture (MOR), qui entraîne une plus grande variabilité du MOR pour un MOE donné, serait compensée par le fait qu'à rigidité équivalente, les espèces feuillues présentent un MOR plus élevé. Les études sur le sujet reconnaissent toutefois que l'utilisation des relations mathématiques développées à partir d'essais sur les espèces résineuses peut engendrer une utilisation très conservatrice de la matière première (Kovryga *et al.*, 2019b, Green *et al.*, 1994). La difficulté de prédire les propriétés mécaniques des espèces feuillues ainsi que des différences significatives entre les relations entre les propriétés mesurées en fonction de l'espèce justifient une étude distincte des caractéristiques des espèces d'intérêt (Kovryga *et al.*, 2019b; Weidenhiller *et al.*, 2019).

Collage structural des bois d'espèces feuillues

L'intégrité de la section transversale d'un élément en bois lamellé-collé est intimement liée à la qualité du collage de face entre les lamelles. En effet, les propriétés mécaniques d'un élément en bois lamellé-collé sont calculées en considérant l'absence de glissement entre les différentes couches composant le produit. Le lien unissant deux lamelles doit donc être suffisamment performant pour résister aux contraintes de cisaillement occasionnées lors de l'application d'une charge.

Dans le cas des espèces feuillues, la résistance de l'assemblage réalisé à l'aide d'un adhésif constitue un enjeu majeur. Il est reconnu que le collage de bois de forte masse volumique fournit des résultats plus variables et moins prévisibles que ceux de plus faible masse volumique. Le seuil critique à partir duquel les résultats deviennent incertains se situerait entre 700 et 800 kg/m^3, tout dépendant des auteurs (Habipi & Ajdinaj, 2015; Ross, 2010).

La structure anatomique des espèces feuillues et conséquemment leur comportement en présence d'humidité exerce une influence marquée sur l'efficacité des collages impliquant ces essences. D'autres paramètres s'appliquant au matériau bois en général et décrits dans la section suivante, sont également à considérer pour conférer une résistance maximale aux assemblages réalisés.

L'influence de la structure anatomique et de la teneur en humidité

La porosité, intimement liée à la masse volumique du bois et à son anatomie, est un facteur crucial puisqu'elle influence grandement la pénétration et le mouillage du bois par l'adhésif. Les fibres plus courtes des feuillus, ainsi que leurs parois plus épaisses et leur lumen réduit, expliquent leur masse volumique élevée, mais aussi la difficulté avec laquelle un fluide peut pénétrer le bois (Ross, 2010; Bandel, 1995). Chez les feuillus davantage que chez les résineux, le mouvement d'un fluide dans les directions radiale et tangentielle est entravé par rapport au mouvement dans la direction longitudinale (Ghazil, 2010; Sellers *et al.*, 1988). L'orientation des cernes de croissance et la distribution des pores dans la section transversale affectent également la pénétration de l'adhésif et l'efficacité du collage (Lehmann *et al.*, 2018; Ross, 2010; Hass *et al.*, 2012; 2009; Xiao *et al.*, 2007; Chui & Delahunty, 2005).

De façon générale, un bois plus dense présentera des changements dimensionnels plus importants lorsqu'exposé à des variations de l'humidité ambiante. De plus, la structure anatomique des feuillus fait qu'à masse volumique égale, leurs changements dimensionnels sont plus importants que ceux des espèces résineuses. Une fois le produit en service, ces changements

dimensionnels engendrent une contrainte considérable sur le plan de colle et sur le bois lui-même (Ross, 2010; Sellers *et al.*, 1988). D'autre part, le comportement anisotrope du bois fait en sorte que les changements dimensionnels ne sont pas de même ampleur dans les axes radial, tangentiel et longitudinal. Il est donc préférable de ne pas combiner des pièces dont les cernes présentent une orientation radiale et tangentielle (coupe sur dosse et coupe sur quartier) en raison de la différence marquée de retrait/gonflement (2:1) entre ces deux directions. Une orientation tangentielle devrait être privilégiée pour les éléments structuraux soumis à des contraintes de traction (Sellers *et al.*, 1988). Toutefois, certains travaux indiquent que cette orientation peut limiter la pénétration de l'adhésif chez certaines espèces et que de meilleurs résultats seraient obtenus avec une coupe radiale (Hass *et al.*, 2012; Xiao *et al.*, 2007).

Le contenu en eau du bois doit également être soigneusement contrôlé. Des résultats mitigés sont obtenus avec des bois dont le contenu en eau dépasse les 25 %, la teneur en humidité optimale se situant entre 6 et 16 % (Ross, 2010; Sellers *et al.*, 1988). Au moment du collage, la différence de contenu en eau entre les pièces assemblées ne doit pas excéder deux pour cent; toute différence supérieure entraînera une contrainte pouvant compromettre l'intégrité du collage. Les pièces assemblées doivent de plus présenter une section transversale relativement symétrique et des caractéristiques semblables en termes de masse volumique et d'espacement des anneaux de croissance. L'épaisseur des lamelles doit également être similaire (Bandel, 1995). Certains travaux (Clerc *et al.*, 2018; Ohnesorge *et al.*, 2010) ont d'autre part révélé que dans le cas des feuillus denses, des lamelles plus épaisses pourraient induire une contrainte supplémentaire liée aux changements dimensionnels, ce qui réduirait la résistance à la délamination du collage.

Influence de la qualité de surface

L'affinité du substrat pour l'adhésif diminue en fonction de l'âge de la surface, puisqu'un nombre réduit de sites actifs sera disponible pour la formation d'un lien solide entre l'adhésif et le bois. Le collage doit donc être effectué dans un court délai (généralement 24 heures) suivant le rabotage ou une quelconque autre forme d'usinage (CSA, 2016; Ross, 2010; Sellers *et al.*, 1988).

L'usinage de la surface doit limiter les dommages aux fibres du bois, puisque les liens formés avec des fibres endommagées n'offriront qu'une fraction de la résistance de ceux formés avec des fibres intactes en plus de limiter la pénétration de l'adhésif dans le substrat (Sellers *et al.*, 1988). Ainsi, une surface usinée au couteau serait plus adéquate qu'une surface sciée (Ross, 2010). Une étude sur le collage de l'érable à sucre a d'autre part révélé qu'une raboteuse à lame fixe produirait les meilleurs résultats (Hernandez, 1994). Les surfaces sablées offriraient quant à elles des résultats variables, une compression des cellules à la surface du bois ayant parfois été constatée (Jiang *et al.*, 2014).

L'Influence de l'adhésif et des paramètres de collage

Les paramètres de collage, notamment le temps d'assemblage et le temps de pressage, doivent être déterminés en fonction de l'adhésif, de l'essence utilisée et de l'orientation du grain des pièces de bois. Le temps d'assemblage et la pression requise pour des joints d'extrémités seront inférieurs en raison de la plus grande facilité de pénétration de l'adhésif dans cette direction. De façon générale, bien que dépendant de leur structure anatomique, le temps d'assemblage et la pression appliquée doivent être plus importants pour les essences de forte masse volumique (Vick, 1999; Sellers *et al.*, 1988; Jokerst, 1981).

Considérant la nature du bois provenant des espèces feuillues, le choix de l'adhésif est critique, d'autant plus lorsqu'une utilisation en structure est prévue. Traditionnellement, les seuls adhésifs capables de remplir les exigences d'une telle utilisation étaient ceux du type résorcinol, phénol-résorcinol-formaldéhyde et mélamine-formaldéhyde (Jokerst, 1981). D'autres adhésifs synthétiques se prêtent aujourd'hui à cet usage, notamment les émulsions d'isocyanate et de polymère ainsi que certains polyuréthanes (Grøstad & Bredesen, 2014; Knorz, 2014; Stoeckel *et al.*, 2013; Ross, 2010). Le collage structural d'espèces feuillues de forte masse volumique pose toutefois encore problème pour certains d'entre eux, principalement en ce qui concerne la délamination lors de variations répétées de la teneur en humidité (Lehmann *et al.*, 2018; Ammann *et al.*, 2016; Konnerth *et al.*, 2016; Knorz *et al.*, 2015; Vick & Okkonen, 1998).

Les principaux adhésifs utilisés aujourd'hui pour la fabrication de bois lamellé-collé structural sont les résines phénol-résorcinol-formaldéhyde (PRF), les polyuréthanes (PUR), les émulsions d'isocyanate et de polymère (EPI) ainsi que les résines mélamines-urée-formaldéhyde (MUF), plus abordables que les résines mélamine-formaldéhyde (MF).

Adhésifs phénol-résorcinol-formaldéhyde (PRF)

Ces adhésifs permettent de bénéficier de la résistance des adhésifs résorcinol à un coût plus abordable. L'ajout de résorcinol lors de la préparation d'un adhésif phénol-formaldéhyde augmente de beaucoup sa résistance à l'humidité et l'efficacité de collage des espèces denses tout en maintenant un coût raisonnable (Sellers *et al.*, 1988). Les composés phénoliques présents dans ces résines leur donnent une couleur rougeâtre foncé, ce qui peut limiter leur intérêt pour une utilisation avec des bois pâles. Les adhésifs contenant du résorcinol peuvent polymériser à température ambiante, ce qui les rend intéressants pour la fabrication de bois lamellé-collé. Une température plus élevée accélère toutefois le processus dans le cas des résines phénol-résorcinol-formaldéhyde (Ross, 2010). De nombreux travaux (Lehmann *et al.*, 2018; Ammann *et al.*, 2016; Konnerth *et al.*, 2016; Knorz, 2014; Knorz *et al.*, 2014) impliquant des espèces feuillues denses, principalement le hêtre et le frêne européens, ont confirmé la supériorité de ce type d'adhésif sur les substituts possibles, principalement en ce qui concerne la résistance à la délamination.

Adhésifs mélamine-urée-formaldéhyde (MUF)

Les adhésifs mélamine-urée-formaldéhyde ont été développés afin de combler les lacunes des résines urée-formaldéhyde. L'ajout de mélamine permet notamment de réduire leur vulnérabilité à l'humidité et les émissions de formaldéhyde une fois en service, tout en conservant un coût inférieur aux adhésifs mélamine-formaldéhyde (Bandel, 1995). La ligne de colle est incolore et la polymérisation s'effectue en présence de chaleur ou à l'aide d'une presse haute fréquence (Ross, 2010). Lorsqu'utilisées pour le collage structural de hêtre européen, les résines MUF ont démontré une résistance au cisaillement équivalente ou légèrement inférieure à celle des résines PRF (Aicher *et al.*, 2018; Lehmann *et al.*, 2018; Franke *et al.*, 2016; Tran *et al.*, 2014, Aicher & Ohnesorge, 2011). Des résultats similaires ont été obtenus pour le collage du frêne européen (Aicher *et al.*, 2018; Knorz, 2014; Knorz *et al.*, 2014) et des chênes européens (Aicher *et al.*, 2018; Tran *et al.*, 2016). Toutefois, une résistance à la délamination inférieure à celle obtenue avec les résines PRF a été constatée dans certains travaux (Lehmann *et al.*, 2018; Ammann *et al.*, 2016; Konnerth *et al.*, 2016).

Adhésifs polyuréthanes (PUR)

On considère généralement deux groupes d'adhésifs de ce type, soit les polyuréthanes à un composant (PUR 1C) et les polyuréthanes à deux composants (PUR 2C). Ces adhésifs sont susceptibles de se lier chimiquement avec certains groupements

fonctionnels du substrat en raison de la présence d'isocyanates. Ils demeurent relativement flexibles une fois la réticulation complétée (Ross, 2010; Bandel, 1995).

Les PUR 1C sont des adhésifs réagissant à l'humidité, c'est-à-dire qu'ils polymérisent en se liant notamment aux groupements hydroxyles présents à la surface du substrat (Dunky & Pizzi, 2002), ou même dans l'air. La réaction de polymérisation entraîne des émissions de gaz carbonique (Pizzi & Mittal, 2003; Strøbech, 1990). La faible résistance à la délamination constatée par certains auteurs (Jiang *et al.*, 2014; Vick, 1995) pourrait être corrigée par l'application d'un apprêt, comme l'ont démontré plusieurs travaux, tant pour le collage de face (Franke *et al.*, 2016; Amen-Chen & Gabriel, 2015; Luedtke *et al.*, 2015; Kläusler *et al.*, 2014; Lehringer et Gabriel, 2014; López-Suevos et Richter, 2009), que le collage de joints en bout (Clerc *et al.*, 2018; Lehmann *et al.*, 2018). En 2014, un apprêt destiné à être utilisé en combinaison avec un PUR 1C a d'ailleurs été intégré à deux homologations techniques en Allemagne pour le collage structural du hêtre européen (DIBt, 2016; 2009).

Les PUR 2C sont composés au minimum d'un prépolymère d'uréthane comprenant une fonction isocyanate et d'un polyalcool. La polymérisation débute dès que les deux composants sont mélangés, sauf dans le cas des formulations dont les fonctions isocyanates sont bloquées, qui nécessitent un apport de chaleur. On a recours à ce type d'adhésif polyuréthane lorsque le durcissement doit être rapide (Pizzi & Mittal, 2003). Très peu d'occurrences d'utilisation des polyuréthanes à deux composants pour le collage d'espèces feuillues ont été recensées dans la littérature. Dagenais et Salenikovich (2008) ont procédé à l'aboutage de pièces d'érable à sucre avec un adhésif polyuréthane à deux composants formulé pour des espèces résineuses et ont obtenu des résultats prometteurs pour une utilisation structurale.

Adhésifs d'émulsion d'isocyanate et de polymère (EPI)

Ces adhésifs à deux composants comprennent une dispersion dans un milieu aqueux d'un polymère comprenant des groupements hydroxyles ainsi qu'un isocyanate agissant comme agent de réticulation. Ces adhésifs présentent à la fois les caractéristiques des adhésifs thermoplastiques et thermodurcissables. Leur résistance à l'humidité serait toutefois limitée (Grøstad & Pedersen, 2010). Les lignes de colles sont incolores et la polymérisation s'effectue rapidement à température ambiante ou élevée en générant des émissions de CO_2. Une pression importante, mais de courte durée est nécessaire (Ross, 2010). Ce type d'adhésif est utilisé principalement dans la fabrication de poutrelles en I et dans l'aboutage par entures multiples (Grøstad & Pedersen, 2010). Une quantité moindre est requise par rapport aux adhésifs MUF, ce qui rend ce produit relativement économique malgré son coût plus élevé à poids égal. D'autre part, la polymérisation de cet adhésif n'est pas affectée par le pH du substrat et la pénétration dans le bois suivrait un mécanisme différent des adhésifs PRF et MUF, ce qui en fait un candidat intéressant pour les espèces dont le collage est plus difficile (Grøstad & Bredesen, 2014). Des travaux de collage impliquant un adhésif EPI réalisés avec du frêne européen ont en effet démontré l'atteinte d'une résistance au cisaillement presque équivalente à celle obtenue pas les PRF et MUF. La résistance à la délamination était toutefois inférieure (Knorz, 2014; Knorz *et al.*, 2014).

Aboutage structural des bois d'espèces feuillues

L'aboutage constitue en cas particulier de collage structural et est un élément critique dans le cas du bois lamellé-collé, en particulier dans les lamelles les plus fortement sollicitées en traction (Brandner & Schickhofer, 2008; Falk & Colling, 1995). La résistance obtenue par cette technique d'aboutage dépend principalement des propriétés du bois, des paramètres de production

et de la géométrie des entures (Dagenais, 2007). L'influence des propriétés du bois ainsi que celle de la qualité de la surface et de l'adhésif, comme discuté précédemment, doit donc être considérée avec attention. L'usinage des entures présente toutefois une difficulté supplémentaire par rapport au rabotage puisque la précision d'assemblage des couteaux, et conséquemment du joint, est critique (Selbo, 1963).

L'influence des paramètres géométriques du joint sur la résistance de ce dernier est largement reconnue (Franke *et al.*, 2014; Ayarkwa *et al.*, 2000; Castro & Paganini, 1997; Jokerst, 1981; Selbo, 1963). Sellers (1988) décrit 4 variables géométriques influençant la résistance d'un joint à entures multiples (Figure 4), soit la longueur des entures (*l*), le pas (*p*), la pente (*s*) et la largeur des pointes (*t*). La résistance obtenue repose d'abord et avant tout sur la maximisation de la surface de contact entre les deux pièces aboutées (Selbo, 1963). La pente des entures doit être faible de manière à présenter une surface presque parallèle aux fibres du bois, ce qui offre une meilleure résistance aux contraintes de traction et de cisaillement, bien que le gain s'atténue au-delà d'un certain seuil (Rao *et al.*, 2012; Bandel, 1995; Jokerst, 1981; Selbo, 1963). Le rapport de la longueur des entures sur le pas (*l/p ou 2l/p*) est donc un indicateur efficace de la résistance d'un joint. Un rapport plus élevé et une pente plus faible entraînent une résistance supérieure, du moins jusqu'à un rapport de 4:1 (Selbo, 1963). Les pointes doivent également être les plus fines possible, puisque le collage bout à bout du bois ne permet la transmission que d'une très faible contrainte en plus de générer une concentration du stress en un endroit précis (Rao *et al.*, 2012; Jokerst, 1981; Strickler, 1980).

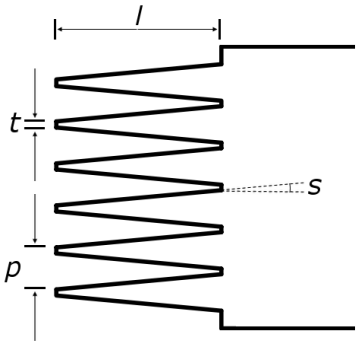

Figure 4. Paramètres géométriques d'un joint à entures multiples.

L'importance de la qualité de l'aboutage est encore plus manifeste dans le cas des espèces feuillues puisque la répartition des défauts ferait en sorte d'augmenter le nombre de joints nécessaires comparativement aux produits faits de bois résineux (Aicher & Stapf, 2014). De plus, les difficultés inhérentes au collage des feuillus denses peuvent grandement affecter le comportement et la nature des ruptures lors du chargement d'un élément en BLC. En effet, alors que l'aboutage par entures multiples des espèces résineuses permet d'atteindre une résistance similaire à celle du bois non jointé, il en va autrement dans le cas des espèces feuillues (Tran *et al.*, 2016; 2014a; 2014b; Aicher & Stapf, 2014; Widmann *et al.*, 2014). Dans une étude portant sur des produits en bois lamellé-collé fabriqués en chêne Européen, Aicher & Stapf (2014) ont aussi conclu que la résistance des joints à entures multiples demeurait le facteur limitant la résistance globale du produit, allant même jusqu'à proposer une approche permettant de calculer la résistance caractéristique de poutres simplement à partir du nombre de joints à entures multiples et des paramètres de la distribution statistique de Weibull de leur résistance en traction.

Au Canada, seulement quelques travaux se sont intéressés à l'aboutage structural des bois d'espèces feuillues nord-américaines (Dagenais & Salenikovich, 2008; Chui & Delahunty, 2005; Verreault, 2000). Les travaux de Verreault (2000) ont démontré qu'il était possible de réaliser un aboutage structural du bois de cœur de bouleau jaune, de bouleau blanc et d'érable à sucre et que les propriétés mécaniques de ces pièces étaient comparables à celles du groupe EPS de catégorie No.1. Chui et Delahunty (2005) ont quant à eux confirmé que l'érable rouge canadien était doté de propriétés mécaniques adéquates pour la fabrication de produits du bois d'ingénierie structuraux. Pour leur part, Dagenais et Salenikovich (2008) ont établi que le bois d'érable à sucre avait le potentiel d'être abouté pour former des pièces à usage structural se comparant en matière de résistance en traction aux pièces

aboutées d'épinette noire. Toutefois, ces travaux étaient réalisés en considérant uniquement la géométrie de joint à entures multiples utilisée traditionnellement dans l'industrie des produits du bois au Canada. Pourtant, d'autres géométries de joint sont possibles et autorisées, par exemple dans la norme EN 14080 (2013). L'aboutage des espèces feuillues tempérées a d'ailleurs fait l'objet de plusieurs travaux en Europe (Franke *et al.*, 2014; Tran *et al.*, 2014b; Aicher *et al.*, 2001) dont les résultats ont été concluants. Considérant l'impact reconnu des paramètres géométriques des joints sur leur résistance, il est essentiel d'étudier ces facteurs en considérant de manière spécifique les espèces feuillues canadiennes afin de sélectionner les paramètres les plus appropriés à leur aboutage structural.

Potentiel des espèces feuillues disponibles au Canada

Les espèces feuillues disponibles dans l'est du Canada présentent des propriétés mécaniques qui se comparent avantageusement à celles des espèces résineuses. Les tableaux 1 et 2 présentent les principales caractéristiques et propriétés mécaniques de petits échantillons clairs (sans défauts) ces espèces.

Tableau 1. Propriétés mécaniques des principales espèces feuillues disponibles au Québec (Jessome, 1977).

Espèce	Masse volumique (kg/m^3)	Flexion statique (MPa)		Retrait vert à anhydre (%)	
		MOR	MOE	Radial	Tangentiel
Betula papyrifera Marsh.	640	94,8	12 893	5,2	7,2
Betula alleghaniensis Britt.	670	106,3	14 065	5,8	7,1
Quercus alba L.	750	120,9	15 513	4,7	6,0
Quercus rubra L.	690	98,7	11 928	3,6	6,7
Acer rubrum L.	610	97,6	11 101	3,6	6,0
Acer saccharum Marsh.	740	115,1	14 065	4,6	8,8
Fraxinus americana L.	690	108,0	12 824	4,2	7,0
Fagus grandifolia Ehrh.	750	116,1	13 996	5,2	10,1
Populus tremuloides Michx.	450	67,6	11 239	3,6	6,6

Tableau 2. Propriétés mécaniques des principales espèces résineuses disponibles au Québec (Jessome, 1977)

Espèce	Masse volumique (kg/m^3)	Flexion statique (MPa)		Retrait vert à anhydre (%)	
		MOR	MOE	Radial	Tangentiel
Picea engelmannii Parry ex Engelm.	450	69,5	11 032	4,2	8,2
Picea glauca (Moench) Voss	420	62,7	9 929	3,2	6,9
Picea mariana (Mill.) Britton, Sterns & Poggenburg	480	78,3	1 0411	3,8	7,5
Larix laricina (Du Roi) K. Koch	560	76,0	9 377	2,8	6,2
Larix occidentalis Nutt.	640	107,1	14 341	5,1	8,9
Pinus banksiana Lamb.	500	77,9	10 204	4,0	5,9
Pinus contorta Douglas	460	76,0	10 894	4,7	6,8
Tsuga canadensis (L.) Carrière	480	67,1	9 722	3,5	6,7
Tsuga heterophylla (Raf.) Sarg.	480	81,1	12 342	5,4	8,5
Pseudotsuga menziesii (Mirbel) Franco	540	88,6	13 514	4,8	7,4
Abies amabilis Douglas ex J.Forbes	430	68,9	11 376	4,2	8,9

Considérant leurs propriétés mécaniques, les bénéfices d'une valorisation de la ressource feuillue, en plus de l'attrait potentiel de tels produits, il apparaît pertinent de poursuivre les efforts de recherche pour aboutir à la fabrication d'un bois lamellé-collé structural entièrement composé d'espèces feuillues indigènes.

La préoccupation de valoriser les essences feuillues est présente au Canada. À l'échelle du pays, la proportion des volumes disponibles qui est récoltée annuellement avoisine les 45% (Ressources Naturelles Canada, 2019). Au Québec, la situation est similaire, avec moins de la moitié de la possibilité annuelle de récolte prélevée (Durocher *et al.*, 2019). En forêt publique, le niveau de récolte des espèces feuillues se situait à 40 % pour l'année 2013-2014 (MFFP, 2015). Les essences principalement disponibles sont le bouleau à papier (6 Mm^3), les peupliers (3,7 Mm^3), les érables à sucre et rouge (1,5 Mm^3), ainsi que le bouleau jaune (1 Mm^3) (BFEC, 2014). L'enjeu est tel qu'entre 2012 et 2017, le gouvernement du Québec a affecté un budget global de 9 millions de dollars au « Chantier sur la forêt feuillue » dans le but d'identifier des débouchés à forte valeur ajoutée pour ces bois (MRNF, 2012).

Parmi les espèces feuillues disponibles dans l'est du Canada, le bouleau à papier (*Betula papyrifera* Marsh.), le bouleau jaune (*Betula alleghaniensis* Britt.), le frêne d'Amérique (*Fraxinus americana* L.) et le chêne blanc (*Quercus alba* L.) présentent un potentiel intéressant pour des raisons variables, liées tant à leurs propriétés mécaniques qu'à leur attrait esthétique et qu'à leur disponibilité.

Le bouleau à papier est l'une des espèces feuillues les plus largement répandues au Canada. Dans la province de Québec, cette espèce représente 40 % de la possibilité annuelle de récolte en espèces feuillues. Le bouleau jaune représente quant à lui 11% de la possibilité annuelle de récolte en espèces feuillues au Québec. Cette espèce emblématique du Québec est reconnue pour sa noblesse et ses sciages arrivent en deuxième position en termes de valeur parmi les espèces feuillues du nord-est de l'Amérique du Nord (Hardwood Publishing Inc., 2020). Parmi les quatre espèces mentionnées, celles du genre *Betula* sont les plus disponibles, avec seulement 21% de leur possibilité annuelle de récolte prélevée chaque année (Durocher *et al.*, 2019). Le frêne d'Amérique est l'espèce du genre *Fraxinus* la plus répandue au Canada, bien qu'elle soit présente exclusivement dans le sud-est du pays (Schlesinger, 1990). Toutefois, la mortalité et l'abatage préventif causés par l'arrivée de l'agrile du frêne pourraient rendre d'importants volumes disponibles dans certaines régions (Herms & McCullough, 2014). Quant au chêne blanc, il s'agit de l'une des espèces feuillues les moins répandues au pays, présente seulement dans l'extrême sud du Québec et de l'Ontario (Tardif *et al.*, 2006). Il s'agit toutefois de l'espèce feuillue dont la valeur des sciages est la plus élevée (Hardwood Publishing Inc., 2020). Son bois noble est recherché par les consommateurs et les espèces de chêne font l'objet d'importations massives en provenance des États-Unis (Statistiques Canada, 2019).

Objectifs du projet

Objectif principal :

Évaluer la faisabilité technique d'un bois lamellé-collé structural composé d'espèces feuillues du nord-est de l'Amérique du Nord.

Sous-objectifs :

- Identifier les propriétés indicatrices pertinentes à la prédiction de la résistance en traction des espèces étudiées et commenter leur importance relative;
- Mesurer la résistance au cisaillement d'assemblages composés de différentes espèces feuillues et adhésifs structuraux et identifier les combinaisons les plus appropriées pour un produit d'ingénierie structural;
- Mesurer la résistance en traction de lamelles aboutées selon différentes configurations de joint à entures multiples et identifier la géométrie la plus appropriée aux espèces étudiées;
- Évaluer les propriétés mécaniques, notamment le module d'élasticité et le module de rupture de poutres pleine grandeur composées des espèces étudiées.

Chapitre 1 – *Strength grading of northern hardwood species for structural engineered wood products: Identification of the relevant indicating properties.*

1.1 Résumé

Afin d'utiliser les espèces feuillues dans la fabrication de produits d'ingénierie structuraux, il est essentiel que leur bois fasse l'objet d'un classement basé sur la résistance. Toutefois, les espèces feuillues canadiennes ne font actuellement l'objet que d'un classement basé sur l'apparence. L'objectif de ce chapitre était d'identifier les propriétés indicatrices pertinentes permettant de prédire la résistance en traction de lamelles de frêne d'Amérique et de bouleau jaune. Une approche de sélection de modèles a été conduite afin d'identifier les modèles les plus performants et de comparer, pour chacune des espèces, l'impact relatif des propriétés indicatrices. Malgré des différences en fonction de l'espèce dans la façon dont les caractéristiques mesurées affectent la résistance en traction, les modèles finaux permettent de prédire la résistance en traction des espèces étudiées avec un coefficient de détermination de 0.82 pour le frêne d'Amérique et de 0.78 pour le bouleau jaune.

1.2 Abstract

Strength grading of hardwoods is a prerequisite to use them in structural engineered wood products. However, hardwood strength grading is considerably less developed than it is for softwood species and no strength grading procedure dedicated to hardwoods is available in Canada. The objective of this study was to identify the most relevant indicating properties for predicting the ultimate tensile strength of the investigated species. A model selection approach was used to identify the most performing models and to compare, for each species, the relative impact of the indicating properties. A final model was created for each species by multimodel inference. The indicating properties included in the final models were the density of the specimens, the dynamic modulus of elasticity, the sinus of the maximum local grain deviation (SGD_{max}) as well as the knot area index (KAI), derived from the knot area ratio. The final models revealed important differences between the two species, indicating that it may be relevant to grade them separately to ensure the most efficient utilization of the resource. The KAI and SGD_{max} variables affected more importantly the UTS of white ash, while for the MOE, the effect on UTS was more pronounced for yellow birch. The effect of the density was also of an opposite direction for both species. The coefficients of determination between the actual and model predicted UTS were respectively of 0.82 for white ash and 0.82 for yellow birch. From our results, we can conclude that it is feasible and relevant to develop a strength grading procedure for both species.

1.3 Introduction

The last decades have seen a renewed interest towards the use of hardwoods in construction (Ross & Erickson, 2020; Aicher *et al.,* 2014; Green *et al.,* 1994). Their availability, impressive mechanical properties and distinctive appearance are among the main factors fostering the development of new structural engineered wood products from various broadleaf species. The value of the timber from hardwood species, as well as the possibility to use it engineered wood products, highly depends on the knowledge of its mechanical properties and behavior under load. However, the inherent variability associated with the structure and anatomical features of hardwoods causes uncertainty with respect to their mechanical properties. The types of cells, their proportion and the relative amount of their chemical constituent as well as the nature and abundance of the strength reducing defects is highly variable between species, but also within the individuals of a given species and even inside a single tree (Ridley-Ellis *et al.,* 2016; Panshin & Zeeuw, 1970).

In engineering applications, this uncertainty is managed by the means of design approaches taking into account the natural variability of the material. One of the most widespread practice is to consider, in the design calculations, the 5th percentile level from the normal distribution of the lumber properties, also called characteristic properties. However, the diversity is so big that the establishment of characteristic properties applicable to all hardwoods, or even to a single species, would lead to a very inefficient utilization of the raw material (Ravenshorst, 2015). The strength grading process allows segregating the timber in groups for which the same strength properties can be assigned, allowing for a more efficient and more economical use of the resource. In the case of engineered wood products, such as glued-laminated timber (glulam), grading of the lumber allows identifying and use the strongest material in the most solicited portions of the beam's cross section for instance.

The strength grading process is based on the measurement of various parameters, called indicating properties (IP), that knowledgeably affect the strength of timber and that can be measured nondestructively (Ross & Erickson, 2020; Schlotzhauer *et al.,* 2019). Most grading methods can be classified either as visual or machine grading. Visual grading is based on limitations of characteristics that can be assessed visually, for instance the position, dimensions and number of knots and the slope of grain, but also the presence of reaction wood, fissures, wane or rot (Ridley-Ellis *et al.,* 2016; Ravenshorst, 2015). Visual grading was the only available method until the 1960's and is based, since the 1990's, on large-scale testing of lumber (Galligan & McDonald, 2000). However, a considerable margin for safety must be added to account for the limited precision of human evaluation and the uncertainty in the relationships between the visual characteristics and the strength. Visual grading is therefore not allowing the most efficient utilization of the real properties of the timber. Machine strength grading is now well established and a variety of methods and equipment are now available to measure properties that can or cannot be assessed visually. Those properties include namely the stiffness, the density, and the direction of the wood fibres (Galligan & McDonald, 2000). As of today, most grading approaches rely on a combination of visual and machine-based methods (Ehrhart *et al.,* 2016a; Niemz & Mannes, 2012). For instance, MSR lumber is also graded visually, because adding knot information to the stiffness significantly improves the precision of the process (Bendtsen & Youngs, 1981).

The structure and mechanical properties of hardwood species are more complex and even more variable than that of softwoods (Bollmus *et al.,* 2017; Panshin & Zeeuw, 1970), making a grading process essential to use them in structural applications. Strength grading of hardwoods is considerably less developed than it is for softwoods (Weidenhiller *et al.,* 2019; Kovryga *et al.,* 2019a), notably because hardwoods mechanical properties are less predictable (Schlotzhauer *et al.,* 2019). In Canada, the dominant use of hardwoods in appearance products has defined the grading method. Hardwood lumber is sawn in factory lumber rather than in dimension lumber and graded for its appearance instead of being graded for its mechanical properties (NHLA, 2019). Moreover, hardwood grading based on the tensile strength, which would be relevant for products such as glulam which are subjected to tensile stresses, is still in its early stages. Despite comprising tensile strength classes for softwoods, European standard EN 338 (2016) does not yet include tensile strength classes dedicated to hardwood species.

Yet, research efforts conducted in the United States in the early 1990s have proved that the relationships between the mechanical properties of softwoods, on which current strength grading methods are based, are also applicable to hardwoods (Green *et al.,* 1994). However, compared to softwoods, most hardwood species appear to have a higher ultimate tensile strength (UTS) for a given bending strength (MOR), and a higher bending strength for a given modulus of elasticity (MOE). It may therefore be over-conservative to use the softwood relationships (Kovryga *et al.,* 2019b; Green *et al.,* 1994) to assign characteristic properties to

hardwood species. Moreover, the mechanical properties of some hardwood species are very difficult to predict (Weidenhiller *et al.,* 2019) and the interrelationships between the indicating properties appear to be variable in function of the species (Kovryga *et al.,* 2019b).

Previous work by the authors have shown that white ash (*Fraxinus americana* L.) and yellow birch (*Betula alleghaniensis* Britt.) are promising species for the manufacture of glulam (Morin-Bernard *et al.*, 2020a; 2020b). However, there is little scientific knowledge on the mechanical properties of these species that are not currently strength graded in Canada. The objective of this study was to identify, using a modelling approach, the most suitable indicating properties to predict the ultimate tensile strength of white ash and yellow birch timber. The relative impact of the IPs on their mechanical properties as well as their adequateness to be subjected to a strength grading process will also be discussed. This study is part of a broader project aiming to foster the use of northern hardwood species in structural engineered wood products.

1.4 Experimental

1.4.1 Materials

Lumber from the investigated hardwood species were purchased from a supplier located in the province of Quebec, Canada. Boards were processed to lamellae with cross-sectional dimensions of 38 x 38 mm and a length of 1830 mm. The resulting samples comprised lamellae presenting a wide range of strength reducing defects but also lamellae clear of knots or any other visible strength reducing defects. When a knot or a major grain deviation was present, the lamella was sawn in such a way that the worst defect was positioned in the central portion of the lamella, within the test span. A total of 62 white ash and 55 yellow birch specimens were prepared and tested.

1.4.2 Methods

Measurement of indicating properties and non-destructive testing

The maximum local grain deviation, the maximum grain deviation on a length equivalent to the width of the specimen, as well as the average slope of grain in the 610 mm test span were recorded on each face of the specimens. The average slope of grain on the four faces of the piece was also derived from the measurements. Considering the difficulties related to the measurement of the fiber direction on hardwoods, multiple methods were used. When a radial surface was present, the growth rings boundaries were used to determine the angle of the grain, as suggested by Koehler (1955). For less evident specimens, a magnifying glass, a scribe and the pattern after tensile failure were used to ensure the accuracy of the measurements. Data relative to the knots were recorded using the concept of the Knot Area Ratio (KAR), which corresponds to the projection of the knot on the cross-sectional area of the piece. The width of the knot, measured on every face where it was visible, was taken as the distance between lines drawn parallel to the length of the board and enclosing the knot. Every specimen comprised only one knot within the test span.

The dynamic modulus of elasticity (MOE_{dyn}) was measured using a HM200 Director acoustic velocity tool on all lamellae. The velocity of the sound wave measured by the tool was used to calculate MOE_{dyn} with Equation 1, where ρ is the density in kg/m^3 and V, the acoustic wave velocity in km/s.

$$MOE_{dyn} = \rho V^2 \quad (1)$$

To confirm the suitability of the HM200 Director (Christchurch, New Zealand) as a tool to measure the stiffness of hardwood lamellae, the apparent modulus of elasticity in third point bending was also measured on 17 white ash and 18 yellow birch specimens. The loading span of 813 mm and the test setup conformed to ASTM D4761 (2013). Equation 2 was used to calculate the apparent modulus of elasticity (MOE_{app}), where *P* is the increment of applied load on the specimen in Newtons, *l* is the span of flexure in mm, *b* is the width of the specimen in mm, *d* is depth of specimen mm and *Δ* is the increment of deflection of the specimen in mm when subjected to the applied load P.

$$MOE_{app} = 23Pl^3 / 108bd^3\Delta \quad (2)$$

Generalized linear models were built with the data from the lamellae that has been subjected to both dynamic and static MOE measurement to establish the relationship between the two methods of measurement.

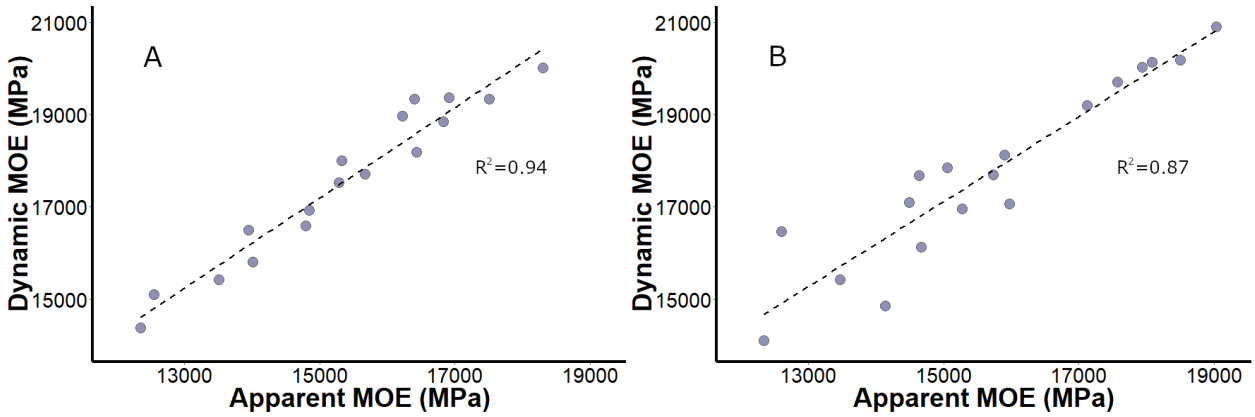

Figure 5. Dynamic MOE values plotted against the apparent MOE measured in third point bending for white ash (A) and yellow birch (B).

In Figure 5, the dynamic MOE values are plotted against the apparent MOE values for white ash (A) and white oak (B) samples. Those results are in line with findings from Liu *et al.* (2014) which concluded that the MOE measured by dynamic techniques leads to 5 to 20 % higher values than that obtained from static measurement methods. In the present study, the linear models relating the two methods showed a coefficient of determination of 0.94 for white ash and 0.87 for yellow birch. Coefficients derived from the linear model were used to assign an apparent modulus of elasticity value to the lamellae for which the MOE has only been assessed using the acoustic velocity tool. The relevant characteristics of the lumber tested in the present study, including the strength reducing defects, are shown in Table 3.

Table 3. Relevant characteristics of the white ash and yellow birch lamellae tested in the study.

		White ash	Yellow birch
Number of specimens		62	55
Density (kg/m^3)			
	Mean	712,7	717,9
	Minimum	634,9	577,9
	Maximum	798,5	794,0
	SD	45,1	41,3
MOE_{app} (MPa)			

	Mean	14 195	15 254
	Minimum	8 806	11 035
	Maximum	18 217	18 972
	SD	2 342	1 857
Maximum local grain deviation (°)			
	Mean	26,3	26,6
	Minimum	1,9	1,9
	Maximum	71,7	62,4
	SD	20,6	18,4
Knot Area Ratio (%)			
	Mean	5,4	3,9
	Minimum	0,0	0,0
	Maximum	50,6	24,7
	SD	11,0	6,1

Tension testing of the lumber

Tension testing of the specimens was realized with an hydraulic tension testing machine in accordance with the standard test method ASTM D4761 (2013) for determination of axial strength in tension, with a test span of 610 mm for a specimen width of 38 mm. The specimens were held in place by grips designed to minimize slip. Samples were collected on each specimen after testing for determination of the moisture content (MC). UTS, MOE and density values were adjusted to a 12% moisture content following procedures from ASTM D1990 (2016).

Model development

With the aim of identifying the explanatory variables influencing the UTS of the lamellae, a model selection process was performed using package AICcmodavg (Mazerolle, 2019) and the R programming environment (R Core Team, 2019). The procedure was realized separately for each of the species. Three groups of candidate models comprising a total of 20 models were built a priori. The first set comprised models with variables related to the characteristics measured by non-destructive testing of the lamellae, namely the dynamic MOE and density, while the second group included the models involving variables linked to the defects recorded during the visual grading process. A third group was created with the models combining variables from the two aforementioned groups. An intercept-only model was also included in the analysis. The variables included in the candidate models are presented in Table 4. Because of the nature of the relationship between the maximum grain deviation and UTS, a transformation was required. Variable SGD_{max} corresponds to the sinus of the maximum local grain deviation in radians. The Knot Area Ratio also needed to be transformed to avoid generating negative UTS in the selected models. Variable KAI, or Knot Area Index, was created by exponential transformation of variable KAR. Therefore, the KAI value tends to zero as the KAR increases.

Table 4. Indicating properties included in the candidate models.

Variable	Description
ρ_{12}	Density adjusted to 12% moisture content ($kg/m^{3)}$
MOE_{dyn}	Dynamic modulus of elasticity adjusted to 12% moisture content (N/mm^2)

SGD_{max}	Sinus of the maximum local grain deviation in radians on the worst face of the lamella
$GD_{max1.5}$	Maximum grain deviation on the worst face of the lamella on a length equivalent to the width of the lamella (°)
$Combined\_SOG_{1.5}$	Average maximum grain deviation on the four faces of the lamella, on a length equivalent to the width of the lamella (°)
$Combined\_SOG_{Span}$	Average slope of grain in the test span of the four faces (°)
KAI	Knot Area Index [$e^{(-0.1*KAR)}$]

When multiple models showed a comparable performance (i.e. similar AICc values), a final model was built by multimodel inference, also known as model-averaging. This approach, described by Mazerolle (2006), uses the Akaike weights of the models to weight the estimates and standard errors (SE) of each parameter, resulting in estimates and SE considering the information of all relevant models. All selected models presented normally distributed errors and homogeneous variances. The interactions between the explanatory variables were dismissed.

1.5 Results and discussion

1.5.1 Results from the tensile strength tests

In Table 5, we show the ultimate tensile strength and other relevant properties of the specimens tested in tension. The mechanical properties determined from the test campaign appears slightly higher than what is published in literature. For white ash, Jessome (1977) declared a mean MOE of 12 800 MPa (13 406 MPa when adjusted to 12% MC) while the declared MOE for yellow birch was 14 100 MPa (14 700 at 12% MC). The respective mean density values from Jessome (1977) are 690 for white ash and 670 kg/m^3 for yellow birch. No data were available regarding the UTS of the investigated species.

Table 5. UTS and other relevant properties of the white ash and yellow birch lamellae tested in tension.

Species	n	Mean density (kg/m^3)	Density SD (kg/m^3)	Mean MC (%)	Median UTS (MPa)	Min. UTS (MPa)	UTS SD (MPa)	Mean MOE_{app} (MPa)	Min. MOE_{app} (MPa)
White ash	62	712.7	45.1	10.0	85.7	16.4	38.0	14 195	8 806
Yellow birch	55	717.9	41.3	11.0	95.3	19.6	32.8	15 254	11 035

1.5.2 Results of the model selection process

Table 6 shows the ranking of the candidate models for white ash after the model selection process based on the AICc. The best model for the prediction of white ash UTS was model 14 (AICc = 533.42, w_i = 0.69). This model included visually assessed variables, namely the maximum local grain deviation (SGD_{max}) and Knot Area Index (KAI) as well as the density and the dynamic MOE (MOE_{dyn}). The second-best model was model 17 (AICc = 535.21, w_i = 0.28) which included all variables from model 14, except the density. The third most performing model was model 16 (AICc 540.17, w_i = 0.02) which included the density, SGD_{max} and KAI.

Table 6. Ranking of the candidate models and related indicators for white ash after model selection.

Model ID	Explanatory variables	K	AICc	Delta AICc	AICc weight	Log-likelihood
14	p_{12} + MOE_{dyn} + SGD_{max} + KAI	6	533.42	0.00	0.69	-259.95
17	MOE_{dyn} + SGD_{max} + KAI	5	535.21	1.78	0.28	-262.07
16	p_{12} + SGD_{max} + KAI	5	540.17	6.74	0.02	-264.55
9	SGD_{max} + KAI	4	550.89	17.46	0.00	-271.09
13	SGD_{max} + Combined_SOG_{Span} + KAI	5	551.28	17.86	0.00	-270.11
15	p_{12} + MOE_{dyn} + Combined_SOG_{Span} + KAI	6	554.31	20.88	0.00	-270.39
4	SGD_{max}	3	565.80	32.37	0.00	-279.69
10	$GD_{max1.5}$ + KAI	4	566.72	33.30	0.00	-279.01
11	Combined_$SOG_{1.5}$ + KAI	4	566.81	33.38	0.00	-279.05
8	KAI	3	585.38	51.95	0.00	-289.48
12	Combined_SOG_{Span} + KAI	4	586.36	52.94	0.00	-288.83
19	MOE_{dyn} + Combined_SOG_{Span}	4	586.40	52.98	0.00	-288.85
5	$GD_{max1.5}$	3	588.46	55.03	0.00	-291.02
18	p_{12} + Combined_SOG_{Span}	4	589.29	55.86	0.00	-290.29
6	Combined_$SOG_{1.5}$	3	590.92	57.50	0.00	-292.25
2	MOE_{dyn}	3	618.39	84.96	0.00	-305.99
3	p_{12} + MOE_{dyn}	4	620.61	87.19	0.00	-305.95
7	Combined_SOG_{Span}	3	628.96	95.54	0.00	-311.27
20	Intercept only	2	630.14	96.71	0.00	-312.97
1	p_{12}	3	630.36	96.93	0.00	-311.97

The multi-model inference allowed to compute model-averaged estimates and their corresponding standard error at a 95% confidence level for the three best-performing models, as presented in Table 7.

Table 7. Model-averaged estimates and 95% confidence level standard error (SE) of the final models for the two investigated species.

	White ash		**Yellow birch**	
Parameter	Model-averaged estimate	SE	Model-averaged estimate	SE
p_{12}	0.1141	0.0572	-0.1373	0.0596
MOE_{dyn}	0.0034	0.0011	0.0058	0.0013
SGD_{max}	-66.46	9.44	-59.31	12.15
KAI	42.78	8.60	23.20	9.59
Intercept	-29.86	45.65	79.68	46.04

Figure 6 shows the model-averaged predictions and unconditional 95% confidence intervals for the best-fit model parameters for white ash.

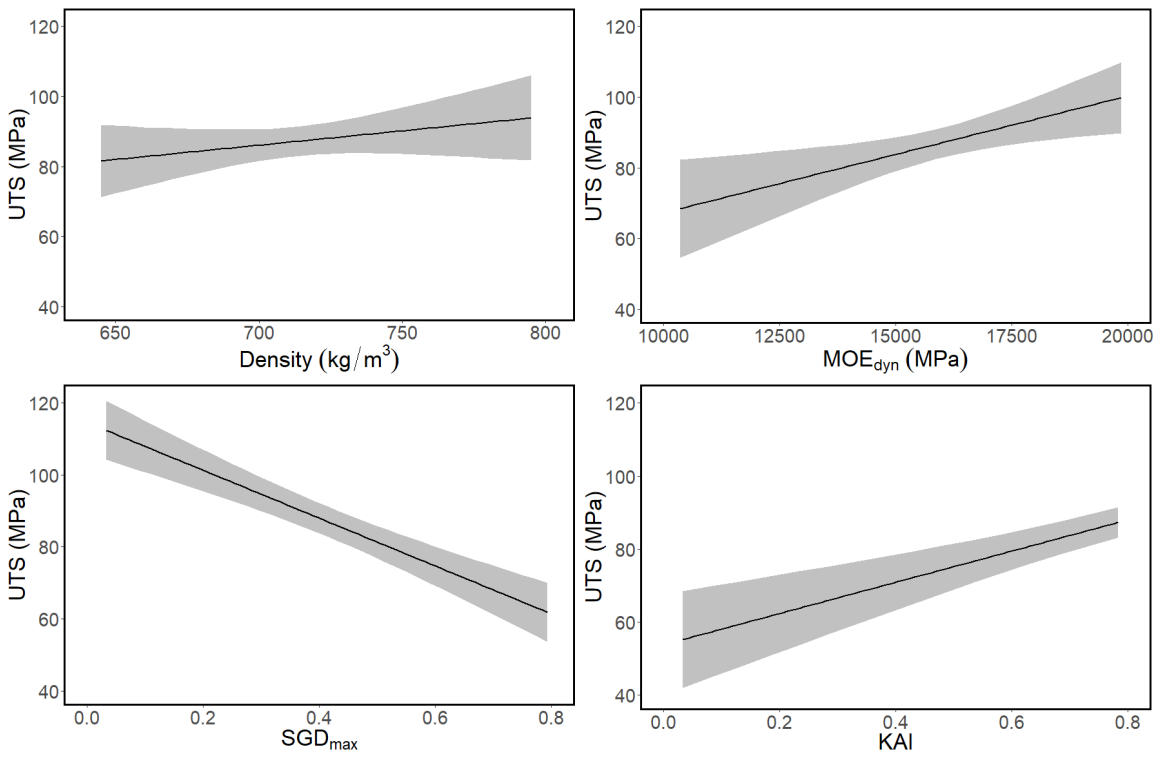

Figure 6. Model-averaged predictions and unconditional 95% confidence intervals for the best-fit model parameters for white ash.

The ranking of the candidate models for yellow birch is presented in Table 8. For this species, model 14 (AICc = 459.83 w_i = 0.81) was also the best model for predicting the UTS. Model 17 (AICc = 462.86, w_i = 0.18) also came in second position, but was followed by model 15 (AICc = 468.88, w_i = 0.1), which included the density, MOE_{dyn}, KAI and the combined average slope of grain in the test span Combined_SOG_{Span}. However, the effect of Combined_SOG_{Span} was not included in the final model because the maximum local grain deviation SGD_{max} proved to be a stronger predictor of the tensile strength.

Table 8. Ranking of the candidate models and related indicators for yellow birch after model selection.

Model ID	Explanatory variables	K	AICc	Delta AICc	AICc weight	Log-likelihood
14	p_{12} + MOE_{dyn} + SGD_{max} + KAI	6	459.83	0.00	0.81	-223.02
17	MOE_{dyn} + SGD_{max} + KAI	5	462.86	3.03	0.18	-225.80
15	p_{12} + MOE_{dyn} + Combined_SOG_{Span} + KAI	6	468.88	9.04	0.01	-227.54
9	SGD_{max} + KAI	4	475.35	15.52	0.00	-233.27
16	p_{12} + SGD_{max} + KAI	5	477.51	17.68	0.00	-233.13
13	SGD_{max} + Combined_SOG_{Span} + KAI	5	477.74	17.91	0.00	-233.25
10	$GD_{max1.5}$ + KAI	4	477.78	17.94	0.00	-234.48
11	Combined_$SOG_{1.5}$ + KAI	4	480.11	20.28	0.00	-235.65
4	SGD_{max}	3	480.45	20.62	0.00	-236.99
19	MOE_{dyn} + Combined_SOG_{Span}	4	482.94	23.11	0.00	-237.06
5	$GD_{max1.5}$	3	484.80	24.97	0.00	-239.16
6	Combined_$SOG_{1.5}$	3	489.02	29.19	0.00	-241.27
18	p_{12} + Combined_SOG_{Span}	4	490.33	30.49	0.00	-240.76
8	KAI	3	497.91	38.08	0.00	-245.71
12	Combined_SOG_{Span} + KAI	4	499.41	39.58	0.00	-245.30

3	p_{12} + MOE_{dyn}	4	505.49	45.66	0.00	-248.34
2	MOE_{dyn}	3	514.96	55.13	0.00	-254.24
1	p_{12}	3	529.51	69.68	0.00	-261.51
20	Intercept only	2	529.58	69.75	0.00	-262.67
7	Combined_SOG_{Span}	3	530.54	70.71	0.00	-262.03

The model-averaged estimates and their corresponding standard error at a 95% confidence level are presented in Table 5, while the model-averaged predictions plots for yellow birch are shown in Figure 7.

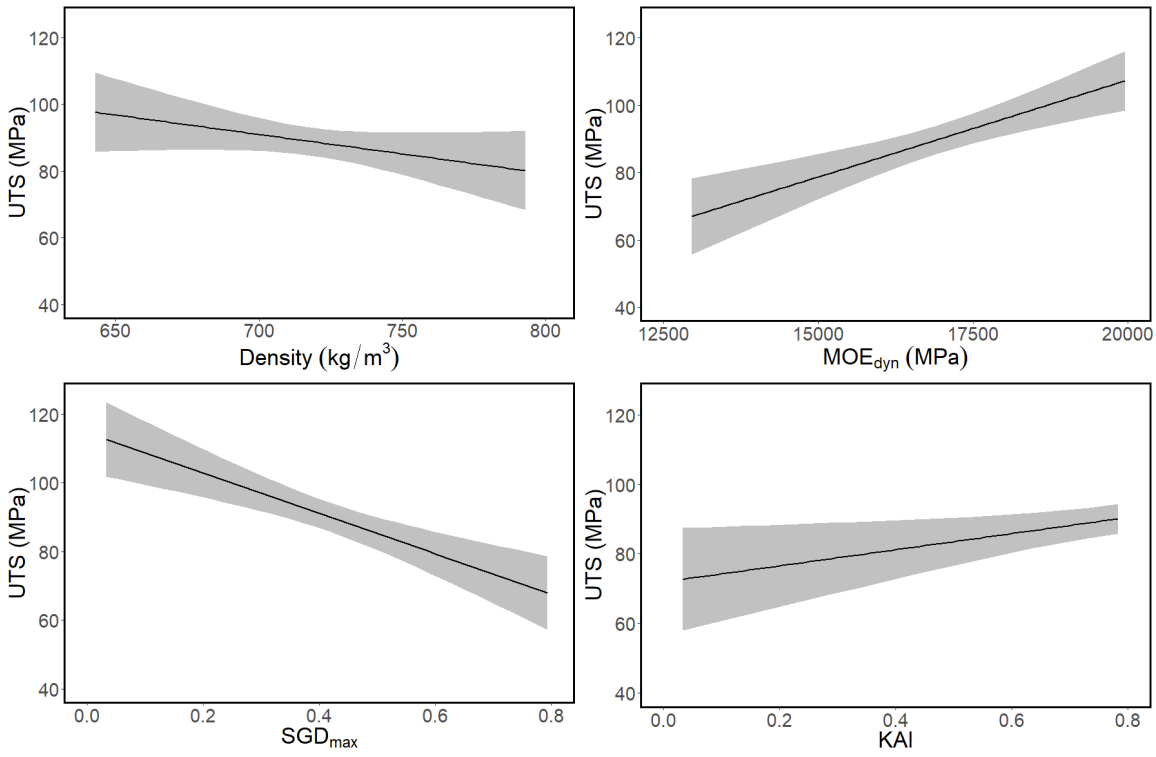

Figure 7. Model-averaged predictions and unconditional 95% confidence intervals for the best-fit model parameters for yellow birch.

1.5.3 Effect of the explanatory variables included in the final models

The final models for white ash and yellow birch, despite showing similitudes, exhibited major differences. The relationships between the mechanical and indicating properties appear to be somehow different for both species. By isolating the effect of each of the explanatory variables included in the final models, as presented in Figures 6 and 7, it is possible to better understand these differences and their implications for the grading of these species.

Effect of the density on the UTS

In this study, the density affected the two species differently, as it can be seen from the estimates presented in Table 7. While the UTS of the white ash specimens tended to get higher as the density increased, the opposite trend was observed for yellow birch. A deeper analysis of the test specimens revealed that the densest yellow birch lamellae that failed at a lower tension stress presented wavy grain (Figure 8) that was not visible on the other specimens. The presence of irregular grain patterns in yellow birch is known for a long time and is generally undesirable except in some specific appearance products (Ross & Erickson, 2020;

Clausen & Godman, 1967). The implications of this characteristic are going to be further discussed in section 3.4. Differences have already been observed between northern hardwood species regarding the effect of the density on their mechanical properties. In a study involving North American white ash, yellow birch and sugar maple specimens, Kretchmann *et al.* (2010) concluded that the density changes affected the three species differently. Although their data suggested a trend for a higher strength with increasing density, it was not possible to conclude definitively. It is also not exceptional that a higher density leads to lower mechanical properties. In a study on grading of European hardwoods, Kovryga *et al.* (2019c) found a negative relationship between density and MOE for European maple.

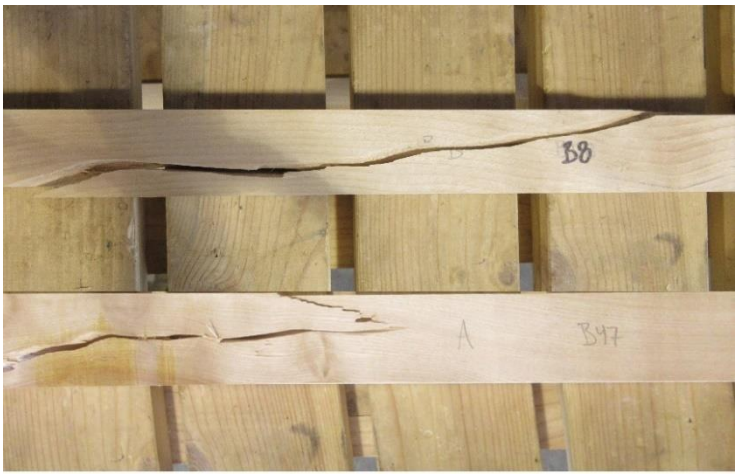

Figure 8. Wavy grained yellow birch specimens after failure.

Nevertheless, it is generally acknowledged that the density of the wood has a direct and positive impact on the strength of both softwoods and hardwoods (Ravenshorst, 2015; Ross, 2010; Bendtsen & Youngs, 1981). A study conducted on small, clear wood specimens from 160 hardwoods species and 32 softwood species revealed a coefficient of determination of 0.64 for the linear model relating the density to the bending strength of all species together (Ravenshorst, 2015). After submitting small, clear wood specimens to bending tests, Zhang (1997) found R^2 values ranging from 0.50 to 0.74 between the density and MOR for four European birches and oak species. In the case of structural timber, the effect of density is less obvious than it is for small, clear wood specimens. The variability in the properties of hardwood species make difficult to base the strength grading on the density (Kovryga *et al.,* 2019b; Brunetti *et al.,* 2019; Frühwald & Schickhofer, 2005). For that reason, Ehrhart *et al.* (2016a) did not even include this property in any of their candidate models. In our study, the generalized linear models in which the density was the sole predicting variable for UTS resulted in R^2 values of 0.015 for white ash (p = 0.167) and 0.024 for yellow birch (p = 0.132). The density, despite not being a good predictor on its own, was still included in the best-performing models retained after the model selection process. In the first-ranked model (Model 14), the effect of the density was significantly correlated to the UTS (p = 0.049). It appears that the inclusion of additional indicating properties in the final models explained a larger proportion of the residual variance, increasing therefore the significance of the density as a predictor of the UTS. Those results, although different from what could have been expected, are still consistent with findings from other studies on hardwood strength grading. When studying the relation between the UTS and the density of European ash timber, Sarnaghi *et al.* (2017) obtained an R^2 of 0.006, while Kovryga *et al.* (2019c) found a slightly higher coefficient of determination (R^2 = 0.034) for the same species. Considering the results of the model selection process as well as the differences in the effect of the density on the UTS of the investigated species, this indicating

property should be considered for the grading of white ash and yellow birch, unless it is possible to account for its influence through other characteristics or indicating properties.

Effect of the grain deviations of the UTS

In this study, the generalized linear models in which the maximum local grain deviation in degrees was the only explanatory variable allowed to conclude that this indicating property had a significant but limited impact on the UTS for both white ash (R^2 = 0.05, p = 0.05) and yellow birch (R^2 = 0.07, p = 0.03). It is already well known that the angle made by wood fibres from the longitudinal axis of a lumber piece affects its bending strength. This effect can be approximated using the Hankinson equation (Ravenshorst *et al.,* 2019; Ross, 2010; Bodig & Jayne, 1982), which is not linear. This non-linear relationship was also observed by Ravenshorst (2015) in a study on tropical hardwoods. In the present study, the maximum local grain deviation had to be transformed to account for the non-linear relationship between the UTS and the maximum local grain deviation. In the models relating the grain deviations to the UTS, the substitution of the maximum local grain deviation in degree by variable SGD_{max} allowed to increase considerably the portion of the UTS explained, with an R^2 of 0.65 ($p < 0.001$) for white ash, and an R^2 of 0.62 ($p < 0.001$) for yellow birch. A common practice for softwood structural grading is to consider the general slope of grain, which is measured on a certain length and ignores the local grain deviations (ASTM D245, 2011; Fruhwald & Schickhofer, 2005). Due to the anatomical differences of hardwoods and their diversity, (Sarnaghi *et al.,* 2017) concluded that we should avoid using the same grading methods as for softwoods. Indeed, in the present study, all the variables expressing the general slope of grain offered a poor performance as predictors of the tensile strength compared to the maximum local grain deviation expressed by variable SGD_{max}. From examination of the final models, one can see that the relative importance of variable SGD_{max} as a predictor of UTS differs between white ash and yellow birch. The reduction in tensile strength caused by the maximum local grain deviation appears to be of a larger magnitude for white ash, with an estimate of -66.46 compared to -59.31 for yellow birch. In a study of the impact of the slope of grain on the bending strength of white ash, yellow birch and sugar maple, Kretschmann *et al.* (2010) came to a similar conclusion, suggesting that grain deviations had a bigger impact on the bending strength of white ash and sugar maple than yellow birch.

Results from other studies on hardwood grading also revealed a certain variability in the relationships between the grain angle and the bending or tensile strength. The main challenge in relating the grain deviations to the mechanical properties comes from the difficulty to assess visually this property on sawn hardwood products (Bollmus *et al.,* 2017; Ravenshorst, 2015; Fruhwald & Schickhofer, 2005), which depends on the species and evaluation method. Fruhwald & Schickhofer (2005) were able to measure the grain deviations accurately on beech only by considering the fracture pattern after test, and obtained a moderate correlation (R^2 = 0.44) with bending strength. However, Brunetti *et al.* (2019) found that neither the slope of grain measured visually or measured after failure was related to any of the mechanical properties of beech timber. Kovryga *et al.* (2019d) measured the slope of grain by transverse ultrasound on the worst 150 mm section of European ash and maple lamellae and concluded that neither this measure nor the slope measured after failure was significantly correlated with tensile strength. With European oak, Riesco-Muñoz & Remacha-Gete (2012) also found that the general slope of grain did not have a significant impact on the bending strength or MOE.

In the present study, the high significance of variable SGD_{max} is attributable to the short span of the measurements, but may also be explained by the limited cross section (38 x 38 mm) of the tested specimens, which resulted in a more accurate estimation of

the real grain deviations. Stapel & van de Kuilen (2014) showed that visual grading techniques are strongly influenced by the cross section of the specimen and that some defects cannot be properly detected on larger cross sections. Nevertheless, from our experience, it was feasible to measure the grain deviations visually for both investigated species. A considerable proportion of the specimens failed in the region where the worst local grain deviation had been measured. The annual rings boundary method was the easiest way to measure the grain deviations and the failure patterns confirmed the suitability of this method, as depicted in Figure 9. However, this technique was only appropriate for specimens presenting an almost perfectly radial face. Grain deviations were more difficult to assess on the other specimens and the process required more time. Grain deviations also proved easier to measure visually on white ash than on yellow birch.

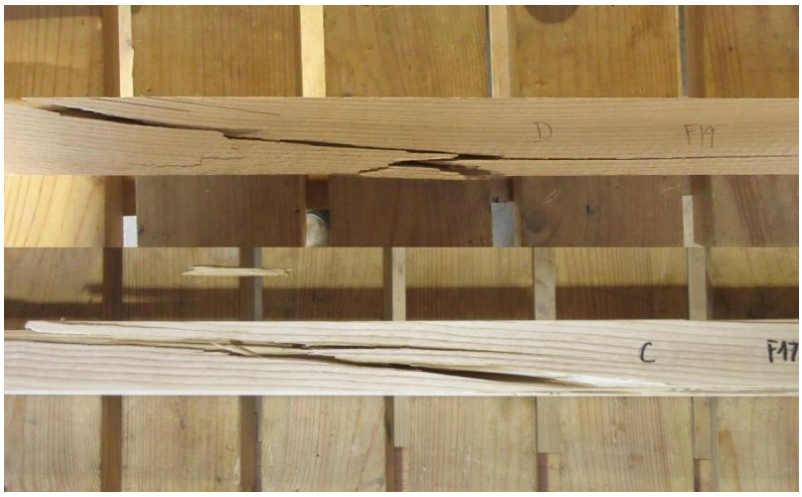

Figure 9. Failure pattern following the ring boundaries on radially sawn white ash specimens.

Results from the present study have confirmed the significant effect of the grain angle on the UTS. The maximum local grain deviation appears to be a relevant indicating property for the strength grading of the investigated species. To accurately and efficiently measure the grain deviations on a greater diversity of cross sections and species, the measurement method needs to be refined, since the measures taken on larger specimens may not be as reliable. To that extent, Ehrhart *et al.* (2018) developed for beech an automatic image analysis that calculates the grain deviations from the spindles formed by the medullary rays. That technique would also be applicable to other species. In a study on strength grading of European ash and European maple, Kovryga *et al.* (2019d) found a strong correlation between the slope of grain measured by transverse ultrasound and the measure taken from the failure pattern. However, the deviation measured on a 150 mm length was not correlated with the tensile strength, but the measurement span could be reduced which may lead to better results. Similar methods could be experimented with the species investigated in the present study. However, the prohibitive cost of some of these scanning technologies may limit their applicability in an industrial context (Ross & Erickson, 2020).

Effect of the modulus of elasticity on the UTS

The effect of the stiffness, accounted by variable MOE_{dyn}, was comparable for both species. A higher stiffness influenced positively the UTS, but the magnitude of the effect appears to be larger for yellow birch, as revealed by the higher model-averaged estimate for the latter (0.0058 vs 0.0034). The coefficient of determination of the linear model relating MOE_{dyn} to the UTS was also higher for yellow birch ($R^2 = 0.28$, $p < 0.001$) than for white ash ($R^2 = 0.19$, $p < 0.001$). The modulus of elasticity is currently the main

indicating property considered in machine grading and its relationship with the bending strength is among the most documented. Experiments conducted by Smulski (1991) on small, straight grained white ash, sugar maple and white oak specimens revealed that the dynamic MOE was significantly correlated with the bending strength. He also concluded, as found for tensile strength in this study, that the MOE explained a bigger portion of the bending strength of yellow birch (R^2 = 0.92) than of white ash (R^2 = 0.85). For hardwoods, the MOE has also been found to be correlated to the tensile strength. However, the power of this indicating property would be lower for temperate hardwoods (R^2 = 0.38) than it is for softwoods (R^2 = 0.48) and tropical hardwoods (R^2 = 0.50) (Ravenshorst, 2015).

In structural timber, the introduction of strength reducing defects reduces the portion of the strength variations explained by the MOE, resulting in lower R^2 values. In a study of strength grading of European ash and European maple, Kovryga *et al.* (2019d) found a coefficient of determination of 0.62 between MOE and UTS, while Sarnaghi *et al.* (2017) found a slightly lower R^2 of 0.41 between the two variables for European ash. For their part, Weidenhiller *et al.,* (2019) reported from other studies an R^2 of 0.19 between tensile strength and dynamic MOE for European ash. However, the different span considered in both measurements would explain the weaker correlation. The prediction accuracy for tensile strength would also depend on the quality of the material. Westermayr *et al.* (2018) reported an R^2 value of 0.48 between UTS and MOE for low quality beech, while Ehrhart *et al.* (2016b) reported R^2 of 0.22 with high quality beech.

The dynamic MOE, as measured in this study, appears to be a reliable indicating property that should be included in strength grading procedures for the investigated hardwood species. However, considering the relatively low coefficients of determination, especially for white ash, other indicating properties shall be included to reach a satisfactory prediction accuracy.

Effect of knots on the UTS

Knots represent a reduction of the cross section and cause a discontinuity of the wood fibres. The distortion of the fibres around the knot generates stress concentrations, which would be directly related to the proportion of the cross section occupied by the knot (Ravenshorst, 2015; Ross, 2010). It is also considered that knots have a bigger impact on strength in axial tension than in bending (Green *et al.,* 1999).

In the present study, knots were among the factors affecting the most importantly the UTS. The KAR measured on the specimens was transformed and expressed by the Knot Area Index (KAI), which prevented the model to generate negative UTS values. There was a direct and highly significant influence of KAI on the UTS, with an R^2 value of 0.52 for white ash ($p < 0.001$) and 0.48 for yellow birch ($p < 0.001$). As it can be seen from Figures 2 and 3, increasing KAI values resulted in a higher UTS, because the KAI value of a knot-free specimen equals unity. Results from the current study also indicated that the relative influence of the knots is considerably higher for white ash than it is for yellow birch, as revealed by their respective estimates (42.78 vs 23.20) in the final models.

Results from this study are coherent with findings from other studies on hardwood species which concluded that the relationship between knots and UTS was existent, but variable among species. When relating the biggest knot parameter to the tensile strength, Fruhwald & Schickhofer (2005) found a coefficient of determination of 0.34 for European ash, beech and oak species, while Ehrhart *et al.* (2016a) reported an R^2 of 0.53 between KAR and UTS of European beech. Kovryga *et al.* (2019d) found an R^2 of 0.78

between KAR measured by transverse ultrasound and UTS. The coefficient of determination was only slightly lower (R^2 = 0.74) when considering the KAR measured visually.

The KAR, expressed here by the KAI, shall be included as an indicating property in grading procedures for the investigated species. However, as for the grain deviations, additional test campaigns are required to confirm the applicability of the results to larger cross sections. The impact of the position of the knot should also be assessed properly. In this study, no difference was made between edge and centre knots. It is well known that knots located on the edge of a board affect its bending strength, depending if the knots are positioned on the tension or compression side of a lumber piece. Edge knots are also presumed to have a bigger impact on tensile strength than knots located in the centre of the boards, because their eccentricity would induce additional stresses (Ross, 2010).

Implications for the strength grading of the investigated species

Results from this study have confirmed some of the difficulties related to hardwood strength grading, which are among the main factors limiting their use in structural engineered wood products (Schlotzhauer *et al.,* 2019). Nevertheless, the final models built from multimodel inference were satisfactorily accurate in predicting the UTS of both species, using the selected indicating properties. In Figure 10, the values predicted from the model-averaged estimates are plotted against the values obtained in the tests. The coefficients of determination of the linear models relating the actual and model predicted UTS were respectively 0.82 for white ash and 0.78 for yellow birch. As observed for the relationship between MOE_{dyn} and MOE_{app}, the coefficient of determination was slightly higher for white ash, indicating that the mechanical properties of this species may be easier to predict than they are for yellow birch.

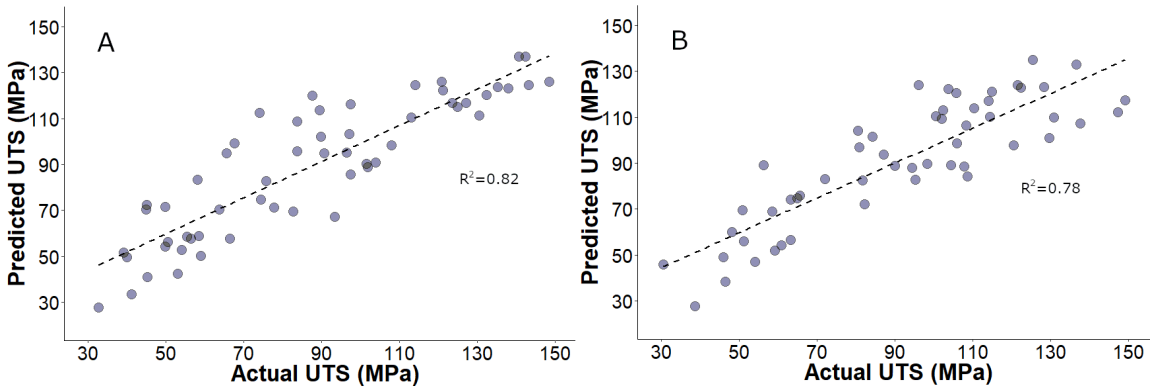

Figure 10. Model-predicted and actual UTS for white ash (A) and yellow birch (B) samples.

The performance of the models developed in this study compares favorably to what can be expected from commercially available machine grading systems for softwoods. With European spruce, Hanhijärvi & Ranta-Maunus (2008) reported R^2 values between 0.55 and 0.61 for the relationship between the UTS and the selected indicating properties, while the most advanced systems could lead to R^2 above 0.70 between the indicating properties and the bending strength (Olsson *et al.,* 2013). The prediction performance of the models from this study is comparable to what was achieved in other studies on hardwood strength grading. Using 3D finite element numerical simulations, Sarnaghi *et al.* (2017) obtained a higher coefficient of determination than in the present study (R^2 = 0.91) for the prediction of the tensile strength of European ash and European maple. For their part, Kovryga *et al.* (2019a)

developed an automated grading system for European ash and European maple, based on the MOE and the detection of knots by X-Ray, resulting in respective coefficients of determination of 0.58 and 0.53.

The species investigated in the current study presented some important differences in their behavior. The KAI and SGD_{max} variables affected more importantly the UTS of white ash, while the effect of MOE_{dyn} on UTS was more pronounced for yellow birch. The effect of an increasing density was also opposite for both species. Because of interrelations between indicating properties and structural differences between hardwood species, it is difficult to conclude on the impact of density on hardwood's strength in general. For instance, the density changes affected more importantly the stiffness of white ash and yellow birch than it did for sugar maple (Kretchmann *et al.,* 2010). Since the stiffness also impacts the bending and tensile strengths, these confounding effects are difficult to distinguish. For its part, Zhang (1997) also found a significant impact of the density on the MOE of hardwood species, but this impact was of larger magnitude for ring-porous species than for diffuse porous species. In the present study, some of the differences between the two species could be attributed to the fact that white ash is a ring-porous species, while yellow birch is a diffuse porous species. However, most of the differences were related to grain irregularities in yellow birch. This characteristic must be investigated to develop an accurate strength grading procedure for this species. A potential solution would be to define the presence of wavy grain as a criterion for exclusion. For instance, Riesco-Muñoz *et al.* (2011) suggested to systematically exclude European oak specimens presenting wavy grain because of their poor mechanical properties. However, before taking such a decision, the incidence of this characteristic must be known, as well as the potential yield if the restriction was to be implemented. Since wavy-grained specimens were also the densest, an abnormally high density could also serve as a criterion for exclusion.

Among the indicating properties included in the final models from the present study, the grain angle was the most challenging to measure. The final models, including all four indicating properties, proved to be more accurate in predicting the UTS than the other candidate models that were more parsimonious. However, for practical reasons, it may be relevant to simplify the grading procedure by removing indicating properties that are too difficult to assess visually. For instance, Ravenshorst *et al.* (2019) suggested that the slope of grain should not be measured but considered indirectly from the MOE and density. Results from the current study allows to confirm that both the maximum local grain deviation and variable SGD_{max} were significantly correlated with the dynamic MOE for yellow birch, with respective p values of 0.037 and 0.029. For white ash however, respective p values of 0.069 and 0.052 were close but slightly over the desired significance level of 0.05. Moreover, candidate model 3 which included MOE_{dyn} and density as explanatory variables, was one of the least performing models for both white ash (AICc = 620.61, $w_i = 0$) and yellow birch (AICc = 505.49, $w_i = 0$). Therefore, more investigations should be conducted on the accuracy of grain deviation measurements and the relationships between the grain deviations and the other indicating properties.

The size effect of the specimens should also be investigated. As discussed earlier, specimens tested in this study had uniform dimensions of 38 x 38 x 1830 mm. The conclusions presented in this study should be verified on larger cross section specimens. It is acknowledged that the probability of occurrence of strength reducing defects increase as the cross section of the specimens increases (Pedersen *et al.,* 2003; Weibull, 1939). For European hardwoods, Schlotzhauer *et al.* (2017) were not able to conclude on the existence of a size effect on the tensile strength of the specimens. However, Kohler (2013) found that the tensile strength of spruce decreased with an increasing specimen's length. Those observations should be validated for white ash and yellow birch.

1.6 Conclusions

1. It is feasible, using a modelling approach, to predict the UTS of white ash and yellow birch lumber from the density, dynamic modulus of elasticity, sinus of the maximum local grain deviation (SGD_{max}) and Knot Area Index (KAI). The final linear models resulted in coefficients of determination (R^2) between the actual and predicted UTS of 0.82 for white ash and 0.78 for yellow birch.

2. The final models revealed important differences between the two species, indicating that it may be appropriate to grade them separately to ensure the most efficient utilization of the resource. The KAI and SGD_{max} variables affected more importantly the UTS of white ash than yellow birch, while the effect of the MOE on the UTS was more pronounced for yellow birch. The effect of an increasing density was also of an opposite direction for both species.

3. Because of interrelations between indicating properties and significant differences in the mechanical behavior of both species, it is difficult to conclude on the impact of the density on the strength of hardwood timber. For instance, some yellow birch specimens with wavy grain had an abnormally high density and failed at a lower tensile strength than expected.

4. This study also brings questionings relative to the measurement of grain deviations on hardwoods. The measurement required considerable time and attention to ensure its accuracy. Other methods to assess the direction of the wood fibers should be investigated to improve the efficiency of the grading process.

Chapitre 2 – *Use of northern hardwoods in glued-laminated timber: a study of bondline shear strength and resistance to moisture.*

2.1 Résumé

Utilisées de façon marginale pour la fabrication de produits d'ingénierie structuraux, les espèces feuillues font aujourd'hui l'objet d'un intérêt grandissant de la part des concepteurs et utilisateurs de bâtiments. Dans le cadre d'un projet visant à évaluer la faisabilité technique d'un bois lamellé-collé composé d'espèces feuillues du nord-est de l'Amérique du Nord, l'objectif de cette étude était d'évaluer la résistance au cisaillement d'assemblages réalisés à partir de blocs de bouleau à papier, de bouleau jaune, de frêne d'Amérique et de chêne blanc assemblés en utilisant un adhésif polyuréthane et un adhésif mélamine-formaldéhyde. Les résultats indiquent qu'une résistance au cisaillement allant de 17,4 à 20,5 MPa à l'état sec peut être atteinte en fonction de l'espèce et de l'adhésif, ce qui se compare avantageusement aux produits composés d'espèces résineuses. La résistance en conditions humides dépendant toutefois fortement de l'adhésif utilisé, la résine mélamine-formaldéhyde offrant les meilleurs résultats.

2.2 Abstract

The growing demand for engineered wood products in the construction sector has resulted in the diversification of the product offer. Used marginally in structural products in North America, northern hardwoods are now attracting a growing interest from industry and policymakers because of their outstanding strength as well as their high availability and distinctive appearance. Currently, there is no standard in Canada governing the use of hardwoods in the manufacturing of glued-laminated timber. As part of a larger project aiming to assemble the basic knowledge that would lead to such standard, the specific objective of this study was to assess the shear strength in dry and wet conditions of assemblies made from different hardwood species and structural adhesives. Results suggest that a mean shear strength as high as 20.5 MPa for white oak, 18.8 MPa for white ash and respectively 18.2 MPa and 17.4 MPa for yellow birch and paper birch can be obtained in dry conditions. The choice of adhesive did not affect the dry shear strength of our specimens, but differences were observed in wet conditions. Specimens bonded with melamine-formaldehyde adhesive had generally the highest wet shear strength and wood failure values. Our results also highlight the important influence of wood density on the percentage of failure that occurs in wood and, to a lesser extent, on shear strength. Further investigations on finger joint strength and full-size bending tests will allow confirming the potential for the investigated species to be used in glued-laminated timber.

2.3 Introduction

The current growing demand for engineered wood products in the construction sector is largely attributable to their outstanding ecological performance. The substitution of materials having a larger ecological footprint, such as steel and concrete, by structural engineered wood products like glued-laminated timber (GLT) have proven to be effective in minimizing the environmental impacts of the building sector (Thormark, 2006). In addition to sustainability-related arguments, building designers also tend to choose wood products because of their aesthetics (Gaston, 2014; Gosselin *et al.*, 2016; Laguarda Mallo & Espinoza, 2015; Markström *et al.*, 2018). Aware of the market opportunities as well as of the lack of high value-added opportunities for some wood species, industry and policymakers from several jurisdictions have recently joined forces to develop products made from non-conventional species, especially with hardwoods. In addition to the possibility of creating products with a noble and distinctive appearance, the high mechanical properties of some hardwood species offer the opportunity to create engineered products of outstanding strength. Several glued-laminated timber products (DIBt, 2009; 2013; ETA-13/0642-02646, 2013) made from various hardwood species

have been approved in the European union, which are largely exceeding the strength of their softwood counterparts. Hardwood glulam products are also available in the United States for over two decades. Work undertaken in this country in the early 1990s with red maple and red oak (Janowiak *et al.*, 1995; Manbeck *et al.*, 1993; Shedlauskas *et al.*, 1996) led to the development of structural products now used in timber bridge design (Manbeck *et al.*, 1996).

As the laminating effect in glued-laminated timber beams stems from the fact that laminations are bonded (Falk & Colling, 1995), the integrity of the cross-section is a key factor in the overall product strength (Dietsch & Tannert, 2015). For hardwood, the bonding quality and resistance to moisture remain issues that cannot be neglected. The thick cell walls and small lumens of hardwood species often lead to a limited penetration of the adhesive, and consequently to weakened bondlines (Frihart & Hunt, 2010; Selbo 1975). Results from the work of Aicher *et al.* (2018), Konnerth *et al.* (2016), Jiang *et al.* (2014), Knorz (2014) and Lehmann (2018) with several European and Tropical hardwoods revealed that bond strength may greatly vary depending on the adhesive system and wood species. The low dimensional stability of hardwoods also induces important stresses on the bondlines when the moisture content fluctuates (Frihart & Hunt, 2010). Several gluing tests (Ammann *et al.*, 2016; Knorz *et al.*, 2015; Konnerth *et al.*, 2016; Vick & Okkonen, 1998) conducted with dense hardwoods in wet conditions or after repeated moisture content variations confirmed the importance of this effect. Considering the inherent difficulties of bonding hardwoods, the achievable bondline strength of a given species and adhesive system must be carefully assessed in order to confirm the relevance of their use in a structural engineered wood product such as glued-laminated timber.

In Canada, no structural GLT products made from hardwood species are currently available on the market. The CSA O122 (2016) standard, governing the manufacturing and quality control testing of structural glued-laminated timber, does not include any provision regarding the use of hardwood species. Moreover, the resource is largely available. Each year in the province of Quebec, half of the annual allowable cut of deciduous trees remains unharvested (Durocher *et al.*, 2019). As part of a project seeking to develop new opportunities for these species and promote the production of high value-added products such as GLT, the objective of this study was to assess the shear strength in dry and wet conditions of assemblies made from different hardwood species and structural adhesives.

2.4 Materials and methods

2.4.1 Materials

White oak (*Quercus alba* Linn.), white ash (*Fraxinus americana* Linn.), yellow birch (*Betula alleghaniensis* Britt.) and paper birch (*Betula papyrifera* Marsh.) were selected as the species to be investigated in this study, according to criteria including their mechanical properties, appearance, desirability on the market and availability. Amongst the four species, white oak is the most valued (Hardwood Publishing Inc. 2020), but also the less widely spread in Canada. At the northern limit of its range, this species is only present in the extreme south of the provinces of Quebec and Ontario (Tardif *et al.*, 2006). However, northern oak species are highly desired in the appearance wood products industry and are therefore largely imported from the United States (Statistics Canada, 2019). White ash range is also limited to the southern part of Canada (Schlesinger, 1990). However, salvage and preemptive harvesting linked to the damages caused by the arrival of the emerald ash borer, an invasive exotic beetle, could make larger volumes available (Herms & McCullough, 2014). Yellow birch is more abundant and, amongst the investigated species,

arrives second in terms of its value on the market (Hardwood Publishing Inc., 2020). Representing almost 11% of the hardwoods allowable annual cut in Quebec (BFEC, 2019), yellow birch is also widely used in appearance wood products. Paper birch is one of the most widely spread hardwood species in Canada, representing 40% of the hardwoods allowable annual cut in the province of Quebec (BFEC, 2019). Amongst the investigated species, the birches are the most available in the province of Quebec, with only 21% of their allowable annual cut harvested each year (Durocher *et al.*, 2019). Some relevant mechanical properties of the investigated species are shown in Table 9.

Table 9. Some mechanical properties of the investigated species according to Jessome (1977).

Species	Density (p_{12})	Modulus of elasticity (MPa)	Modulus of rupture (MPa)
Paper birch	640	12 900	94.8
Yellow birch	670	14 100	106.0
White ash	690	12 800	108.0
White oak	750	15 500	121.0

Lumber was purchased from various local merchants and sawmills. Birch trees were harvested in Duchesnay, near Quebec City, Canada, but the exact provenance of the white oak and white ash lumber is unknown. It was not possible to know the diameter or age of the trees at the time of harvest. White ash and white oak lumber was bought from a different supplier in the two test campaigns, mainly because the density of the material obtained from the first supplier was considerably lower than values stated in literature (Jessome, 1977). For each species, four to six boards with lengths between 1830 and 2430 mm, widths between 102 and 203 mm and a thickness of approximately 25 mm were purchased. Pieces to be used in the experiment were selected in accordance with the quality criteria provided in CSA O112.9 (2010).

All pieces used in this experiment showed a maximum slope of grain of 1 in 15, were free of knots and any other defects. Growth rings were making an angle of less than 45° with the wider face of the pieces. Lumber was conditioned at 20°C and 65% relative humidity until constant mass was reached. Density at equilibrium moisture content (ρ) was measured by the volumetric method described in ASTM D2395 (2017a), but the exact moisture content was not determined. Mean values and standard deviation (SD) are presented in Table 10.

Table 10. Mean density (ρ) values from preliminary trials and main test campaign.

Species	Preliminary trials		Main campaign	
	Mean density ρ (kg/m^3)	SD	Mean density ρ (kg/m^3)	SD
Paper birch	634.6	30.6	613.3	13.7
Yellow birch	664.0	15.6	667.6	30.7
White ash	659.0	85.5	731.8	22.9
White oak	739.4	39.4	766.2	87.4

Two adhesive systems, approved both for interior and exterior exposure in structural applications, were used in this study. A melamine-formaldehyde (MF) and a two-component polyurethane (2C-PUR) adhesives were chosen after preliminary tests conducted with five different adhesive systems. The final selection was made according to the performance of the adhesives in the preliminary tests, their ease of use and their applicability in the context of an industrial production. Two major adhesive manufacturers and the industrial partner involved in the project were also consulted. Names and specifications of the adhesives used in this study are shown in Table 11.

Table 11. Adhesives and gluing parameters.

Adhesive type	Resin	Hardener	Glue spread (g/m^2)	Mixing ratio	Pressure (psi)	Press time (h)
Melamine-Formaldehyde (MF)	Cascomel™ 4720	Wonderbond™ 5025A	390	4:1	150	15
Two-component Polyurethane (2C-PUR)	Purbond® GT20	Purbond® GT205	340	100:15	200	2.3

2.4.2 Block shear tests

In glued-laminated timber quality-control process, block shear tests are widely used to assess the shear strength and wood failure of gluelines. In the United States, AINSI A190.1 (2017), the standard establishing performance requirements for GLT products, relies on the block shear test method described in ASTM D905 (2013). Its counterpart in the European union, EN 14080 (2013), also relies on a block shear test method, described earlier in former standard EN 392 (1995). Block shear test is also the testing method prescribed by international standards ISO 6238 (2018) and ISO 12579 (2007) for determining the glueline shear strength in glued-engineered wood products.

In Canada, block shear tests are an integral part of the quality control testing of glulam as specified in CSA O122 (2016), the standard governing the manufacturing of softwood GLT in Canada. Standard CSA O112.9 (2010) «*evaluation of adhesives for structural wood products (exterior exposure)*» is also largely based on block shear tests. In accordance with this standard, tests must be conducted in dry condition and in wet conditions, after the specimens are subjected to a vacuum-pressure cycle. Wet tests are used because they allow discriminating easily between performing and non-performing adhesives-species combinations in wet conditions.

2.4.2.1 Preparation of test specimens

Lumber from the four species was cut into billets of 21 mm thick, 65 mm wide and 350 mm along the grain. All billets were planed to a final thickness of 19 mm on the same day when they were bonded, using a planer with a rotary cylindrical cutter. Knives were sharpened just before processing the pieces from the preliminary trial. In the main test campaign, it was decided not to do so, to make the surface preparation process more representative of a factory production.

For each combination of wood species and adhesive, the billets were grouped by pairs of similar density and assembled with the growth rings concave from the bondline. Adhesives application rates, assembly times, pressures and pressing times were specified after consulting the technical data sheets and the manufacturers (Table 11). After bonding, assemblies were placed in a conditioning room at 20°C and 65% relative humidity for at least two days before the preparation of test specimens. Five blocks of approximately 50 x 50 mm were cut from each assembly, as specified in standard CSA O112.9 (2010) and ASTM D905 (2013). A 5-mm notch extending to without going beyond the bondline was cut on each side of the test specimens. The bondline area was approximately 2000 mm^2. Figure 11 shows the configuration and measurements of test specimens. Specimens were returned in the conditioning chamber until tested. The exact contact surface was measured to the nearest 0.01 mm immediately before testing. In the main test campaign, thirty test specimens were obtained for each species-adhesive combination while only twenty specimens were prepared for each sample in the preliminary trials.

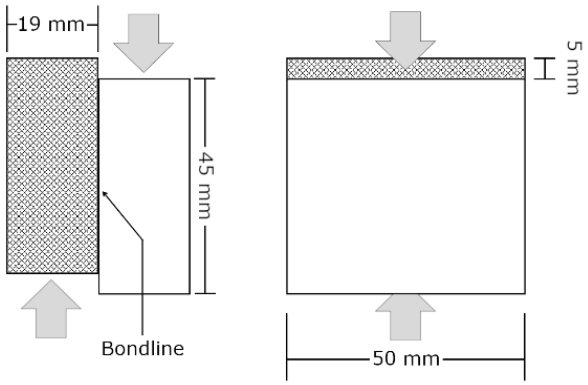

Figure 11. Geometry and measurements of block shear test specimens from CSA O112.9 (2010).

2.4.2.2 Testing procedure

In the main test campaign, fifteen specimens were randomly selected and subjected to a vacuum-pressure cycle as specified in CSA O112.9 (2010) standard before being tested. In the preliminary trials, only five specimens were submitted to the vacuum-pressure cycle. The cycle consisted of submerging specimens in water, holding a vacuum of 75 kPa ± 10 kPa for thirty minutes and then applying a pressure of 540 kPa ± 20 kPa for two hours. These specimens were tested in wet conditions, while the remaining fifteen specimens were tested in dry conditions.

Block shear tests were conducted on an MTS QTest load frame (Eden Prairie, USA) fitted with a 50 kN load cell and a compression shearing tool. The load was applied parallel to the grain direction in a continuous motion rate of 5 mm/minute. The wood failure levels were estimated visually, without the use of a colouring agent since the adhesive could be discriminated from the wood fibres easily in most cases. A magnifying glass was used for certain specimens for which the contrast was not evident. The test apparatus and shearing tool shown in Figure 12 complied with ASTM D905 (2008). The maximum load was used to calculate the bondline shear strength with the following equation:

$$f_v = \frac{F_{max}}{A} \quad \text{in N/mm}^2\text{, where: } f_v\text{: Shear strength (MPa), } F_{max}\text{: Maximum load applied (N) and } A\text{: Bondline area (mm}^2\text{)} \qquad (3)$$

Figure 12. Block shear testing device.

2.4.3 Data analysis

From the shear strength data, the mean value and standard deviation for each species-adhesive combination were calculated. A mixed-effects analysis of variance was conducted to compare means, using adhesive and wood species as fixed effects and the assembly from which specimens were cut out as a random effect. Assumptions were verified and confirmed. When a significant effect of one of the explanatory variables was detected, multiple comparisons were conducted using Tukey's test. Analyses were made using the *lme4* (Bates *et al.*, 2015) and *emmeans* (Lenth *et al.*, 2018) packages in the R software, version 3.5.2 (R Core Team, 2018). Median and mean wood failure percentages were computed for each group as standards rely on either one or the other.

2.5 Results and discussion

2.5.1 Results from the preliminary test campaign

Table 12 shows the results of the preliminary test campaign. The highest dry shear strength was achieved by yellow birch specimens glued with 2C-PUR adhesive and was significantly higher (p = 0.0095) than the lowest strength value, which was observed with white ash specimens bonded with the MF adhesive. Strength of yellow birch specimens was also significantly higher (p = 0.0416) than that of paper birch specimens glued with MF adhesive. The differences between all other species-adhesive combinations were not statistically significant (p > 0.05).

In tests realized after the vacuum-pressure cycle, white oak specimens bonded with MF adhesive and white ash specimens bonded with 2C-PUR adhesive attained an equivalent strength, which corresponded to reductions of respectively 46.5 and 49.7 % from the dry shear strength. The strength of those groups was significantly higher (p = 0.0271, 0.0287) than the strength of white oak specimens bonded with 2C-PUR, for which the loss of strength reached 64.0 %. Tukey's test did not reveal other statistically significant differences. Specimens from the birch species bonded with the MF adhesive attained an intermediate strength, with reductions from the dry strength of 60.7 % for yellow birch and 50.9 % for paper birch, respectively. Yellow birch and paper birch specimens bonded with 2C-PUR attained a slightly higher strength than the MF bonded specimens, but the loss of strength was comparable, with reductions of respectively 57.6 and 52.3 % from the dry test values. White ash specimens bonded with MF achieved strength close to that of the birch samples, with a reduction of 43.0 % from the dry shear strength. In the dry test, the mean level of wood failure ranged from 59 to 98 % while it ranged from 2 to 99 % in the wet test. In both tests, the lowest wood failure percentage was observed on white oak specimens bonded with the 2C-PUR adhesive. In the wet test, wood failure of specimens bonded with 2C-PUR adhesive was always lower than those glued with the MF adhesive.

Table 12. Shear strength (MPa), mean density (kg/m^3), median and mean wood failure percentage from the preliminary trials.

Test	Species	Adhesive	n	Mean density (kg/m^3)	Mean f_v (MPa)	SD	Median WF (%)	Mean WF (%)
Dry	Paper birch	MF	15	615.4	16.9	0.9	80	81
		2C-PUR	15	653.2	19.5	1.7	100	97
	Yellow birch	MF	15	653.6	20.6	1.0	100	89
		2C-PUR	15	675.9	22.4	1.1	90	79
	White ash	MF	15	633.0	15.8	4.2	100	95

	White oak	2C-PUR	15	684.9	19.9	2.4	100	98
		MF	15	756.8	18.7	2.4	90	75
		2C-PUR	15	722.0	17.2	1.4	55	59
Wet	Paper birch	MF	5	626.8	8.3	0.3	90	93
		2C-PUR	5	644.0	9.3	0.4	75	78
	Yellow birch	MF	5	649.8	8.1	0.5	100	99
		2C-PUR	5	673.8	9.5	0.8	25	31
	White ash	MF	5	651.3	9.0	2.6	100	81
		2C-PUR	5	672.3	10.0	0.3	50	62
	White oak	MF	5	774.7	10.0	1.0	85	75
		2C-PUR	5	730.1	6.2	2.5	0	2

Consecutively to these tests, as density of the wood material between subsamples varied substantially and was most of the time lower than values stated in literature (Jessome, 1977), it was decided to better control this parameter in the main test campaign.

2.5.2 Results from the main test campaign

Figure 13 shows the mean dry bondline shear strength from the main test campaign for paper birch, yellow birch, white ash and white oak specimens, glued with MF and 2C-PUR adhesives. White oak specimens glued with MF adhesive exhibited the highest shear strength (20.5 MPa), followed by white oak specimens glued with 2C-PUR adhesive (19.3 MPa). White ash specimens had very similar values regardless of the adhesive used (18.6-18.8 MPa). Paper birch specimens glued with the MF adhesive attained the lowest strength (16.4 MPa). This value was significantly lower than the strength of MF (p = 0.0001) and 2C-PUR (p = 0.0078) bonded white oak specimens as well as that of white ash specimens bonded with the MF adhesive (p = 0.0376). Paper birch and yellow birch specimens bonded with the polyurethane adhesive (17.4-17.5 MPa) also achieved a significantly lower shear strength (p = 0.0057, 0.0059) than white oak specimens bonded with the melamine adhesive. Yellow birch specimens glued with the MF adhesive achieved the higher mean shear strength amongst birch samples, with 18.2 MPa, but this value was not significantly different from any other group (p > 0.05). No other statistically significant differences were unveiled by Tukey's multiple comparison test.

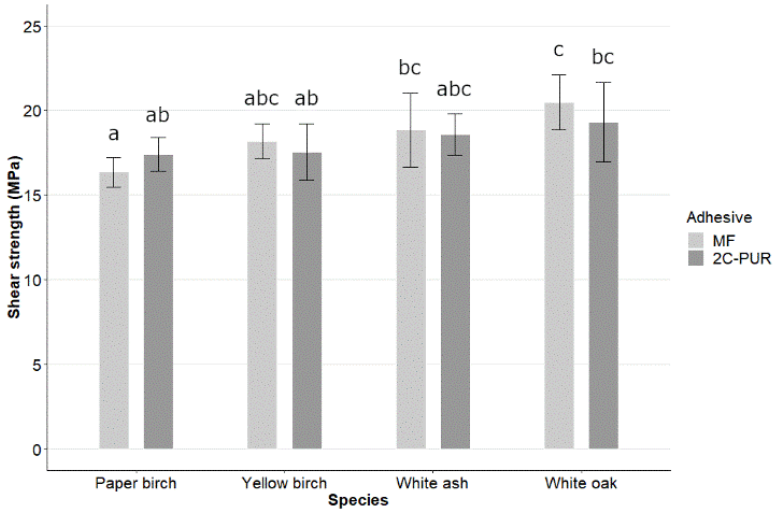

Figure 13. Bondline shear strength (MPa) in dry conditions of paper birch, yellow birch, white oak and white ash specimens bonded with two adhesives.

Figure 14 shows the mean bondline shear strength obtained from the wet test in the main test campaign. The shear strength achieved by the birches specimens was not significantly impacted by the adhesive choice ($p > 0.05$). Paper birch specimens attained a shear strength of 7.6 MPa with MF and 2C-PUR adhesives, corresponding to reductions of respectively 53.7 and 56.3 % compared to strength values from the dry test. Yellow birch specimens achieved slightly higher but not statistically different strengths ($p > 0.05$), with a mean value of 8.6 MPa for specimens glued with MF adhesive, and 7.8 MPa for specimens glued with 2C-PUR adhesive. The corresponding reductions from the dry shear strengths are respectively 52.8 and 55.4 %.

Oak and ash specimens glued with MF adhesive showed significantly higher shear strength than specimens from the same species glued with 2C-PUR adhesive, with values of 10.3 and 10.1 MPa for white oak ($p = 0.0001$) and white ash ($p = 0.0097$), which corresponded to reductions of 49.8 and 46.3 % from the dry shear strength, respectively. The strength of the oak and ash specimens glued with 2C-PUR was substantially lower with values of 7.3 MPa for white oak and 7.8 MPa for white ash, which corresponded to reductions of 62.2 and 58.1 %, respectively, compared to the dry test values. For specimens glued with the 2C-PUR adhesive system, differences between species were not significant according to Tukey's test ($p > 0.05$). However, the strength of white oak and white ash specimens bonded with the MF adhesive was significantly higher than the strength of paper birch specimens bonded with the same adhesive ($p = 0.0009$, 0.003).

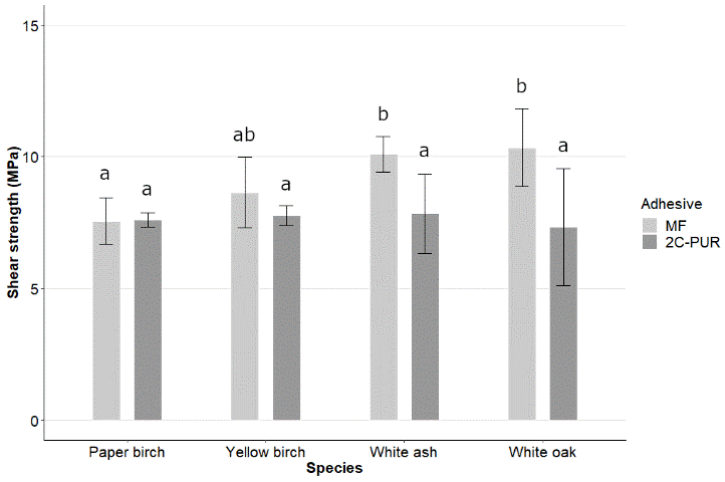

Figure 14. Bondline shear strength (MPa) in wet conditions of white oak and white ash specimens bonded with two adhesives.

Table 13 presents the detailed density values as well as mean and median wood failure percentages for every group from the main test campaign. In dry conditions, the mean wood failure levels of paper birch specimens were the highest amongst all species. Yellow birch specimens showed slightly lower levels, especially those bonded with the 2C-PUR adhesive. White ash and white oak groups followed in order and showed, for a given species, comparable wood failure levels irrespectively of the adhesive used, although slightly better results were achieved for white ash specimens glued with 2C-PUR. Figure 15 presents the wood failure level as a function of the density of the specimens. The strength of the relationship between WF and density increased as the density of the samples was increasing, with R-squared values ranging from 0 for the paper birch sample to 0.61 for the white oak sample.

Compared to wood failure levels in dry conditions, wood failure in wet conditions was lower for all species-adhesive combination, exception made of the paper birch specimens bonded with the polyurethane adhesive and of the white ash specimens bonded with the melamine adhesive. Yellow birch, white oak and white ash specimens bonded with the 2C-PUR adhesive exhibited considerably lower wood failure levels in the wet test than their counterpart bonded with the MF adhesive, but this was not the case with paper birch specimens, for which the opposite trend was observed.

The relation between the bondline shear strength and the density of the specimens was also investigated. The dry shear strength tended to get higher as the density of the specimens increased, but the strength of the relation between the two variables was very low, with R-squared values ranging from 0.003 for yellow birch to 0.3 for white oak. No clear trend was visible when we considered the wet shear strength, with R-squared values under 0.11 for all groups. Those observations are in line with previous work on the bondline shear strength of hardwood GLT elements. Because of the low correlation between wood shear strength and density, it is unlikely to find a strong correlation between the bondline shear strength and the density of the specimens, even when wood failure levels are high (Aicher *et al.*, 2018).

Table 13. Density and wood failure (WF) percentages of species-adhesive groups tested in dry and wet conditions.

Test	Species	Adhesive	n	Mean density (kg/m³)	Density SD	Median WF (%)	Mean WF (%)	WF SD
Dry	Paper birch	MF	15	617.7	13.9	95	94	7.0
		PUR2	15	614.4	11.0	100	95	8.3
	Yellow birch	MF	15	645.7	29.3	100	88	15.7
		PUR2	15	660.1	23.2	80	76	24.9
	White ash	MF	15	736.5	23.5	70	60	34.7
		PUR2	15	729.3	23.0	75	78	17.3
	White oak	MF	15	783.0	91.1	60	56	38.3
		PUR2	15	756.2	87.7	60	54	28.4
Wet	Paper birch	MF	15	609.4	16.1	75	69	22.5
		PUR2	15	611.7	13.1	95	94	10.2
	Yellow birch	MF	15	691.9	30.5	70	53	32.6
		PUR2	15	672.5	20.1	30	32	31.7
	White ash	MF	15	734.2	23.3	80	76	26.8
		PUR2	15	727.4	23.0	15	29	27.0
	White oak	MF	15	777.9	94.0	50	47	32.5
		PUR2	15	747.8	80.0	10	17	19.1

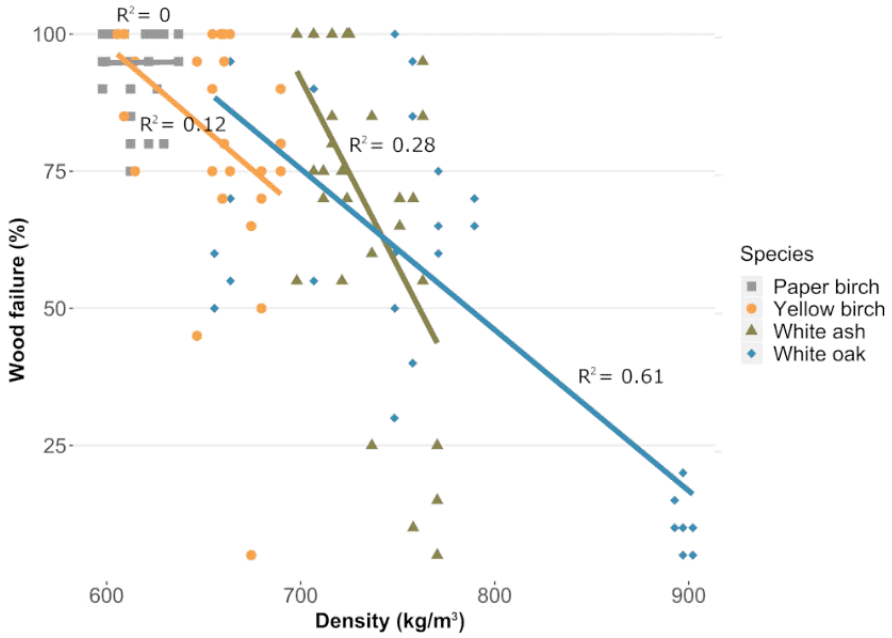

Figure 15. Wood failure level (%) of specimens tested in dry conditions from all investigated species as a function of the density.

2.5.3 Comparison of results with requirements from GLT standards and comparable studies

Various standards issued in different countries comprise shear strength and wood failure requirements for glued-laminated timber products. However, one should be careful when comparing values from a given test campaign with requirements from a standard or with results from another study conducted using a different test method or apparatus. In some cases, the specimen's dimensions, the shearing tool as well as the test procedure may differ, leading likely to discrepancies between the results. Okkonnen & River (1989) have shown that different block shear test methods can lead to discrepancies as high as 60 % in the results. Even when the same test method is used, Steiger *et al.* (2010) shown that the testing device alone can induce significant differences, making the comparison of the results hazardous. For instance, European standard EN 14080 (2013) relies on a slightly different method than that used in this study. Moreover, in EN 14080 (2013), the requirements for shear strength as well as wood failure are exclusively differentiated between softwoods and hardwoods by means of thresholds for the lowest single values.

In Canada, since no standards regulate the use of hardwoods in GLT, threshold values for shear strength and wood failure percentage are only available for softwood GLT in CSA O122 (2016). However, standard CSA O112.9 (2010) provides qualification requirements for adhesives used in products made from hardwoods and softwoods and intended for load-bearing applications in exterior conditions. Requirements for hardwoods are based on tests conducted exclusively on hard maple (*Acer saccharum* Marsh., *Acer nigrum* Michx. f.). The minimum bondline shear strength requirements of 19 MPa in dry conditions and 11 MPa in wet conditions set out in this standard can therefore not be compared directly with our results.

In the United States, standard ANSI A190.1 (2017) defines the bond shear strength requirement as a ratio of the clear wood shear strength. In dry conditions, bonded specimens must reach at least 90 % of the clear wood shear strength value as indicated in the ASTM D2555 (2006) reference tables. In this study, all groups achieved a shear strength considerably higher than this minimum

requirement, which was obtained by multiplying by 0.9 the clear wood shear strength values given in ASTM D2555 (2006). However, the significance of this criterion should be interpreted with caution because values from this standard do not account for variation within species. Strength values provided in ASTM D2555 (2006) were obtained from tests on lumber that is not necessarily representative of the lumber used in this study, especially regarding its provenance or growth conditions. As suggested by River *et al.* (1991) and Aicher *et al.* (2018), comparing the bondline shear strength with a clear wood strength value obtained from the same sample of wood material would be more meaningful. Moreover, the shear strength should always be interpreted in conjunction with the level of wood failure. Shear strength values are a good indicator of the product's strength only if wood failure levels are sufficiently high (Frihart & Hunt, 2010).

Any comparison of our results with reference values from other studies is difficult since very little literature on bonding of northern hardwood species is available. In a study of the impact of block shear test method on shear strength values, Okkonen & River (1989) conducted tests with bonded and clear wood white oak specimens using a phenol-resorcinol-formaldehyde (PRF) resin as adhesive. Amongst others, they used testing method ASTM D905 (2008) and a testing device comparable to that used in this study. White oak lumber had a mean density of 740 kg/m^3 and clear wood specimens achieved a mean shear strength of 18 MPa, while bonded specimens reached 17 MPa. In addition to the difference in the adhesive used, the higher mean density of the white oak used in our study may explain why our bonded specimens reached higher strength than the clear wood specimens from Okkonen & River (1989). Unlike what we observed in our tests, almost all failures occurred entirely at the bondline in the case of their glued specimens. Our review of the literature did not lead to any results on the bondline shear strength of North American white ash. Even if shear strength values cannot be compared directly because of the different testing procedures and apparatus, experiments conducted in Europe with species related to those investigated in this study, namely common ash (*Fraxinus excelsior* L.), common oak (*Quercus robur* L.) and sessile oak (*Quercus petraea* (Matt.) Liebl.) provide the best available basis for comparison. In that way, findings of the current study are not consistent with those of Aicher *et al.* (2018). In block shear tests conducted on specimens originating from industrially manufactured hardwood glued-laminated timber beams, common ash attained higher wood and bondline shear strengths than common/sessile oak with density of 695 kg/m^3 and 752 kg/m^3, respectively. No reference to shear strength of glued assemblies made from the investigated or related birch species was found in literature.

However, our results are consistent with the mechanical properties of the investigated species, as white oak is known to be slightly stronger in longitudinal shear than white ash, followed in decreasing order by yellow and paper birch (Jessome, 1977). It must be noted, however, that mechanical properties from the work of Jessome (1977) were obtained from block shear tests conducted following standard ASTM D143, which involves a different specimen geometry and test apparatus than that used in this study. In wet conditions, shear strength values were considerably lower. However, all species-adhesive combinations did not suffer an equivalent loss in strength. The observed loss ranged from 46.3 to 62.2 % depending on the adhesive and species. In comparison, the deemed-acceptable reduction in median shear strength for hard maple bonded specimens in CSA O112.9 (2010), when submitted to the vacuum-pressure cycle, is 42.1 % (i.e. 19 MPa to 11 MPa). The substantial loss of strength observed in our experiment can be explained partially by the occurrence of bondline failures during the wet test. Indeed, very low wood failure percentages were observed on specimens with the higher density, mainly within the yellow birch, white ash and white oak samples bonded with 2C-PUR. The wet shear strength values were therefore lower than what could have been expected if failure has occurred mainly in the wood. Furthermore, the wet shear strength that was reached by paper birch specimens was similar to that

of the yellow birch specimens bonded with the 2C-PUR adhesive. The lower wood failure level observed for the latter and the difference in density between the two species are the most likely factors explaining this result.

Wood failure percentage provides much information as it allows knowing if bonding took full advantage of the wood material's strength. In the dry test, wood failure percentages suggest that the maximum strength potential of the wood material was not always reached, particularly in the case of white ash and white oak specimens. With respect to wood failure requirements, ANSI A190.1 (2017) defines a specific category for dense hardwoods and different thresholds for Initial Type Testing (ITT) and Factory Production Control (FPC). Mean wood failure percentages in dry conditions must be at least 60 % for ITT and 50 % for FPC. Every combination of adhesive and wood species tested in the main test campaign reached the mean wood failure requirement in FPC for dense hardwoods from AINSI A190.1 (2017). For ITT however, white oak specimens bonded with MF and 2C-PUR adhesives did not reach the required mean wood failure percentage. Although requirements from CSA O112.9 (2010) apply to different species, our results in dry conditions are close to the minimum median wood failure requirement of 60 % set out in this standard, but only paper birch specimens glued with 2C-PUR adhesive and white ash specimens glued with MF adhesive fulfilled the threshold value of 80 % for the test in wet conditions. Since CSA O112.9 (2010) expects higher wood failure percentage in the wet test than in the dry test, our results are not entirely satisfactory. Only the white ash specimens bonded with the MF adhesive have met this criterion.

In comparable studies, Aicher *et al.* (2018) obtained higher mean wood failure percentages, with 89 % for the common/sessile oak sample (752 kg/m^3) bonded with melamine-urea-formaldehyde (MUF) and 79 % for the common ash sample (695 kg/m^3) bonded with a PRF adhesive. In block shear tests on bonded common ash specimens (661 kg/m^3), Knorz *et al.* (2014) obtained a mean wood failure percentage of 63 % with a one-component polyurethane (1C-PUR) adhesive and 99 % with a MUF adhesive. In tensile shear tests with common ash (638 kg/m^3) specimens bonded with MUF, PRF, 1C-PUR and emulsion polymer isocyanate adhesives, Jiang *et al.* (2014) obtained mean wood failure values of at least 70 % with all four adhesives tested. No reference to wood failure levels from shear strength tests on glued assemblies of paper birch or yellow birch was found in the literature. The differences between our results and comparable studies might be due to the adhesive system and gluing parameters, but also to the density of the wood material.

2.5.4 Impact of wood density on bondline strength and wood failure

Differences observed in wood failure between the preliminary trials, the main test campaign and comparable studies tend to confirm the impact of wood density on the adhesive performance. For both white oak and white ash, the species showing the highest specific gravity, specimens made of higher density material showed most of the time lower wood failure percentage. In the first series of tests, average density of white oak and white ash were lower. Some ash specimens had density as low as 522 kg/m^3, which is far from the mean value of 690 kg/m^3 stated in literature (Jessome, 1977). Therefore, it was decided to increase the minimal density of the white oak and white ash sample to obtain more representative results. As a result, dry shear strengths for these species were higher in the main test campaign than in preliminary trials, even if for three of the four species-adhesive combinations, mean wood failure was considerably lower. The significant increase in the white ash sample density resulted in a 30 % reduction of the mean wood failure percentage.

When comparing all four species in the main test campaign, the density of the wood material seemed to have a direct influence on the wood failure levels observed in the dry test, although other anatomical and chemical factors could also be responsible for the differences. Paper birch and yellow birch specimens achieved, with only a few exceptions, consistently high wood failure levels. Above a certain density value located near that of our white ash sample, the adhesive performance in dry conditions appears to be affected by an increase in the density of the adherent. Very low wood failure levels were observed on some of the ash specimens with the highest density (> 750 kg/m^3). The same effect is visible within the white oak sample, where all the specimens that showed an extremely high density (i.e. 897-902 kg/m^3) achieved a very low wood failure level. If those specimens were excluded from the analysis, mean and median wood failure percentages would have been considerably higher. These observations are in line with the threshold zone proposed by Frihart & Hunt (2010) of 700 to 800 kg/m^3. In the wet test, the same general trend could be observed, especially for specimens bonded with the polyurethane adhesive.

These results show the interactions occurring between material density, shear strength and wood failure. To facilitate the use of hardwood species in structural glued-engineered wood products, it is important to consider the hardwoods intraspecies variability in the establishment of standardized shear strength and wood failure requirements. Grading requirements for lumber to be used in the manufacture of this type of product might also include provisions related to density. Nevertheless, if bonded satisfactorily, denser wood offers the possibility to increase the strength of the product.

2.5.5 Impact of adhesive on wet conditions resistance

In dry conditions, no statistically significant differences between adhesive performance were detected for a given species. In wet conditions, wood failure percentage was particularly low for yellow birch, white ash and white oak specimens bonded with the 2C-PUR adhesive. The loss of strength induced by the vacuum-pressure cycle was also greater for specimens of these species bonded with the same adhesive.

However, in the main test campaign, paper birch specimens showed higher wood failure levels when bonded with the 2C-PUR adhesive rather than with the MF adhesive. This inconsistent result coincides with the fact that paper birch is the least dense amongst all tested species. The magnitude of the stress induced on the gluelines by wood swelling is thought to increase proportionally to the density of the material (Selbo, 1975; River *et al.*, 1991; Frihart & Hunt, 2010). Therefore, because of their low density compared to the specimens from the other species, the stress induced on the glueline of the paper birch specimens glued with the 2C-PUR adhesive may have been contained under a certain threshold that is within the limits of the 2C-PUR performance. This performance threshold is also likely to explain why despite showing similar wood failure levels in the dry test, yellow birch and paper birch performed differently in the wet test.

The link between density and shrinkage properties also provides an explanation regarding the discrepancies between the results of the preliminary trials and main test campaign. In the preliminary trials, paper birch specimens bonded with 2C-PUR showed lower wood failure levels than the specimens bonded with the MF adhesive. In addition to the limited number of specimens submitted to the wet test in the preliminary trials, the difference in the mean density of the two paper birch subsamples can be identified as a cause. The mean density of the paper birch specimens bonded with the polyurethane adhesive was higher than the mean density of the specimens glued with the MF adhesive (644.0 vs 626.8 kg/m^3). The lower wood failure levels observed in the preliminary trials for the paper birch specimens bonded with the polyurethane adhesive are therefore more likely to be attributable

to the limited sample size and different mean density rather than to the impact of the adhesive system used. The shrinkage properties of a given wood species is therefore a determining factor for the bondline shear strength and wood failure levels achieved by specimens submitted to moisture content variations.

Thus, our findings are globally consistent with studies conducted in the past years on moisture resistance of several adhesive systems used to bond hardwood species. Work from Ammann *et al.* (2016) with common ash of a density of approximately 650 kg/m^3 glued with six adhesive systems revealed that the two-component polyurethane adhesive was one of the least efficient in wet tensile shear tests and in resistance to delamination tests. In studies of structural bonding in common ash, Knorz *et al.* (2015, 2014) stated that polyurethane adhesives showed the highest delamination rates amongst multiple adhesive systems when submitted to repeated moisture content variations. In these studies, melamine-urea-formaldehyde (MUF) adhesives, which are recognized to have a lower moisture resistance than MF adhesives (Frihart & Hunt, 2010), still offered a higher performance than polyurethane based adhesives. Delamination and shear strength tests conducted on GLT elements made from a poplar species from Portugal also led to similar conclusions. Despite involving a species with a density considerably lower (442 – 492.8 kg/m^3) than that of the species investigated in our study, Martins *et al.* (2017) concluded that the polyurethane-based adhesive showed less resistance to moisture than the melamine-based adhesive. Melamine-formaldehyde adhesive therefore appears to be suitable for structural products exposed to weather. However, results in wet conditions with white oak and MF might have been better in regard to the results obtained with white ash. In the main test campaign, the fact that knives were not perfectly sharpened before planing may have limited adhesive penetration, as shown by Knorz *et al.* (2015). This effect could have been added to that of density, explaining the low wood failure percentage observed on some specimens. However, these conditions are more realistic in the context of an industrial production, since it is unlikely that knives would be sharpened as frequently as they were in our preliminary test campaign.

2.6 Conclusion

In this study, white oak, white ash, yellow birch and paper birch specimens bonded with MF and 2C-PUR adhesives were submitted to block shear tests in dry and wet conditions. Results suggest that a mean shear strength as high as 20.5 MPa for white oak, 18.8 MPa for white ash and respectively 18.2 MPa and 17.4 MPa for yellow birch and white birch can be obtained in dry conditions. For a given species, results from the dry test were similar, regardless of the adhesive. The loss of strength induced by the moisture and mainly by the differential wood swelling caused by the vacuum-pressure cycle was considerable, especially for high-density specimens bonded with 2C-PUR adhesive. Therefore, the MF adhesive appears more suitable for such products exposed to weather. However, since the products investigated in this study are more likely to be used in a weather-protected environment, 2C-PUR adhesive may also be adequate.

The results also highlight the major influence of wood density on wood failure percentage and, to a lesser extent, on shear strength. In both test conditions, several bondline failures occurred in specimens of higher density. In this sense, it is important to account for extreme density values in the selection of lumber destined to the manufacture of structural glued engineered wood products made from hardwoods. A microscopic examination of the gluelines could be carried out to better understand the impact of material density and specific anatomical features on the adhesive penetration.

Additional tests are required to confirm the potential use of the investigated species and adhesives in commercial glued-laminated timber production. For example, previous work with related species in Europe has pointed out the challenge that represents the fulfilment of delamination tests requirements. Such tests will be performed with the species and adhesives investigated in this study. Also in line with the aim of this project to assess the potential use of the investigated species in glued-laminated timber production, the next experiments will focus on determining the finger-joint strength and the bending strength of full-size beams.

Chapitre 3 – *Glued-laminated timber from northern hardwoods: effect of finger-joint profile on lamellae tensile strength and study of the bending properties from full-size beams.*

3.1 Résumé

Les propriétés mécaniques d'un élément en bois lamellé-collé dépendent de la qualité de la matière première, de la qualité du collage entre les lamelles et également de la résistance des joints à entures multiples. L'aboutage structural des espèces feuillues canadiennes a été assez peu étudié et les travaux réalisés se concentraient uniquement sur le type de joint traditionnellement utilisé dans l'industrie des produits de bois résineux. Pourtant, les paramètres géométriques du joint peuvent avoir un impact majeur sur sa résistance. L'objectif de ce chapitre était d'évaluer la résistance en traction de lamelles de frêne d'Amérique et de bouleau jaune aboutées selon deux profils de joints qui ne sont actuellement pas utilisés dans les produits structuraux au Canada. Les résultats confirment l'impact des paramètres géométriques sur la résistance et ont permis de sélectionner le profil le plus performant. Des poutres pleine grandeur ont été fabriquées à partir des connaissances acquises, puis soumises à des essais de résistance en flexion afin d'en déterminer les propriétés mécaniques.

3.2 Abstract

The use of hardwood species in glued-laminated timber is the subject of a growing interest because of their availability, mechanical properties and distinctive appearance. Previous work on bonding and structural grading of northern hardwoods have shown that white ash, yellow birch and white oak are promising species for the manufacture of a Canadian hardwood glulam. The objective of this study was to investigate the impact of the finger joint profile on the tensile strength of jointed hardwood lamellae and to assess the bending properties of full-size beams made from the investigated species. Tensile tests conducted on finger-jointed lamellae confirmed the possibility to achieve characteristic tensile strengths up to 36.4 MPa for white ash, 33.6 MPa for yellow birch and 35.8 MPa for white oak. White ash and yellow birch full-size beams submitted to bending tests achieved bending strengths of respectively 47.0 and 41.6 MPa, while a serial failure probability model have been proved adequate to predict the characteristic bending strength from the finger joints Weibull distribution. The investigated species appear promising for the manufacture of glued-laminated timber, but further research work should be conducted on hardwood finger-jointing to optimize the machining and gluing parameters and increase the joint efficiency.

3.3 Introduction

Glued-laminated timber (glulam) is among the structural engineered wood products showing the strongest growth. Although it is predominantly made from softwood species, the last decade has seen a growing interest towards the use of hardwood species. In the United States, AITC 119-96: *Standard specifications for structural glued-laminated timber of hardwood species* (1996) allows the manufacture of glulam from various North American hardwood species up to an allowable bending stress of 30.6 MPa. In Europe, many technical approvals have been issued for such products made from beech (*Fagus sylvatica* L.), oak (*Quercus sp.*) and chestnut (*Castanea sativa* Mill.) (ETA-13/0646, 2013; ETA-13/0642, 2013; DIBt, 2013; 2012; 2009), with characteristic bending strengths of up to 33 MPa for oak and 48 MPa for beech. In addition to their high mechanical properties, broadleaved species are widely available and using their timber in engineered wood products provides great opportunities for some undervalued species (Ross & Erickson, 2020; Aicher & Stapf, 2014; Franke *et al.*, 2014). Moreover, since one of the key drivers behind the prescription

of wood as a primary structural material by building designers in the aesthetics of the products (Markström *et al.*, 2018; Gosselin *et al.*, 2016; Laguarda Mallo & Espinoza, 2015; Gaston, 2014), the noble and distinctive appearance of hardwood species could foster their use in structural engineered wood products.

Currently, glulam products made from hardwood species have yet to be manufactured in Canada and the idea has received little scientific attention. However, with only about 45% of the country's allowable annual cut (AAC) for hardwoods harvested each year, the resource is undoubtedly available (Durocher *et al.*, 2019; Natural Resources Canada, 2018). To this end, white ash (*Fraxinus americana* L.), yellow birch (*Betula alleghaniensis* Britt.) and white oak (*Quercus alba* L.) appear to offer a promising combination of mechanical properties, appearance and availability. As white ash is the most common ash species in Canada, its lumber is increasingly available as a consequence of mortality caused by the emerald ash borer (Herms & McCullough, 2014). Yellow birch is highly valued by consumers and represents 11% of the hardwoods AAC in the province of Quebec (BFEC, 2019), which accounts for about half of the overall AAC of hardwoods in Canada. Despite not being widely distributed in Canada, white oak highly desired by consumers and is commonly imported by Canadian mills from the United States (Statistics Canada, 2019).

Introducing new species in the manufacture of glued-laminated timber induces uncertainty and requires extensive study and testing. The quality of the laminations, the strength of the finger joints and the quality of the gluelines, are the main factors affecting the strength of a glued-laminated timber element (Dietsch & Tannert, 2015; Brandner & Schickhofer, 2008). Previous work by Morin-Bernard *et al.* (2020a) on white ash, yellow birch and white oak have shown that acceptable wood failure levels can be achieved in bondline shear strength tests with commercially available structural adhesives. However, the strength of the finger joints still appears to be the most limiting factor for the production of hardwood glulam, as confirmed by studies conducted in Europe with oak and beech glulam (Tran *et al.*, 2016; Tran *et al.*, 2014a; Aicher & Stapf, 2014).

In Canada, only a few authors (Dagenais & Salenikovich, 2008; Chui & Delahunty, 2005; Verreault, 2000) have investigated the finger-jointing performance of northern hardwoods species. These studies only involved the finger joint profile typically used in the Canadian softwood products industry, which may not be the most appropriate for the end jointing of northern hardwoods. Preliminary finger-jointing trials with dense hardwoods conducted by a glulam manufacturer involved in this project have caused tear out of the boards and breakage of the cutting tools. Structural finger-jointing with other profiles is allowed by glulam standard EN 14080 [28] and has been studied extensively with various European hardwood species (Franke *et al.*, 2014; Tran *et al.*, 2014b; Aicher *et al.*, 2001). The impact of the geometrical parameters of the finger joint on its performance is widely recognized (Franke *et al.*, 2014; Ayarkwa *et al.*, 2000; Castro & Paganini, 1997; Jokerst, 1981; Selbo, 1963) and must be assessed in light of the particular characteristics of our domestic hardwood species. The objectives of this study were to 1) investigate the impact of the finger joint profile on the tensile strength of jointed hardwood lamellae and 2) assess the bending properties of full-size beams made from the investigated species. This work is part of a broader project aiming to support the production of high value-added construction products from northern Canadian hardwood species.

3.4 Materials and method

3.4.1. Finger-jointing test campaign

3.4.1.1. Investigated species, finger-joint profiles and adhesives

The finger-jointing trials were conducted with three hardwood species, namely white ash, yellow birch and white oak. Tests were also conducted on softwoods species to provide a basis for comparison and validate the adequateness of the manufacturing process. Softwood species comprised black spruce (*Picea mariana* (Mill.) B.S.P), red spruce (*Picea rubens* Sarg.) and white spruce (*Picea glauca* (Moench) Voss), which are used indiscriminately in dimension lumber and in engineered wood products in Canada. A review of finger-jointing studies involving related hardwood species in Europe and discussions with a tool manufacturing company led us to select, in addition to the profile commonly used in Canada, two additional joint profiles to be included in this study. Fig. 16 presents the geometrical parameters of the selected profiles, which will be referred to as '15 mm', '22 mm' and '28 mm' in the remainder of the text. The effective glue joint area (*2l/p*) corresponds to the shear area parallel to the grain of the joint as defined by Selbo (1963) and Jokerst (1980). Considering the damage caused to the hardwood boards and jointing machine parts during preliminary trials with the 28 mm profile, the latter was only included in the softwoods test program.

Joint profile	15 mm	22 mm	28 mm
Finger length *l* (mm)	15.00	22.22	28.27
Pitch *p* (mm)	3.80	5.67	6.70
Tip thickness *t* (mm)	0.60	0.88	0.76
Effective glue joint area *(2l/p)*	3.95	3.92	4.22
Angle of fingers Θ (°)	4.57	5.12	5.24

Figure 16. Geometrical parameters of the finger-joint profiles investigated in this study.

Two structural adhesives were selected for the finger-jointing of the hardwood lamellae, namely the LOCTITE PURBOND® GT20/GT205 two-component polyurethane adhesive system (PUR) and the Cascomel™ 4720 with Wonderbond™ Hardener 5025A melamine formaldehyde resin (MF). These structural adhesives are approved for use in softwood glulam in North America. Softwood lamellae were jointed using only the PUR adhesive on an industrial jointing line.

3.4.1.2. Preparation *of the finger-jointed lamellae*

Hardwood lumber was purchased from a local supplier near Quebec City, Canada. Sixty white ash, sixty-four yellow birch and sixteen white oak boards were cut and planed to lamellae with cross-sectional dimensions of 39 x 39 mm and a length varying between 900 to 1100 mm. All lamellae were free of knots and of any local grain deviation superior to 15 degrees. The processed lamellae were stored in a conditioning chamber at a temperature of 20°C and 65% relative humidity until they reached a constant mass. The density of each lamella was determined in accordance with method A from ASTM D2395 (2017a). Lamellae were ordered according to their density and distributed in subsamples having a similar mean density and standard deviation. Softwood boards from the SPF species group, graded to MSR strength class 2100 Fb-1.8E and fulfilling the requirements of laminating stock

grade B in accordance with CSA O122 (2016), were provided by an industrial partner of the project. The grading criteria included a general slope of grain limitation of 1:16 and a minimum modulus of elasticity requirement of 11 000 MPa. Density was measured after testing.

Finger joints were manufactured under industrial conditions at the facility of the glulam manufacturer involved in the project, with the exception that the adhesives were applied manually. Boards were jointed continuously, at a feeding speed of 14.9 m/min for softwood lamellae and 12.5 m/min for hardwoods. An end pressure of 7.72 and 12.35 MPa was applied to the softwood and hardwood lamellae, respectively. Final specimens with a 1830 mm length and a joint positioned in the middle were cut out of the continuous lamellae, planed to a final cross-section of 38 x 38 mm, and stored back in the conditioning chamber until they reached a constant mass. Between 11 and 25 unjointed lamellae per species, satisfying the same knot and grain deviation limitations as the finger-jointed specimens were extracted from the dataset and analysed to determine the UTS of the three species. The unjointed lamellae had the same dimensions (38 x 38 x 1830 mm), originated from the same batch of timber and were tested following the same test procedure as the finger-jointed lamellae. The distribution of test specimens in the different sample groups is presented in Table 14.

Table 14. Experimental design and density of the sample groups included in the present study.

Species	Joint profile	Adhesive	Density (kg/m³)		Number of specimens
			Mean	Standard deviation	
White ash	15 mm	MF	711.0	50.6	33
		PUR	713.2	52.8	34
	22 mm	MF	712.5	50.9	33
		PUR	709.2	51.0	33
	Unjointed		719.5	42.0	25
Yellow birch	15 mm	MF	717.9	37.1	32
		PUR	717.4	41.4	33
	22 mm	MF	719.2	37.0	32
		PUR	716.7	37.5	32
	Unjointed		706.2	49.5	22
White oak	15 mm	MF	783.3	55.2	12
		PUR	777.0	65.4	12
	22 mm	MF	779.4	55.4	12
		PUR	782.6	63.4	12
	Unjointed		809.3	52.6	11
Softwoods	15 mm	PUR	504.0	26.5	43
	22 mm	PUR	494.8	20.7	42
	28 mm	PUR	491.5	29.5	41

The finger-jointed lamellae were tested using a hydraulic tension testing machine conforming to the requirements of ASTM D7469 (2016a) for determination of axial strength in tension. Tensile tests were preferred to bending tests because they allow for a better consideration of the negative influence of the slope of grain on the UTS (Lehmann *et al.*, 2018). Specimens were held in place by grips designed to minimize slip, resulting in a clear test span of 610 mm, with a single finger joint positioned approximately in the center. The failure of each specimen was classified according to the six modes described in ASTM D7469 (2016a). Specimens that failed in mode 6 (i.e. failure away from the joint) or inside the grips were rejected. The moisture content at the time of testing was determined from samples collected on from both sides of the joint after failure. For softwood lamellae, these samples were

also used to determine the density of the specimens. Since many hardwood lamellae exhibited bondline failures, UTS values were not adjusted to a uniform moisture content.

3.4.1.3. Analysis of finger-jointing results

Data from tests on hardwood species were used to build generalized linear models relating the measured UTS with the species, adhesive and joint profile, as well as the interactions between variables. An analysis of variance was conducted to identify the variables significantly impacting the UTS. In the presence of a significant effect of one of the investigated variables or interactions, Tukey's test was used to identify the significant differences between each factor levels. A generalized linear model was also built with data from the softwood samples with the joint profile as the only explanatory variable included in the model. An analysis of variance was conducted to conclude if significant differences existed among sample groups. A third analysis including data from both hardwood and softwood samples was performed in order to assess the differences of UTS between species-adhesive-joint profile combinations. In the presence of a significant effect, multiple comparisons using Tukey's test were performed using *emmeans* R package (Length *et al.*, 2018) to identify the significant differences between hardwoods and softwoods groups. The 5th percentile of UTS values was determined for each jointed and unjointed sample group, assuming a two-parameter Weibull distribution. The distribution fitting was performed using the *fitdistrplus* R package (Delignette-Muller & Dutang, 2015). Considering the limited sample size, the minimum test value is also reported in the results, as recommended in ASTM D2915 (2017b) for representing the 5th percentile value using a nonparametric analysis with a 75% confidence level.

A three-factor logistic regression model was built from the hardwood samples data to analyse the impact of the investigated variables on the failure modes. Specimens that failed in modes 1 or 2 were grouped together (i.e. failure mostly along the bondline surfaces) while another group comprised specimens that failed in modes 3, 4 or 5 (i.e. failure mostly along the joint profile to failure beginning at the joint). A Firth correction was applied to account for the bias caused by a quasi-complete separation of the data, using *brglm* R package (Kosmidis, 2019). For the softwood sample groups, a one-factor multinomial regression with a Firth correction was used to analyse the impact of the joint profile on the failure mode. Specimens that failed in modes 1, 2 and 3 were grouped and compared to specimens that failed in mode 4 and specimens that failed in mode 5.

3.4.2. Manufacture and testing of full-scale beams

Two yellow birch and one white ash beams with finished dimensions of 130 x 243 x 5500 mm were manufactured under fully industrial conditions from the boards remaining after the finger-jointing trials, using the 15 mm joint profile. The two-component polyurethane adhesive system was chosen because this product was already being used by the manufacturer involved in the project, in addition to its ease of use and shorter curing time. Gluing parameters for both finger-jointing and face-gluing are shown in Table 15.

Table 15. Adhesive and gluing parameters for the manufacture of the full-size beams.

Adhesive type	Resin	Hardener	Glue spread – face bonding (g/m^2)	Mixing ratio	Face bonding pressure (MPa)	Press time (h)	End-jointing pressure (MPa)
Two-component Polyurethane (PUR)	Purbond® GT20	Purbond® GT205	340	100:15	1.42	2.3	12.35

Combined glued-laminated timber lay-ups with seven laminations were designed, requiring the boards to be graded to three different classes. A schematic representation of the cross-section of the manufactured beams with the three different stiffness zones, as well as the stress distribution within the cross-section is shown in Fig. 17. Capital letters represent the grade of the lamellae used in the lamination zone, where $MOE_A > MOE_B > MOE_C$.

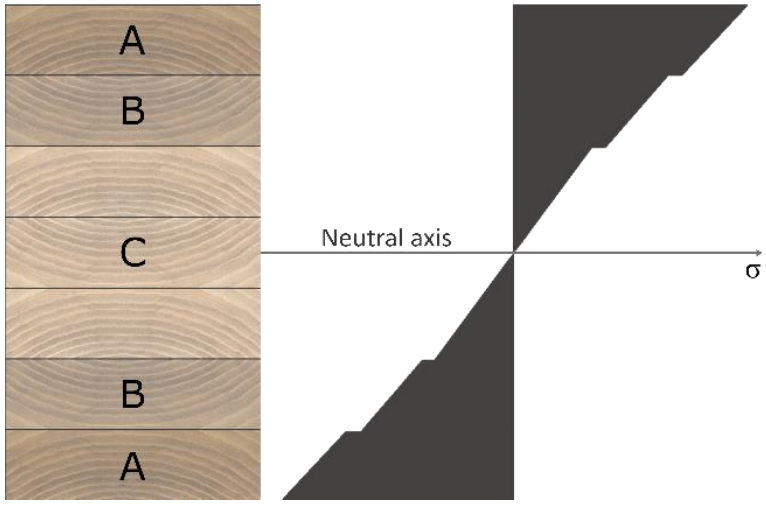

Figure 17. Glued-laminated timber beams lay-up configuration and stress distribution within the cross-section.

3.4.2.1. Grading of the lamellae

Thirty-four white ash boards and fifty-four yellow birch boards with lengths ranging between 500 and 2400 mm were processed to lamellae with a uniform width of 140 mm and a thickness of 38 mm. Measurement of visual defects and nondestructive testing was realized as described in Morin-Bernard *et al.* (2020b). The dynamic modulus of elasticity (MOE_{dyn}) and density were measured on each board, as well as the knot area ratio (KAR) and maximum local grain deviation on the worst face. Splits, shakes, insect holes and decay were removed as well as edge knots, to ensure the visual quality of the beams. Twenty boards per species for which the MOE_{dyn} was known were submitted to a non-destructive bending test using a third-point loading configuration and a span to depth ratio of 1 in 60, in conformity with ASTM D198 (2015).The apparent modulus of elasticity (MOE_{app}) of each lamella was derived from the MOE_{dyn}, using coefficients of linear models established for each species and shown in Table 16.

Table 16. Equations and R^2 values of the generalized linear models linking the apparent and dynamic MOEs (MPa).

Species	Equation	R^2 value
White ash	$MOE_{app} = 0.9138 * MOE_{dyn} – 332.0998$	0.98
Yellow birch	$MOE_{app} = 0.9492 * MOE_{dyn} – 3.3424$	0.95

Since the standard grading rules for Canadian dimension lumber (NLGA, 2017) do not comprise provisions specific to structural hardwoods, custom grades were established for this study. With the aim of using most of the available material, the threshold value for each grading parameter was set in order to meet the expected proportion of the respective grade in the cross-section. Three grades comprising different visual defect limitations as well as minimum stiffness requirements were formed as shown in Table 17. Considering the high quality of the available boards, knots were allowed only in grade C i.e. the lowest quality grade. In addition to the criteria presented in Table 4, a minimum distance of 1800 mm between finger joints was set for grade A lamellae, in accordance with provisions from CSA O122 (2016) for spacing of end-joints located within the outer 1/8 of the total depth on the tension sides.

Grade A lamellae were also manufactured in order to avoid finger joints positioned in the central portion of the beam. Minimum spacings between finger joints of 1100 mm and 500 mm for grades B and C lamellae, respectively, were established considering the length of the available lamellae after the grading process.

Table 17. Relevant properties and visual defects limitations for the three custom lamination grades.

Species	Grade	Nb. of lamellae	Density (kg/m³)			Apparent MOE in third-point bending (MPa)			Maximum local grain deviation (°)	Maximum Knot Area Ratio (%)	Moisture content (%)
			Mean	Minimum	SD	Mean	Minimum	SD			
White ash	A	6	746.3	697.0	30.4	16 593.9	15 425.4	842.4	12.8	0.0	10.7
	B	8	714.9	664.8	37.8	15 234.7	13 621.1	1 083.6	10.6	0.0	10.4
	C	14	689.9	634.8	35.8	13 131.1	10 711.6	1 246.4	26.7	15.0	10.6
Yellow birch	A	14	732.3	681.9	32.3	18 496.7	17 624.7	635.0	14.2	0.0	11.3
	B	18	745.0	664.9	40.7	17 497.2	15 964.8	825.4	15.7	0.0	11.4
	C	30	731.2	590.4	50.8	15 157.3	9 740.1	2 614.3	30.0	17.1	11.4

3.4.2.2. Assessment of the mechanical properties by testing of full-size beams

The manufactured beams were submitted to destructive bending tests using a third-point loading configuration conforming with ASTM D198 (2015). The support span was 5100 mm for a span to depth ratio of 1 to 21, while the loading span was 1700 mm. The modulus of elasticity (MOE) was calculated using Eq. 4, while the modulus of rupture (MOR) was calculated using Eq. 5, where P is the increment of applied load on the specimen in Newtons, P_{max} is the load at failure in Newtons, l is the span of flexure in mm, b is width of the specimen in mm d is depth of specimen mm and Δ is the increment of deflection of the specimen in mm when subjected to the applied load P.

$$MOE_{app} = \frac{23\,Pl^3}{108bd^3\Delta} \quad (4)$$

$$MOR = \frac{P_{max}l}{bd^2} \quad (5)$$

Six samples were collected on three different bondlines of each beam to perform bondline shear strength tests and assess the wood failure levels. The obtained results were then compared to previous block shear tests results conducted by Morin-Bernard *et al.* (2020a) with the investigated species.

3.4.2.3. Estimations of the mechanical properties of full-sized beams

Effective bending stiffness and modulus of elasticity

The effective bending stiffness $(EI)_{ef}$ including the modulus of elasticity were determined by the means of the elastic composite beam theory, using Eq. 6 from Eurocode 5 Annex B (EN 1995-1-1:2004+A2:2014), adapted for a glued-laminated beam, where E_i is the mean modulus of elasticity of the boards used in the lamination zone, I_i is the second moment of area of the lamination zone in mm⁴, γ is the gamma factor, or connection efficiency factor, A_i is the cross-sectional area of the lamination zone in mm² and a_i is the distance in mm between the neutral axis of the beam and the centroid of the lamination zone. The gamma factor γ value

has been set to unity in all calculations considering the perfectly rigid connection between the lamellae. This approach provides a suitable result for most engineering applications (Thelandersson & Larsen, 2003).

$$(EI)_{ef} = \sum_{i=1}^{n}(E_i I_i + \gamma E_i A_i a_i^2) \quad (6)$$

The mean modulus of elasticity of the beams was derived from the effective bending stiffness by dividing the $(EI)_{ef}$ value by the second moment of area I_{beam}, as shown in Eq. 7.

$$MOE_{mean} = \frac{\sum_{i=1}^{n}(E_i I_i + E_i A_i a_i^2)}{I_{beam}} \quad (7)$$

To achieve the best possible precision in the results, the stiffness properties were calculated separately for each beam considering the measured stiffness of the lamellae composing each layer and are therefore not based on the grade-averaged values as presented in Table 17.

Characteristic bending strength

Equations from the European softwood glued-laminated timber model included in EN 14080 (2013) and required for the calculation of the characteristic bending strength are assumed to remain valid for hardwood beams, provided the ratio of the finger joints characteristic bending strength ($f_{m,j,k}$) on the lamellae characteristic tensile strength ($f_{t,0,l,k}$) is within the range presented in Eq. 8 (Aicher & Stapf, 2014; EN 14080, 2013).

$$1.4\, f_{t,0,l,k} \leq f_{m,j,k} \leq 1.4\, f_{t,0,l,k} + 12 \quad (8)$$

In this study, none of the hardwood samples fulfilled this assumption. The characteristic bending strength of the beams was therefore predicted following the approach of Aicher & Stapf (2014), using a simple modified serial failure probability model considering exclusively the finger joints number and strength distribution parameters. The two outermost laminations of the beams and an average of 2.5 finger joint per lamination were considered in the calculations. Eq. 9 was adapted from Aicher & Stapf (2014) to account for the uneven stiffness distribution through the cross-section of the beams manufactured in the present study. σ_{max} is the stress at the extreme fibre, σ_1/σ_{max} is the proportion of the stress σ_{max} on the second lamination zone, m is the shape parameter from the Weibull distributions and λ is the scale parameter of the corresponding Weibull distributions.

$$F_g = 1 - e^{\left\{-n_{fj}\left[1+\left(\sigma_1/\sigma_{max}\right)^m\right]\left(\sigma_{max}/\lambda\right)^m\right\}} \quad (9)$$

The scale and shape parameters of the 2-Parameter Weibull distributions of the finger-joint strength that were used in the calculations are presented in Table 18.

Table 18. Scale and shape parameters of the finger joint 2-P Weibull distributions.

	White ash	Yellow birch	White oak
Shape parameter *m*	8.83	10.76	15.74
Scale parameter λ	49.58 N/mm^2	44.28 N/mm^2	51.45 N/mm^2

3.5 Results

3.5.1 UTS of unjointed hardwood lamellae

The highest median UTS of unjointed lamellae was obtained in the white ash specimens (124.8 MPa), followed by white oak and yellow birch with respective median UTS values of 115.2 and 114.6 MPa (Table 19). When considering the 5th percentile and minimum values, yellow birch came out as the strongest species (80.5 – 83.3 MPa), followed by white ash (74.0 – 78.9 MPa) and white oak (60.5 – 62.6 MPa).

Table 19. Density, median UTS and 5th percentile UTS from the 2-parameter Weibull distribution (X_{05} 2P-Weibull) of the unjointed hardwood lamellae.

Species	n	Density (kg/m³)		Ultimate tensile strength (MPa)			
		Mean	SD	Median	SD	Minimum	X_{05} 2P-Weibull
White ash	25	719.5	42.0	124.8	25.5	74.0	78.9
Yellow birch	22	706.2	49.5	114.6	16.7	80.5	83.3
White oak	11	809.3	52.6	115.2	31.0	60.5	62.6

3.5.2 UTS and failure modes of finger-jointed lamellae

Among the three investigated hardwood species, the highest median UTS was achieved by specimens jointed with the 15 mm profile and bonded using the MF adhesive, with 50.4 MPa for white oak, 48.0 MPa for white ash and 43.6 MPa for yellow birch (Figure 18, Table 20), which correspond to 43.75, 38.46 and 38.05 % of the unjointed lamellae UTS, respectively. The highest 5th percentile value was also attained by the specimens jointed with the 15 mm profile and MF adhesive in the case of white oak and white ash (42.6 and 36.4 MPa), but not in the case of yellow birch, for which the highest 5th percentile was obtained by specimens jointed with the 15 mm profile and PUR adhesive (33.6 MPa) (Table 20). Specimens jointed with the 22 mm profile exhibited considerably lower UTS values. In this case, the highest median UTS was 39.5 MPa for white oak specimens bonded with the PUR adhesive, followed by white ash (37.0 MPa) and yellow birch (36.5 MPa) specimens also bonded with PUR (Table 20), which correspond to 34.29, 29.65 and 31.85 % of the unjointed lamellae UTS values, respectively. The highest 5th percentile was also observed on white oak specimens bonded with PUR (31.5 MPa), followed by yellow birch specimens bonded with PUR (27.5 MPa) and white ash specimens bonded with MF (26.3 MPa). The median UTS values for the softwood lamellae were similar regardless of the joint profile (36.3 – 38.1 MPa), as were the 5th percentile values (23.8 – 25 MPa).

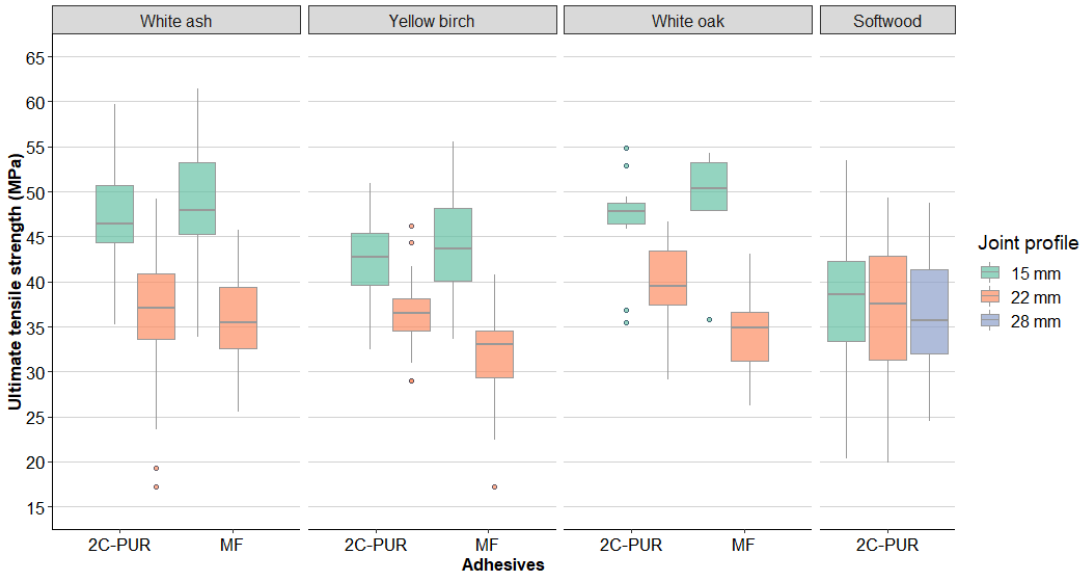

Figure 18. UTS of finger-jointed lamellae as a function of the species, joint profile and adhesive.

Table 20. Median UTS, 5th percentile UTS from the 2-parameter Weibull distribution (X_{05} 2P-Weibull) of finger-jointed lamellae as well as the density and moisture content of the specimens.

Species	Joint profile	Adhesive	n	Density ρ (kg/m3)		Ultimate tensile strength (MPa)			X_{05} 2P-Weibull	Moisture content (%)
				Mean	SD	Median	SD	Minimum		
White ash	15 mm	MF	32	707.8	48.5	48.0	6.5	33.8	36.4	10.2
		PUR	32	715.0	51.8	46.4	5.7	35.2	35.4	10.3
	22 mm	MF	30	720.0	47.0	35.5	5.1	25.6	26.3	10.3
		PUR	31	712.7	51.0	37.0	7.2	17.2	24.5	10.2
Yellow birch	15 mm	MF	27	719.3	37.6	43.6	5.9	33.6	32.4	11.2
		PUR	33	717.4	41.6	42.8	4.5	32.5	33.6	11.2
	22 mm	MF	29	716.7	38.2	33.0	5.2	17.2	23.3	11.2
		PUR	27	718.1	37.7	36.5	4.1	29.0	27.5	11.3
White oak	15 mm	MF	11	780.4	58.2	50.4	5.2	35.8	42.6	9.9
		PUR	12	777.0	66.8	47.8	5.6	35.5	37.7	9.9
	22 mm	MF	10	763.8	47.4	34.8	5.2	26.2	24.8	9.9
		PUR	11	785.7	67.1	39.5	5.1	29.1	31.5	9.9
Softwoods	15 mm	PUR	42	504.0	26.5	38.1	7.0	20.3	25.0	13.4
	22 mm	PUR	35	494.8	20.7	36.8	7.7	19.9	23.8	13.4
	28 mm	PUR	37	491.5	29.5	36.3	6.6	24.5	24.2	13.4

The statistical analysis of the hardwood results revealed that both the species and joint profile had a significant impact on the obtained UTS values ($p < 0.001$). The 15 mm joint profile had significantly higher median UTS values than the 22 mm profile ($p < 0.001$), while white ash and white oak jointed lamellae reached significantly higher UTS values than their yellow birch counterparts ($p \leq 0.001$). The results for white ash and white oak were not significantly different between them ($p = 0.68$). The adhesive did not

come out as a significant factor affecting UTS (p = 0.33). Contrarily to hardwoods, the joint profile did not have a significant impact on the UTS values of the softwood jointed lamellae (p = 0.52).

The analysis of variance including both hardwood and softwood samples showed that the sample group (species-adhesive-profile combination) had a significant impact on the median UTS ($p < 0.001$). Multiple comparisons between hardwoods and softwoods revealed that all hardwood samples jointed using the 15 mm profile reached a significantly higher median UTS than the three softwood groups, with p values under 0.001 for white ash and white oak, and under 0.03 for yellow birch samples. The yellow birch lamellae jointed using the 22 mm profile and the MF adhesive had a significantly lower median UTS than the 15 mm and 22 mm jointed softwood lamellae with p values of 0.001 and 0.025, respectively. There were no other significant differences between the UTS values of the hardwood lamellae jointed using the 22 mm profile and the three softwood groups.

Only the species (p = 0.001) had a significant impact on the proportion of failure modes 3 to 5 versus modes 1 and 2 of the hardwood specimens. The effect of the adhesive system (p = 0.17) or of the joint profile (p = 0.36) were not statistically significant. Most of the white ash specimens failed in modes 2 and 3 (Fig. 19A), while yellow birch specimens failed mostly is mode 1 (Fig. 19B), and only occasionally in mode 2. White oak specimens exhibited the highest proportion of failure modes 3, 4 or 5 (Fig. 19C). For their part, softwood specimens exhibited a high proportion of failure modes 3, 4 and 5, thus meeting ANSI A190.1 (2017) requirement for softwoods. The impact of the joint profile on the relative proportion of failure modes 1-2-3 versus mode 4 and mode 5 was not significant (p = 0.15). Specimens jointed with the 22 mm and 28 mm joint profile failed mainly in mode 4, while the 15 mm jointed specimens failed mainly in mode 3 (Fig. 19D).

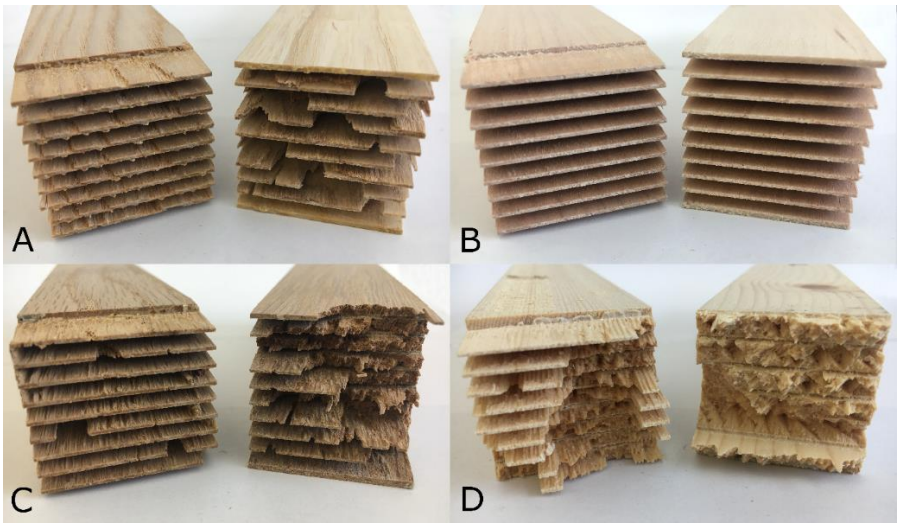

Figure 19. A) Failure modes 2 and 3 on white ash specimens B) Failure modes 1 and 2 on yellow birch specimens C) Failure modes 2 and 3 on white oak specimens D) Failure modes 3 and 4 on softwood specimens.

3.5.3 Bending properties of full-size beams

With a MOR of 47.0 MPa, the white ash full-sized beam had the highest bending strength, but the lowest stiffness (15 078 MPa) (Table 21). The yellow birch beams reached bending strengths of 39.7 and 41.6 MPa and MOE of 16 712 and 16 007 MPa, when adjusted to a 12% MC. Data from the finger-jointing trials led us to an estimated characteristic bending strength of 40.19 MPa for

white oak beams, when considering a stress distribution throughout the cross-section similar to that of the yellow birch beams, which would have been the highest among the investigated species.

Table 21. Predicted and observed mechanical properties of the beams (adjusted to 12% MC) and wood failure levels (WF) obtained in bondline shear strength tests.

Beam	Predicted properties				Properties from tests			
	$f_{m,g,k}$ (MPa)	$(EI)_{ef}$ (N·mm^2)	*MOE* (MPa)	*MOR* (MPa)	$(EI)_{ef}$ (N·mm^2)	*MOE* (MPa)	f_v (MPa)	*WF* (%)
White ash	31.84	2.513E+12	15 880	47.0	2.386E+12	15 078	18.3	97.5
Yellow birch A	30.82	2.833E+12	17 930	39.7	2.641E+12	16 712	20.2	92.0
Yellow birch B	30.81	2.828E+12	17 890	41.6	2.530E+12	16 007	22.8	95.0

Both the wood failure levels (WF), and the mean shear strength (f_v) obtained in the block shear tests were higher than the values obtained by Morin-Bernard *et al.* (2020a) in a previous test campaign conducted with the same species, adhesive and testing procedure. However, contrarily to what was observed in the previous test campaign, the yellow birch specimens collected from the beams had a significantly (p = 0.003) higher mean shear strength (20.22 – 22.75 MPa) than their white ash counterparts (18.32 MPa).

3.6 Discussion

3.6.1 Comparison of results with relevant standards and studies

Although not designed for hardwood species, standards NLGA SPS-4 (2014a) and SPS-1 (2014b) remain relevant to compare the results with the products that are currently predominant on the market. All the hardwood samples jointed with the 15 mm profile, either when considering the 2-P Weibull 5th percentile or minimum test value, greatly exceeded the characteristic tensile strength of 27.9 MPa required for 2400Fb-2.0E softwood fingerjoined machine-graded lumber under short-term load duration, which is the highest finger-jointed product grade marketed in Canada. In contrast, the softwood sample groups met the 5th percentile requirement of 22.8 MPa from NLGA SPS-4 (2014a) for 2100Fb-1.8E fingerjoined machine graded lumber. However, only the 28 mm profile fulfilled this requirement if we consider the most conservative minimum value. All hardwood and softwood groups, regardless of the joint profile and adhesive, exceeded the tensile strength requirement of 15.3 MPa for SPF Select Structural fingerjoined structural lumber from NLGA SPS-1 (2014b). Regarding the wood failure levels, ANSI A190.1 (2017) requires an average wood failure level of 60% for end jointed specimens from dense hardwoods and 80 % for softwoods. In this study, this requirement was assumed to correspond to failure mode 3 or higher. Failure modes lower than 3 represent a failure mostly along the joint profile with no damage to the fingers, and are thus considered as indicators of a poor-quality gluing. Failure modes 3 and higher represent a gradient from partial failure at the finger roots or tips with good wood shear failure along the joint profile to failure outside the joint profile [39]. None of the hardwood groups met this requirement, while softwood groups all exceeded the 80% wood failure threshold.

Very few finger-jointing studies have been conducted on the hardwood species included in this study, yet some results from the literature offer an interesting point of comparison. To the knowledge of the authors, North American white ash has not been the object of any finger-jointing studies. In a study of finger-jointed yellow birch heartwood lamellae, Verreault (2000) subjected specimens jointed using the 28 mm profile and a resorcinol-formaldehyde adhesive to axial tensile tests. The author observed a

mean UTS of 30.46 MPa and a minimum/5th percentile value of 18.15 MPa, the specimens failing exclusively in modes 4,5 and 6. Yellow birch specimens from this study, jointed with the 15 mm profile and the PUR adhesive, reached a considerably higher 5th percentile value (33.6 MPa) despite failing almost exclusively in modes 1 and 2. The lower density of the material (668.0 vs 717.8 kg/m^3) tested by Verreault (2000) as well as its lower quality may explain this counter-intuitive result, in addition to the fact their analysis included the specimens that failed in mode 6. For white oak, however, the present results seem slightly lower than what could have been expected. In a study of finger-jointed North American oak lamellae jointed using a profile almost identical to the 15 mm profile, Aicher & Stapf (2014) reported a median UTS of 63.9 MPa, which represented 55 % of the clear wood strength and a 5th percentile of 41.9 MPa, equivalent to 61 % of the clear wood 5th percentile strength. In this study, the white oak specimens jointed using the 15 mm profile and the MF adhesive achieved a lower median UTS (50.4 MPa) but a similar parametric 5th percentile value (42.6 MPa). However, the minimum test value (35.8 MPa) may be more representative of the real population's 5th percentile, considering the limited number of repetitions. With a joint efficiency of 43.75% for the median UTS and 59.2 % if we consider the minimum value, the joint efficiency was also lower than expected. The higher density of the specimens tested in the present study (780.4 kg/m^3 vs 697.0 kg/m^3) may have led to weaker bondlines and finger joint strength, considering that the median UTS of the unjointed lamellae was almost identical in their investigation (115.9 MPa).

The results of this study with the 15 mm profile compare favourably to finger-jointing trials realized with other north-eastern North American hardwood species. Studies conducted on red maple jointed specimens with a density of 634 and 622 kg/m^3 have shown that it is possible to reach a mean UTS between 33.67 MPa (Chui & Delahunty, 2005) and 44.7 MPa (Janowiak *et al.*, 1995), respectively. A study on sugar maple finger-jointed lamellae (density unknown) resulted in a mean UTS reaching 47.1 MPa and a corresponding 5th percentile of 32.2 MPa, representing, respectively, 62.2 % and 65.7 % of the unjointed wood strengths (Dagenais & Salenikovich, 2008). Results from the present study, however, seem unsatisfactory when compared to highly conclusive results involving European beech. After testing beech lamellae jointed using a profile almost identical to the 15 mm profile used in the present study, Lehmann *et al.* (2018) reported a 5th percentile UTS of 52.2 MPa (density unknown), while Franke *et al.* (2014) reached 60 MPa for the same metric with 700 kg/m^3 density material. With a different joint configuration and beech lamellae with densities ranging between 640 and 720 kg/m^3, Aicher *et al.* (2001) reported a mean UTS of 69 MPa and a minimum value of 48.9 MPa, with 90 % of the failures occurring along the finger joint profile. In a study involving three African tropical hardwoods, Ayarkwa *et al.* (2000) obtained a joint efficiency reaching 82.9 % with a high-density species (891 kg/m^3).

Results gathered from tests on hardwood samples appear promising when compared to results with softwoods. The joint efficiency achieved by the combinations tested in this study appears relatively low when compared with values from the literature, but this issue could be addressed through a more careful optimization of the production parameters. The absence of significant wood failure levels on the yellow birch specimens indicates that several improvements could be made to the machining and gluing parameters that were not considered in the present study. Moreover, the high quality of the hardwood lamellae used in this study have also probably contributed to the limited finger-joint efficiency by reducing the probability of failures outside the joint zone.

3.6.2 Impact of the species on the UTS and failure modes

The differences observed between species confirm the acknowledged difficulties of hardwood gluing and finger-jointing, resulting in more frequent failures along the joint profile and a reduced finger-joint efficiency (Aicher & Stapf, 2014; Franke *et al.*, 2014;

Aichet *et al.*, 2001; Ahmad *et al.*, 2017). These challenges are closely related to the anatomical structure and higher density of the hardwood species, which limits the adhesive penetration (Bandel, 1995; Sellers *et al.*, 1988; Selbo, 1963) and mechanical anchoring. X-Ray tomography images of the finger joints bondlines (Fig. 20) shows clear differences between species. In the case of white ash (Fig. 20A), the adhesive penetrated deeply in the large vessels of the earlywood, providing a good mechanical anchoring. However, the penetration was limited or almost inexistent in the latewood, causing a discontinuity of the bondlines, which may explain the high occurrence of modes 3 failures (i.e. partial failure of the finger roots or tips, Fig. 20A). For yellow birch specimens (Fig. 20B), the adhesive penetration was more superficial, despite being consistent throughout the length of the bondline. Damage caused to the surface by inappropriate machining parameters is a likely explanation for this observation. Regarding the softwood specimens (Fig. 20C), the depth of the adhesive penetration was limited, but consistent throughout the length of the bondline, several rows of tracheids being entirely filled with adhesive.

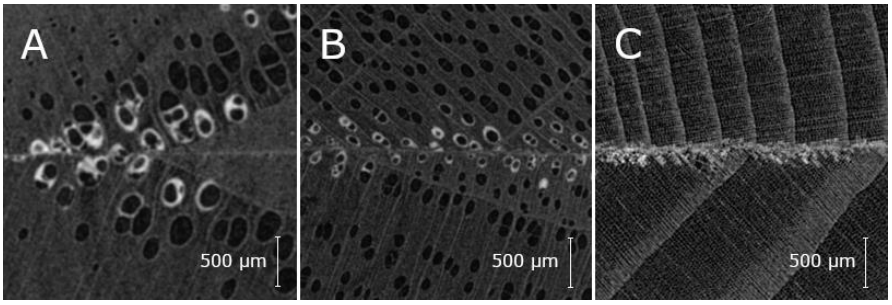

Figure 20. A) Adhesive penetration at a finger joint bondline on white ash B) Adhesive penetration at a finger joint bondline on yellow birch C) Adhesive penetration at a finger joint bondline on softwood.

Some studies on hardwood finger-jointing concluded that the differences in UTS, finger-joint efficiency and failure modes could be attributed to the density of the wood material (Ahmad *et al.*, 2017; Ayarkwa *et al.*, 2000; Castro & Paganini, 1997). However, results from the present study show that other factors are also involved. Although the species had a significant impact on both the UTS and the failure mode, there was no correlation between these variables and the density of the specimens, as Aicher *et al.* (2000) also observed with beech finger-jointed timber. Despite a similar density, white ash and yellow birch behaved differently. Conversely, white ash and white oak showed statistically equivalent results, even if the density of the white oak specimens was higher. This observation highlights the importance of considering the anatomical characteristics of the species. While white ash and white oak are ring-porous hardwoods, yellow birch is a diffuse-porous species. Tran *et al.* (2016) observed similar results, with mostly adhesive failures for beech (diffuse-porous to semi-ring-porous) and wood failures for oak. Considering the high variability among the anatomical features of hardwood species, the machining, surface preparation and gluing of hardwoods requires an even more precise optimization than for softwoods. Results from Dagenais & Salenikovich (2008) with maple have shown that a careful optimization of the cutting speed can increase the joint efficiency from 47 % up to 66 %. The optimal end pressure also depends on the species (Castro & Paganini, 1997) and the optimal end-pressure time is not the same for ring-porous and diffuse-porous species (Sellers *et al.*, 1988) In the present study, these parameters were kept constant for all three hardwood species, making the results suboptimal by introducing a manufacturing bias. Considerable improvements could be obtained if the production parameters were optimized for each of the investigated species.

3.6.4 Impact of the finger joint profile on the UTS and failure modes

As expected, results from the present study confirm that the geometrical parameters of the finger joint have a significant impact on the strength of finger-jointed hardwood lamellae. The 15 mm joint profile, which performed the best with all species-adhesive combinations, showed the highest effective glue joint area. This observation supports the assumption that performing joint profiles maximize the effective glue joint area by adjusting the geometrical parameters such as the finger length, slope, pitch and tip thickness (Franke *et al*., 2014; Bustos, 2003; Ayarkwa *et al*., 2000; Selbo, 1963). However, with an effective glue joint area of 7.89 for the 15 mm profile and 7.84 for the 22 mm, the minor difference may not explain by itself the considerable discrepancies in the performance of both profiles. Low finger slopes, making the surface of the fingers close to parallel to the wood fibres, have also been identified as a major factor impacting the joint efficiency. While Rao *et al.* (2012) reported an optimal slope of 1:12, Selbo (1963) concluded that gains between slopes of 1:12 and 1:16 were present but was reduced beyond 1:16. The width of the fingertips also have to be minimized. Tips are in fact butt joints with a low capability of transmitting the stress, and are also a source of local stress concentration that can lead to failure (Jokerst, 1981; Sellers, 1975; Rao *et al.*, 2012; Strickler, 1980). In this study, the 15 mm joint profile had both the lowest slope and the smallest fingertips, which may explain its performance.

Regarding the length of the fingers, the present results are not in accordance with those of studies suggesting that longer fingers should systematically be preferred (Franke *et al*., 2014; Ahmad *et al*., 2017). In most cases, longer fingers increase the effective glue joint area and should be preferred, but other configurations with shorter fingers could offer good alternatives in certain conditions. Unfortunately, as explained earlier, it was not possible to test the 28 mm profile with the hardwood species. Such results could have confirmed or overturned the observed trend since this profile presents the largest effective glue joint area, but the highest finger slope and tip width. However, considering the damage to the equipment and boards that occurred in the preliminary trials on hardwoods with the 28 mm profile, these technical considerations could justify the use of shorter finger length, especially when dense hardwood species are involved. The 15 mm joint profile therefore appears promising for the finger-jointing of the investigated species in an industrial context. Tests conducted with softwood species did not reveal any significant differences in the UTS as a function of the joint profile. This observation confirms, once again, the bonding issues related to dense hardwoods. In the case of the softwood lamellae, the bond quality was sufficient to result in high levels of wood failure with all joint configurations, masking differences in the actual performance of the joint profile. Results with softwood also showed, despite some differences in the distribution of the failure modes, that it is possible to use short finger lengths to manufacture structural softwood finger-jointed lumber, as also demonstrated by Rao *et al.* (2012).

3.6.5 Performance of full-scale beams

For both white ash (Fig. 22) and yellow birch (Fig. 23) beams, the failure initiated at one of the finger joints was located in the outermost lamellae located in the tension-stressed side of the beam. The tensile failure of the joints led to a shear failure propagating through the cross-section of the beams. No delamination of the bondlines due to shear stress was observed. The cracks propagated into sound wood, with occasional partial failure of finger joints in the inner lamellae. The block shear tests conducted on samples collected from the beams confirmed that the bond quality between the lamellae was satisfactory, with mean wood failure levels largely above the 60 % requirement for Initial Type Testing of glulam products according to ANSI A190.1 (2017). For the two birch beams, the finger joints that initiated the failure failed in mode 1, while the joint failed in mode 2 in the ash beam. These results are coherent with the conclusions from the finger jointing trials, indicating that the bonding quality of the finger joints

was not optimal. This was especially true for the finger joints located in the outermost lamellae, since the latter had the highest density and presented fewer defects than the lamellae positioned in the central portion of the beams. In the finger jointing trials, the strengths of the white ash jointed lamellae were higher than those of the yellow birch lamellae, which resulted in a higher bending strength for the white ash beam than for the yellow birch ones. These results are in accordance with the literature identifying the finger joints as the weakest point of hardwood glulam elements (Tran *et al.*, 2016; 2014a). The MOR values from the bending tests were considerably higher than the predicted 5th percentiles, which was expected considering the limited number of beams tested. According to the serial failure probability model, the obtained bending strength values would correspond to the 89th percentile for the white ash beam, and the 62nd and 81st percentiles for yellow birch beams A and B, respectively. The present results therefore provide preliminary evidence that the calculation approach proposed by Aicher & Stapf (2014) is suitable or conservative for non-homogeneous glulam made from the investigated hardwood species. However, bending tests should be repeated on a larger number of beams to conclude on the real value of the population's 5th percentile. The bending strength of all beams exceeded the requirement for 24f-EX glulam of 37.03 MPa when adjusted to the dimensions of the tested beams following the procedure described in CSA O86 (2014). With respect to the MOE, results of both white ash and yellow birch beams are largely superior to the MOE of the highest softwood glulam strength class available in Canada, which is, when adjusted with ASTM D1990 A1.5 (2016b) to a 12% moisture content, 13 406 MPa for 24f-EX glulam (CSA, 2016).

Figure 21. Failure of a white ash glulam beam initiated at a finger joint.

Figure 22. Failure of a yellow birch glulam beam initiated at a finger joint.

The results obtained in this study are promising when compared with available hardwood glued-laminated timber products. In the United States, standard AITC 119.96 (1996) provides lay-up configurations for the manufacture of glued-laminated timber made from the investigated species up to an allowable bending stress of 30.6 MPa, and an MOE of 10 342 MPa (24f-E2). The corresponding 5th percentile bending strength for 24f-E2 glulam determined in accordance with ASTM D3737 (2018) and adjusted to the dimensions of the beams tested in this study in conformity with the procedure from AITC 119-96 (1996) is 36.37 MPa. The corresponding MOE when adjusted to a 12% moisture content in accordance with ASTM D1990 A1.5 (2016b) is 12 998 MPa. Build-ups provided in AITC 119.96 (1996) allow using timber with a lower quality than that used in the present study to reach a comparable or higher strength. We can conclude that in its current state, the manufacturing process used in this study does not allow taking full advantage of the wood material's strength. However, by using high quality timber, it is possible to succeed at increasing the MOE considerably, which is one of the most limiting factors in structural design.

There is still a potential of improving the bending strength of the product in its current form, considering the properties of currently available products. Technical approvals for glued-laminated timber products made from European oak species declare characteristic bending strengths of 31.5 (DIBt, 2013) for Holz-Schiller glulam, and 33 MPa (ETA-13/0642, 2013) for VIGAM glulam, with respective MOE values of 14 000 and 14 400 MPa for various beam dimensions. To facilitate the comparison with the present study, results from Aicher & Stapf (2014) from bending tests on both Holz Schiller and VIGAM products were adjusted to the depth of the beams tested in this study using the k_h factor from Eurocode 5 (EN 1995-1-1:2004+A2:2014). The size-adjusted 5th percentile bending strengths from tests were 30.9 MPa for Holz-Schiller and 34.2 MPa for VIGAM, while the respective adjusted median test values are 45.27 and 42.10 MPa. With beech timber, a characteristic bending strength of 48 MPa (52.8 MPa when adjusted with k_h factor) and a mean MOE of 15 100 MPa are achievable (DIBt, 2009). Similarly, Frese and Blaß (2006) tested glulam beams made from the highest available grade of lamellae to bending tests. Once adjusted to the dimensions of the beams from the present study using the k_h factor from Eurocode 5 (EN 1995-1-1:2004+A2:2014), the minimum test value of 52.8 MPa and a corresponding mean bending strength of 70.5 MPa. The mean MOE was 15 500 MPa.

The effective properties of a glulam element are the result of a dynamic interaction between several factors, including the quality of the lamellae, their density and the anatomical structure of the species, which all have to be considered in the optimization of the manufacturing process. While high quality lamellae allow manufacturing beams with a high stiffness and a high strength potential,

the latter is rarely achieved because of bonding issued. The strength of the product is therefore governed exclusively by the strength of the finger joints. Conversely, lower quality material allows reducing the gap between the strength of the wood material and the finger joints, increasing therefore the joint efficiency. The downside to this approach is the foreseeable reduction in the stiffness of the product. One should therefore find the equilibrium between these factors, considering the end-use of the product, the characteristics of the available material as well as their impacts on the production costs and value. In this study, the aim was to manufacture a noble and distinctive product with an exceptional visual quality. Considering the limited gain in bending strength compared to hardwood glulams made from lower timber grades, the additional cost for high quality timber can only be justified by the improved visual aspect of the product. When the aesthetic of the product is less of a consideration, the use of lower quality timber would allow significant cost savings.

3.7 Conclusions

Tensile tests on finger-jointed lamellae were realized, using two and three different joint configurations for hardwoods and softwoods, respectively. These tests allowed to conclude that the 15 mm joint profile can be suitable for the finger-jointing of both dense hardwoods and softwoods. However, to maximize the potential of the product, the joint efficiency should be improved, particularly in the case of yellow birch. A careful optimization of the finger-jointing machining and gluing parameters could allow a better penetration of the adhesive, and thus a higher proportion of failure modes 3, 4 and 5. For this to materialize, it is hoped that future development of adhesives will lead to new products on the market that are optimized for hardwood structural bonding.

Bending tests conducted on full-size hardwood glued-laminated timber beams, manufactured in industrial conditions without extensive optimization and using the 15 mm finger joint profile, confirmed the possibility to achieve a bending strength up to 47.0 MPa for white ash and 41.6 MPa for yellow birch. Such results are promising because they are comparable or superior to the properties of the strongest softwood products currently available in Canada. The impressive stiffness of the beams, also confirmed by the bending tests, likely represent the most important outcome of this study. With respective MOE values of 15 078 MPa for white ash and 16 712 MPa for yellow birch, these products have the potential to expand the potential uses of glulam in construction, for instance by reducing the required cross-section of the beams. However, the results revealed that the set of tested adhesives and joint profiles did not take full advantage of the strength of the wood material as failure was initiated at the finger joints in the bending tests. Further study and optimization of the finger-jointing parameters could lead to a superior bending strength that would compare advantageously to the best performing hardwood glulam products currently available. Opting for lamellae free of finger joints in the outermost sections of the beams would also lead to an increased strength, but would limit the achievable span.

Both white ash and yellow birch are promising species for the manufacture of glued-laminated timber. Despite the fact that no white oak beams were manufactured in this study, this species also appears promising since it exhibited a similar or better behaviour than white ash in the finger joints tensile tests, as well as in bondline shear strength tests conducted by Morin-Bernard et al. (2020a). Research is currently underway to better understand the mechanical properties of the investigated species and to propose relevant indicating properties required for the development of a strength grading process, which is a prerequisite for the use of these hardwood species in structural applications. In addition to providing high value-added opportunities for broadleaved species, hardwood glulam has the potential of multiplying the design possibilities and diversifying the aesthetic offer of structural engineered wood products.

Conclusion

Longtemps utilisées pour la construction de charpentes et d'éléments structuraux divers, les espèces feuillues font aujourd'hui un retour dans l'industrie de la construction. La structure anatomique complexe et variable de ces espèces entraîne certains défis, mais offre également l'occasion de créer des produits aux propriétés mécaniques impressionnantes, dotés d'un attrait esthétique indéniable. À ce titre, les travaux réalisés dans le cadre du présent mémoire ont permis de répondre à l'objectif général du projet ainsi qu'aux objectifs spécifiques.

Le chapitre consacré au classement structurel a permis de constater que malgré des particularités anatomiques, il est possible de prédire la résistance en traction des lamelles de frêne d'Amérique et de bouleau jaune avec une précision satisfaisante pour une application industrielle. Les indicateurs utilisés, soient la masse volumique, le module d'élasticité dynamique, la déviation maximale du fil et la proportion de la section transversale occupée par des nœuds sont généralement applicables dans un contexte industriel. Le processus pourrait toutefois être davantage simplifié en étudiant des méthodes de mesure plus rapides ou indirectes pour les propriétés les plus difficiles à mesurer visuellement, notamment les déviations du fil du bois. Les propriétés mécaniques du frêne d'Amérique semblent être davantage prévisibles que celles du bouleau jaune, bien que cette différence soit principalement due aux irrégularités du fil présentes chez ce dernier.

Le chapitre dédié à l'étude de la résistance au cisaillement d'assemblages collés à l'aide de différents adhésifs structuraux a démontré qu'avec les paramètres de production appropriés, il est possible d'utiliser ces adhésifs pour le collage de face de plusieurs espèces feuillues, tout en obtenant des résistances de loin supérieures à ce qu'il est possible d'atteindre avec des espèces résineuses. Les taux élevés de rupture dans le bois ont également confirmé la qualité du collage. Au terme des essais inclus dans ce chapitre, un adhésif polyuréthane a deux composantes ainsi qu'une résine mélamine-formaldéhyde ont été retenus pour leur performance générale et dans le cas de la résine mélamine-formaldéhyde, pour sa résistance à l'humidité.

L'aboutage structural constitue un cas particulier de collage et, dans le cas des espèces feuillues, présente plusieurs défis. Le chapitre y étant dédié a confirmé l'impact des paramètres géométriques du joint sur la résistance des pièces aboutées. Le joint présentant des entures d'une longueur de 15 mm a offert une résistance en traction supérieure à celle du joint dont les entures avaient une longueur de 22,22 mm. La plus faible pente des entures du joint de 15 mm, ainsi qu'une surface de collage effective supérieure expliqueraient les résultats obtenus. D'importantes différences ont également été observées entre les espèces étudiées. Toutefois, il n'est pas possible de lier ces différences à la géométrie du joint. Les écarts dans les résultats obtenus seraient plutôt liés aux paramètres d'usinage du joint, qui auraient été plus adéquats pour les espèces à zone poreuses (frêne d'Amérique et chêne blanc) que pour le bouleau jaune, espèce à pores diffus. Les modes de rupture observés ont d'ailleurs confirmé cette conclusion. Il a été presque impossible d'obtenir une rupture dans le bois avec le bouleau jaune, alors que ce type de rupture était fréquent avec

les deux autres espèces. Une comparaison des résultats avec ceux d'essais réalisés sur des lamelles non jointées a permis de constater que la présence d'un joint affaiblit considérablement la résistance en traction. En ce sens, les joints à entures multiples demeurent l'élément limitant la résistance que les poutres composées des espèces étudiées peuvent atteindre. Il existe cependant un potentiel significatif d'amélioration puisque les essais réalisés dans le cadre de ce chapitre ne cherchaient pas à optimiser les paramètres de production. Une étude attentive des paramètres d'usinage et de collage permettrait certainement d'améliorer la résistance des lamelles jointées et conséquemment, des éléments en bois-lamellé collé qui en sont composés. À partir des propriétés des lamelles jointées, il a été possible, dans le cadre de ce chapitre, d'estimer de façon conservatrice la résistance de poutres pleine grandeur fabriquées à partir de lamelles de frêne d'Amérique et de bouleau jaune. Ces poutres ont par la suite été soumises à des essais en flexion qui ont permis de mesurer leurs propriétés mécaniques effectives.

Les travaux réalisés dans le cadre des trois chapitres ici présentés ont ainsi permis de répondre à l'objectif principal de ce mémoire en démontrant la faisabilité technique d'un bois lamellé-collé composé d'espèces feuillues. En utilisant des installations industrielles et des adhésifs conçus à la base pour la fabrication de produits d'ingénierie structuraux en résineux, il a été possible de fabriquer des poutres en bois lamellé-collé composées d'espèces feuillues dont la résistance se compare avantageusement aux produits en bois résineux les plus résistants et à d'autres produits composés d'espèces feuillues. Ces poutres présentaient d'autre part un atout majeur conféré par leur rigidité impressionnante. Afin de répondre aux exigences esthétiques établies de pair avec le partenaire industriel impliqué dans le projet, nous avons fait le choix d'utiliser des lamelles de qualité supérieure dont la rigidité était impressionnante. Ce faisant, le module d'élasticité des poutres fabriquées dépasse grandement celui de la plupart des produits comparables, surpassant même celui du bois lamellé-collé en hêtre européen, qui est reconnu pour cette caractéristique. Les produits composés d'espèces feuillues disponibles aux États-Unis permettent l'utilisation de lamelles de qualité inférieure. Les spécifications incluses dans la norme AITC 119-96 permettent d'atteindre une résistance équivalente ou supérieure à celle des poutres développées dans le cadre de ce projet, mais leur rigidité demeure de loin inférieure. Ce constat incite à réfléchir sur l'adéquation entre les produits offerts et les besoins des concepteurs et utilisateurs de bâtiments. L'apparence noble et distinctive des espèces feuillues semble constituer un avantage majeur qui pourrait justifier le coût plus élevé engendré par l'utilisation d'une matière première de meilleure qualité. Ce coût pourrait limiter la demande sur les marchés, mais ce constat s'applique également aux produits moins coûteux dont l'attrait esthétique se trouve toutefois limité par la présence de nœuds et d'autres irrégularités. Bien que développés au courant des années 1990, les produits en bois lamellé-collé composés d'espèces feuillues offerts aux États-Unis semblent faire l'objet d'un intérêt limité, principalement concentré autour de la fabrication de ponts. Il serait ainsi pertinent de considérer les deux approches, qui présentent chacune des avantages spécifiques. L'utilisation de volumes de moins bonne qualité permet d'utiliser la ressource de façon plus rationnelle en valorisant des bois qui ne le seraient pas dans les produits d'apparence par exemple. L'utilisation de matériel de première qualité permet d'accroître de façon importante la rigidité des éléments, propriété qui est généralement le facteur limitant dans la

conception de charpentes en bois. Ainsi, ces propriétés impressionnantes pourraient permettre d'utiliser le bois en substitution d'autres matériaux à l'empreinte écologique plus importante, et ce, dans une plus grande diversité d'applications.

D'autre part, l'un des constats majeurs émergeant de ce projet est que les produits fabriqués à partir d'espèces feuillues présentent des différences fondamentales quant à leurs propriétés mécaniques par rapport aux produits composés d'espèces résineuses. Afin d'accroître l'utilisation des espèces feuillues dans les produits d'ingénierie structuraux, il est essentiel de développer des normes qui considèrent ces particularités, en particulier la rigidité supérieure des feuillus à résistance égale. Il serait fortement pénalisant de classer les produits ici développés dans les classes de résistances établies pour les résineux, puisque l'on ne tirerait pas parti du principal avantage des produits composé d'espèces feuillues développés dans le cadre du présent mémoire. En l'absence de normes dédiées à ces espèces, il demeure possible de soumettre un éventuel produit composé d'espèces feuillues au Conseil canadien des matériaux de construction qui pourrait émettre un certificat pour ce bois lamellé-collé propriétaire, rendant son utilisation possible. Ce processus nécessitera toutefois une optimisation plus rigoureuse des paramètres d'aboutage ainsi qu'une campagne d'essais d'envergure sur des poutres pleine grandeur.

Bibliographie

Ahmad, Z., Lum, W.C., Lee, S.H., Razlan, M.A., & Mohamad, W.H.W. (2017). Mechanical properties of finger jointed beams fabricated from eight Malaysian hardwood species. *Construction and Building Materials*, 145, 464–473.

Aicher, S., Höfflin, L., & Behrens, W. (2001). A study on tension strength of finger joints in beech wood laminations. *Otto-Graf-Journal*, 12, 169-186.

Aicher, S., & Ohnesorge, D. (2011). Shear strength of glued laminated timber made from European beech timber. *European Journal of Wood and Wood Products*, 69(1), 143–154.

Aicher, S., Christian, Z., & Dill-Langer, G. (2014). Hardwood glulams - Emerging products of superior mechanical properties. *Proceedings of WCTE 2014*, Quebec, Canada. doi: 10.13140/2.1.5170.1120

Aicher, S., & Stapf, G. (2014). Glulam from European white oak: finger joint influence on bending size effect. *Materials and Joints in Timber Structures – recent developments of technology*, Eds. Aicher, S., Reinhardt, H.-W., Garrecht, H., RILEM Bookseries, Vol. 9, pp. 641-656. ISBN 978-94-007-7811-5

Aicher, S., Ahmad, Z., & Hirsch, M. (2018). Bondline shear strength and wood failure of European and tropical hardwood glulams. *European Journal of Wood and Wood Products,* 76(4), 1205–1222. doi:10.1007/s00107-018-1305-0

AITC. (1996). *Standard specifications for structural glued laminated timber of hardwood species AITC 119-96*. American Institute of Timber Construction. Englewood, Colorado.

Allied Market Research. (2016). *Engineered Wood Market Overview - Global Opportunity Analysis and Industry Forecast, 2014-2022*. Allied Market Research. Récupéré de: https://www.alliedmarketresearch.com/engineered-wood-market

Amen-Chen, C., & Gabriel, J. (2015). Wet adhesion durability improvement of polyurethane wood adhesives with primer. *European Journal of Wood and Wood Products,* 73(5), 697–700. doi: 10.1007/s00107-015-0942-9

Ammann, S., Schlegel, S., Beyer, M., Aehlig, K., Lehmann, M., Jung, H., & Niemz, P. (2016) Quality assessment of glued ash wood for construction engineering. *European Journal of Wood and Wood Products*, 74(1), 67–74. doi: 10.1007/s00107-015-0981-2

ANSI. (2017). *Standard for wood products—structural glued laminated timber.* ANSI A190.1. APA—The Engineered Wood Association. Tacoma, WA

APA. (2015). Engineered Wood Demand Predicted To Rise. *Engineered Wood Journal*, 18(2),9.

ASTM. (2006). *Standard Practice for Establishing Clear Wood Strength Values ASTM D2555.* American Society for Testing and Materials, West Conshohocken, PA.

ASTM. (2011). *Standard Practice for Establishing Structural Grades and Related Allowable Properties for Visually Graded Lumber ASTM D245*. American Society for Testing and Materials, West Conshohocken, PA.

ASTM. (2015). *Standard Test Methods of Static Tests of Lumber in Structural Sizes ASTM D198.* American Society for Testing and Materials, West Conshohocken, PA.

ASTM. (2016a). *Standard Test Methods for End-Joints in Structural Wood Products ASTM D7469*. American Society for Testing and Materials, West Conshohocken, PA.

ASTM. (2016b). *Standard Practice for Establishing Allowable Properties for Visually-Graded Dimension Lumber from In-Grade Tests of Full-Size Specimens ASTM D1990*. American Society for Testing and Materials, West Conshohocken, PA.

ASTM. (2017a). *Test Methods for Density and Specific Gravity (Relative Density) of Wood and Wood-Based Materials ASTM D2395*. American Society for Testing and Materials, West Conshohocken, PA.

ASTM. (2017b). *Standard Practice for Sampling and Data-Analysis for Structural Wood and Wood-Based Products ASTM D2915*. American Society for Testing and Materials, West Conshohocken, PA.

ASTM. (2018). *Standard Practice for Establishing Allowable Properties for Structural Glued Laminated Timber (Glulam) ASTM D3737*. American Society for Testing and Materials, West Conshohocken, PA.

Ayarkwa, J., Hirashima, Y., & Sasaki, Y. (2000). Effect of finger geometry and end pressure on the flexural properties of finger-jointed tropical African hardwoods. *Forest Products Journal*, 50(11/12), 53-63.

Bandel, A. (1995). *Gluing wood*. CATAS, San Giovanni al Natizone. 301 p.

Bates, D., Maechler, M., Bolker, B., & Walker, S. (2015). Fitting Linear Mixed-Effects Models Using lme4. *Journal of Statistical Software*, 67(1), 1-48.

Bendtsen, A., & Youngs, R.L. (1981). Machine stress rating of wood: An overview. *Proceedings of XVII IUFRO World Congress, Division 5,* Kyoto, Japan, pp. 21-34.

BFEC. (2014). *Volumes non récoltés pour la période 2008-2013 potentiellement disponibles à la récolte pour la période 2013-2018.* Bureau du forestier en chef du Québec. Récupéré de: http://forestierenchef.gouv.qc.ca/wp-content/uploads/2014/10/D%C3%A9cision_Forestier_VRN_2014-09-26_Version_Corrigee.pdf.

BFEC. (2019). *Détermination de la possibilité forestière 2018-2023, synthèse provinciale.* (Annual allowable cut determination 2018-2023, provincial synthesis) (in French). Office of the Chief Forester of Quebec (BFEC). Récupéré de: https://forestierenchef.gouv.qc.ca/wp-content/uploads/2019/11/rxx_synthese_provinciale_nov_2019.pdf.

Bodig J., & Jayne BA, 1982. Mechanics of Wood and Wood Composites. Van Nostrand Reinhold, New York.

Bollmus, S., Gellerich, A., Schlotzhauer, P., Behr, G., & Militz, H. (2017). Hardwood research at the Georg-August University of Goettingen*,* in: *Proceedings of the 6th International Scientific Conference on Hardwood Processing*. Lahti, Finland, pp. 116-122.

Brandner, R., & Schickhofer, G. (2008) Glued laminated timber in bending: new aspects concerning modelling. *Wood Science and Technology,* 42(5), 401–425. doi: 10.1007/s00226-008-0189-2

Brunetti, M., Nocetti, M., Pizzo, B., Aminti G., Cremonini C., Negro F., Zanuttini R., Romagnoli M., & Scarascia Mugnozza G. (2019). Glued structural products made of beech wood: quality of the raw material and gluing issues, in: *Proceedings of the 7th International Scientific Conference on Hardwood Processing*. Delft, The Netherlands, pp. 230-242.

Bustos, C. (2003). *Optimisation du procédé d'aboutage par entures multiples du bois d'épinette noire* (Thèse de doctorat, Université Laval, Québec, Canada)

Castro, G., & Paganini, F. (1997). Parameters affecting end finger joint performance in poplar wood. *Proceedings of International Conference of IUFRO S 5.02 Timber Engineering 1997*. Copenhagen, Denmark.

Cecobois. (2019). *Étude sur les parts de marché du matériau bois dans la construction non résidentielle de 4 étages ou moins au Québec*. Rapport réalisé par FEA pour Cecobois.

Cecobois. 2015. *Guide technique sur la conception de poutres et colonnes en gros bois*. Récupéré de: https://www.cecobois.com/publications/guide-technique/guide-technique-sur-la-conception-de-poutres-et-colonnes-en-gros-bois.

Clausen, K.E., & Godman, R.M. (1967). *Selecting superior yellow birch trees – A preliminary guide*, U.S. Department of Agriculture, North Central Forest Experiment Station, St-Paul, MN.

Clerc, G., Lehmann, M., Gabriel, J., Salzgeber, D., Pichelin, F., Strahm, T., & Niemz, P. (2018). Improvement of ash (Fraxinus excelsior L.) bonding quality with one-component polyurethane adhesive and hydrophilic primer for load-bearing application. *International Journal of Adhesion and Adhesives*, 85, 303–307. doi: 10.1016/j.ijadhadh.2018.06.017

Chui, Y.H. & Delahunty, S. (2005). *Glued Engineered Products Made of Red Maple*. UNB6 Research report. University of New Brunswick, Canada.

Cumbo, D., Smith, R., & Araman, P. (2003). Low-grade hardwood production, markets, and issues. *Forest Products Journal*, 53(9),17–24.

CSA. (2006). *Qualification Code for Manufacturers of Structural Glued-Laminated Timber CAN/CSA O177*. Association Canadienne de Normalisation, Etobicoke, Ontario.

CSA. (2010). *Evaluation of adhesives for structural wood products (exterior exposure) CAN/CSA O112.9-10.* Association Canadienne de Normalisation, Etobicoke, Ontario.

CSA. (2014). *Règles de calcul des charpentes en bois CAN/CSA O86-14.* Association Canadienne de Normalisation, Etobicoke, Ontario.

CSA. (2016). *Structural glued-laminated timber CAN/CSA 0122-16*. Association Canadienne de Normalisation, Etobicoke, Ontario.

Dagenais, C. (2007). *Aboutage de l'érable à sucre pour la fabrication de produits de bois d'ingénierie structuraux* (Mémoire de maîtrise, Université Laval, Québec, Canada.)

Dagenais, C., & Salenikovich, A. (2008). *Influence of Machining Parameters on the Tensile Strength of Finger-Jointed Sugar Maple Lumber. Wood and Fiber Science* 40(1), 55–61.

DIBt. (2004). *German technical approval Z-9.1-577 "Glulam from Dark Red Meranti."* Approval holder : Enno Roggemann, Bremen, Issued by DIBT, Germany.

DIBt. (2009). *General technical approval Z-9.1-679. BS-Holz Glulam from beech and glulam from beech-hybrid.* Approval holder: BS-Holz, Issued by DIBT, Germany.

DIBt. (2012). *German Technical Approval Z-9.1-704. Glulam made of oak.* Holder of approval: Elaborados y Fabricados Gámiz. S.A. Spain. Issued by DIBT, Germany.

DIBt. (2013). *German Technical Approval Z-9.1-821. Holz Schiller oak post and beam glulam.* Holder of approval: Holz Schiller GmbH. Germany. Issued by DIBT, Germany

Dietsch, P., & Tannert, T. (2015). Assessing the integrity of glued-laminated timber elements. Construction and Building Materials, 101, 1259–1270. doi: 10.1016/j.conbuildmat.2015.06.064

Dunky, M. & Pizzi, A. (2002). *Chapter 23 - Wood adhesives. In: Adhesion Science and Engineering Volume 2*. A.V. Pocius, D.A. Dillard & M. Chaudhury eds. Elsevier.

Durocher, C., Thiffault, E., Achim, A., Auty, D., & Barrette, J. (2019). Untapped volume of surplus forest growth as feedstock for bioenergy. *Biomass and Bioenergy*, 120:376–386. doi:10.1016/j.biombioe.2018.11.024

Egner, K., & Kolb, H. (1966). Geleimte Träger und Binder aus Buchenholz. *Bau. Mit Holz.,* 68(4), 147–154.

Ehrhart, T., Fink, G., Steiger, R., & Frangi, A. (2016a). Strength grading of European beech lamellas for the production of GLT and CLT. *Proceedings of INTER—Meeting Forty-Nine*, Graz, Austria, pp. 29–43.

Ehrhart, T., Fink, G., Steiger, R., & Frangi, A. (2016b). Experimental Investigation of Tensile Strength and Stiffness Indicators Regarding European Beech Timber, in: *Proceedings of WCTE 2016*, Vienna, Austria, pp. 600-607.

Ehrhart, T., Steiger, R., & Frangi, A. (2018). A non-contact method for the determination of fibre direction of European beech wood (Fagus sylvatica L.), *European Journal of Wood Products*, 76(3), 925–935. DOI: 10.1007/s00107-017-1279-3

EN 338. (2016). *Structural timber – Strength classes*, CEN European Committee for Standardization, Brussels, Belgium.

EN 392. (1995). *Glued laminated timber — shear test of glue lines*. European Committee for standardization (CEN). Brussels

EN 1995-1-1:2004+A2:2014. *Eurocode 5: design of timber structures – Part 1–1: General – Common rules and rules for buildings*, Comité Européen de Normalisation, Bruxelles, Belgique.

EN 14080. (2013) *Timber Structures-Glued laminated timber and glued solid timber—Requirements*. Comité européen de Normalisation, Bruxelles, Belgique.

ETA-13/0642. (2013). *European Technical Approval VIGAM-Glued laminated timber of oak*. Holder of approval: Elaborados y Fabricados Gámiz. S.A. Spain. Issued by OIB, Austria.

ETA-13/0646. (2013). *European Technical Approval SIEROLAM-Glued laminated timber of chestnut*. Holder of approval: Grupo Gamiz SA. Issued by OIB, Austria.

Falk, R.H., & Colling, F. (1995). Laminating Effects in Glued-Laminated Timber Beams. *Journal of Structural Engineering*, 121(12), 1857–1863. doi:10.1061/(ASCE)0733-9445(1995)121:12(1857)

FCBA. (2017). *Valorisation des feuillus dans la construction*. Récupéré de: https://www.fcba.fr/sites/default/files/fcbainfo_2017_8_valorisation_feuillus_construction_guillaume_legrand_morgan_vuillermoz.pdf.

Franke, B., Schusser, A., & Müller, A. (2014). Analysis of finger joints from beech wood. *Proceedings of WCTE 2014*. Quebec, Canada.

Franke, B., Lehringer, C., Müller, A., & Sauser, F. (2016). Beech Glulam - Investigations of surface preparation and gluing. *Proceedings of WCTE 2016*, Vienne, Autriche.

Frese, M., & Blaß, H.J. (2006). Characteristic bending strength of beech glulam. *Materials and Structures*, 40:3–13. doi: 10.1617/s11527-006-9117-9

Frihart, C.R., & Hunt, C.G. (2010). Chapter 10: Adhesives with Wood Materials- Bond Formation and Performance. in: *Wood Handbook: Wood as an engineering material*. U.S. Department of Agriculture, Forest Service, Forest Products Laboratory. Madison, Wisconsin, pp 10-1 - 10-24

Frühwald, K., & Schickhofer, G. (2005). Strength grading of hardwoods, in *Proceedings of the 14th International Symposium on Nondestructive Testing of Wood*, Eberswalde, Germany, pp. 198-210.

Galligan, W.L., & McDonald, K.A. (2000). *Machine Grading of Lumber – Practical concerns for lumber producers*. (FPL-GTR-7). U.S. Deptartment of Agriculture, Forest Service, Forest Products Laboratory, Madison, WI. 39 p.

Gaston, C.W. (2014). Visual Wood Product Trends in North American Nonresidential Buildings. *Forest Products Journal*, 64(3–4),107–115. doi:10.13073/FPJ-D-13-00077

Ghazil, S. (2010). *Étude de la migration des fluides dans le bois* (Thèse de doctorat, Université Henri Poincaré, Nancy-1, Nancy).

Gosselin, A., Blanchet, P., Lehoux, N., & Cimon, Y. (2016). Main Motivations and Barriers for Using Wood in Multi-Story and Non-Residential Construction Projects. *BioResources* 12(1), 546-570. doi:10.15376/biores.12.1.546-570

Green, D.W. (1993). Investigation of the mechanical properties of red oak 2 by 4's. *Wood and Fiber Science*, 25(1), 33–45.

Green, D.W., Ross, R.J. & McDonald, K. (1994). Production of hardwood machine stress rated lumber. *Proceedings of 9th International symposium on nondestructive testing of wood 1993*, Madison, WI. 141-150.

Green, D.W., Winandy, J.E., & Kretschmann, D.E. (1999). *Mechanical properties of wood - Chapter 4. In: Wood handbook—Wood as an engineering material (FPL–GTR–113),* U.S. Department of Agriculture, Forest Product Laboratory, Madison, WI.

Grøstad, K., & Bredesen, R. (2014). EPI for Glued Laminated Timber. in *Materials and Joints in Timber Structures*, Aicher, S., H.-W. Reinhardt, and H. Garrecht (eds.). Springer Netherlands, Dordrecht. pp. 355–364.

Grøstad, K., & Pedersen, A. (2010). Emulsion Polymer Isocyanates as Wood Adhesive: A Review. *Journal of Adhesion Science and Technology*, 24(8–10), 1357–1381. doi: /10.1163/016942410X500981

Habipi, B., & Ajdinaj, D. (2015). Wood Finger-Joint Strength as Function of Finger Length and Slope Positioning of Tips. *International Journal of Engineering and Applied Sciences*, 2(12), 128–132.

Hanhijärvi, A., & Ranta-Maunus, A. (2008). *Development of strength grading of timber using combined measurement techniques*. Report of the Combigrade Project—Phase 2, VTT Publications 686, 55 pp. ISBN 978-951-38-7106-2

Hardwood Publishing Inc. (2020). *Hardwood Review Express – Northern Pricing*. Hardwood Publishing Inc. Charlotte, NC. 19(24), 6-7

Hass, P., Müller, C., Clauss, S., & Niemz, P. (2009). Influence of growth ring angle, adhesive system and viscosity on the shear strength of adhesive bonds. *Wood Material Science & Engineering*, 4(3–4), 140–146.

Hass, P., Wittel, F.K., Mendoza, M., Herrmann, H.J., & Niemz, P. (2012). Adhesive penetration in beech wood: experiments. *Wood Science and Technology*, 46(1–3), 243–256. doi: 10.1007/s00226-011-0410-6

Herms, D.A., & McCullough, D.G. (2014). The emerald ash borer invasion of North America: history, biology, ecology, impacts and management. *Annual Review of Entomology*, 59, 13-30. doi:10.1146/annurev-ento-011613-162051

Hernandez, R.E. (1994). Effect of two wood surfacing methods on the gluing properties of sugar maple and white spruce. Forest Products Journal, 44(7,8), 63.

Hetzer, O. (1906). *Patent for curved, glued laminated beams composed of two or more lamellas*. DRP No. 197773. Germany.

ISO. (2007). *Timber structures—glued laminated timber—method of test for shear strength of glue lines ISO 12579*. International Organization for Standardization ISO. Geneva.

ISO. (2018). *Adhesives - Wood-to-wood adhesive bonds - Determination of shear strength by compressive loading ISO 6238*. International Organization for Standardization ISO. Geneva.

Janowiak, J.J., Manbeck, H.B., Wolcott, M. P., & Davalos, J. F. (1992). *Preliminary refinement of hardwood stress values*. (Final Rep. Project SS-047). Pennsylvania Department of Transportation, Office of Special Studies, Harrisburg, PA.

Janowiak, J.J., Kessler, K.R., Manbeck, H.B., Blankenhorn, P.R., & Labosky, P. (1994). *Compression strength properties for two hardwood glulam materials*. Forest Products Journal, 44(2), 62.

Janowiak, J.J., Manbeck, H.B., Hernandez, R., Moody, R.C., Blankenhorn, P.R., & Labosky, P. (1995) *Efficient Utilization of Red Maple Lumber in Glued-Laminated Timber Beams.* (Res. Paper FPL–RP–541). U.S. Department of Agriculture, Forest Service, Forest Products Laboratory. Madison, WI

Janowiak, J.J. (1997). Red Maple Lumber Resources for Glued-Laminated Timber Beams. in *Undervalued Hardwoods for Engineered Materials and Components*, Forest Products Society, Madison, WI : Marquette, MI. pp. 93–114.

Jessome, A.P. (1977). *Resistance and Related Properties of Native Wood Species in Canada*. Eastern Forest Products Laboratory. Ottawa, Canada.

Jiang, Y., Schaffrath, J., Knorz, M., Winter, S., and van de Kuilen, J.W.G. (2014). Applicability of various wood species in glued laminated timber - Parameter study on delamination resistance and shear strength. *Proceedings of WCTE 2014*, Quebec, Canada.

Jokerst, R.W. (1980). The effect of geometry on the performance of structural finger-joints. in: *Proceedings of Production, Marketing and Use of Finger-Jointed Sawnwood*, 15-19 September 1980, Timber Committee of the UN Economic Commission for Europe. Martinus Nijhof/Dr. W. Junk Publishers, The Hague, The Netherlands. pp.169-180

Jokerst, W.R. (1981). *Finger-Jointed Wood Products*. (Res. Paper FPL-RP-382), U.S. Department of Agriculture, Forest Service, Forest Products Laboratory, Madison, WI

Kläusler, O., Hass, P., Amen, C., Schlegel, S., & Niemz, P. (2014). Improvement of tensile shear strength and wood failure percentage of 1C PUR bonded wooden joints at wet stage by means of DMF priming. *European Journal of Wood Products*, 72(3), 343–354. doi:10.1007/s00107-014-0786-8

Knorz, M. (2014). *Investigation of structurally bonded ash (Fraxinus excelsior L.) as influenced by adhesive type and moisture* (Thèse de doctorat, Technischen Universität München, Germany). Récupéré de: https://mediatum.ub.tum.de/1274270. Accessed 6 December 2018

Knorz, M., Neuhaeuser, E., Torno, S., & van de Kuilen, J.W.G. (2015). Influence of surface preparation methods on moisture-related performance of structural hardwood–adhesive bonds. *International Journal of Adhesion and Adhesives*, 57, 40-48. doi:10.1016/j.ijadhadh.2014.10.003

Knorz, M., Schmidt, M., Torno, S., & van de Kuilen, J.W.G. (2014). Structural bonding of ash (*Fraxinus excelsior* L.): resistance to delamination and performance in shearing tests. *European Journal of Wood and Wood Products,* 72(3), 297–309. doi:10.1007/s00107-014-0778-8

Koehler, A. (1955). *Guide to determining slope of grain in lumber and veneer*, U.S. Department of Agriculture, Forest Products Laboratory, Madison, WI.

Kohler, J., Brandner, R., Thiel, A.B., & Schickhofer, G. (2013). Probabilistic characterisation of the length effect for parallel to the grain tensile strength of Central European spruce, *Engineering Structures*, 56, 691-697. DOI: 10.1016/j.engstruct.2013.05.048

Konnerth, J., Kluge, M., Schweizer, G., Miljković, M., & Gindl-Altmutter, W. (2016). Survey of selected adhesive bonding properties of nine European softwood and hardwood species. *European Journal of Wood and Wood Products,* 74(6), 809–819. doi:10.1007/s00107-016-1087-1

Kosmidis, I. (2019). *Brglm: Bias Reduction in Binary-Response Generalized Linear Models*. R package version 0.6.2. Récupéré de : https://cran.r-project.org/package=brglm.

Kovryga, A., Schlotzhauer, P., Stapel, P., Militz, H., & van de Kuilen, J.W.G. (2019a). Visual and machine strength grading of European ash and maple for glulam application. *Holzforschung 2019*, 73(8), 773-787.

Kovryga, A., Stapel, P., & van de Kuilen, J.W.G. (2019b). Mechanical properties and their interrelationships for medium-density European hardwoods, focusing on ash and beech. *Wood Material Science & Engineering*, doi:10.1080/17480272.2019.1596158

Kovryga, A., Chuquin Gamarra, J.O., & van de Kuilen, J.W.G. (2019c). Machine strength and stiffness prediction with focus on different acoustic measurement methods, in: *Proceedings of the 7th International Scientific Conference on Hardwood Processing,* Delft, The Netherlands, pp. 211-219.

Kovryga, A., Sarnaghi, A.K., & van de Kuilen, J.W.G. (2019d). Strength grading of hardwoods using transversal ultrasound, in: *Proceedings of the 7th International Scientific Conference on Hardwood Processing*, Delft, The Netherlands, pp. 220-229.

Kretschmann, D.E., Bridwell, J.J., & Nelson, T.C. (2010). Effect of changing slope of grain on ash, maple and yellow birch bending strength, in: *Proceedings of WCTE 2010*, Riva Del Garda, Italy.

Laguarda Mallo, M.F., & Espinoza, O. (2015) Awareness, perceptions and willingness to adopt Cross-Laminated Timber by the architecture community in the United States. *Journal of Cleaner Production*, 94, 198–210. doi:10.1016/j.jclepro.2015.01.090

Lehmann, M., Clerc, G., Lehringer, C., Strahm, T., & Volkmer, T. (2018) Investigation of the bond quality and the finger joint strength of beech glulam. *Proceedings of WCTE 2018*, Seoul, Republic of Korea.

Lehringer, C., & Gabriel, J. (2014). Review of Recent Research Activities on One-Component PUR-Adhesives for Engineered Wood Products. in *Materials and Joints in Timber Structures*, Aicher, S., H.-W. Reinhardt, and H. Garrecht (eds.). Springer Netherlands, Dordrecht. pp. 405–420.

Lenth, R., Singmann, H., Love, J., Buerkner, P., & Herve, M. (2018). *Emmeans: Estimated marginal means, aka least-squares means*. Henrik Singmann [ctb], Jonathon. Récupéré de: https://CRAN.R-project.org/package=emmeans.

Liu, Y., Gong, M., Li, L., & Chui, Y.H. (2014). Width effect on the modulus of elasticity of hardwood lumber measured by non-destructive evaluation techniques, Construction and Building Materials, 50, 276-280. DOI: 10.1016/j.conbuildmat.2013.09.029

López-Suevos, F., & Richter, K. (2009). Hydroxymethylated Resorcinol (HMR) and Novolak-Based HMR (n-HMR) Primers to Enhance Bond Durability of Eucalyptus globulus Glulams. *Journal of Adhesion Science and Technology*, 23(15), 1925–1937. doi:10.1163/016942409X12508517390914

Luedtke, J., Amen, C., van Ofen, A., & Lehringer, C. (2015). 1C-PUR-bonded hardwoods for engineered wood products: influence of selected processing parameters. *European Journal of Wood and Wood Products*, 73(2), 167–178. doi:10.1007/s00107-014-0875-8

Manbeck, H.B., Blankenhorn, P.R., Janowiak, J.J., Witmer, R.W., Labosky, P., Powers, P.S., & Schram, P.D. (1999). Northern Red Oak Glued-Laminated Timber Bridge. *Journal of Bridge Engineering*, 4(4), 269–278.

Manbeck, H.B., Janowlak, J.J., Blankenhorn, P.R., Labosky, P. Jr., Moody, R.C., & Hernandez, R. (1993). *Performance of Red Maple Glulam Timber Beams (FPL–RP–519).* U.S. Department of Agriculture, Forest Service, Forest Products Laboratory. Madison, WI.

Manbeck, H.B., Janowiak, J.J., Blankenhorn, P.R., Labosky, P. (1996). Standard Designs for Hardwood Glued-laminated Highway Bridges, in *Proceedings of the National conference on wood transportation structures (FPL-GTR-94)*. Ritter, M.A., Duwadi, S.R., Lee, P.D.H., ed(s). Madison, WI. pp. 351–360.

Markström, E., Kuzman, M.K., Bystedt, A., Sandberg, D., & Fredriksson, M. (2018) Swedish architects view of engineered wood products in buildings. *Journal of Cleaner Production*, 181, 33–41. doi:10.1016/j.jclepro.2018.01.216

Martins, C., Dias, A.M.P.G., & Cruz, H. (2017), Glulam made by Poplar: delamination and shear strength tests. in: *Proceedings of the 6th International Scientific Conference on Hardwood Processing*. Lahti, Finland. pp. 222–231

Mazerolle, M.J. (2006). Improving data analysis in herpetology: using Akaike's Information Criterion (AIC) to assess the strength of biological hypotheses, *Amphibia-Reptilia,* 27, 169–180. DOI: 10.1163/156853806777239922

Mazerolle, M.J. (2019) AICcmodavg: Model selection and multimodel inference based on (Q)AIC(c), R package version 2.2-2. Récupéré de : (https://cran.r-project.org/package=AICcmodavg).

MFFP. (2015). *Ressources et industries forestières du Québec - Portrait statistique 2015*. Récupéré de: https://mffp.gouv.qc.ca/wp-content/uploads/portrait-statistique-2015.pdf.

Moody, R.C., Hernandez, R., Davalos, J. F., & Sonti, S. S. (1993). *Yellow Poplar Glulam Timber Beam Performance*. (Res. Paper FPL-RP-520), U.S. Department of Agriculture, Forest Service, Forest Products Laboratory, Madison, WI. 28 p.

Morin-Bernard, A., Blanchet, P., Dagenais, C. & Achim, A. (2020a). Use of northern hardwoods in glued-laminated timber: A study of bondline shear strength and resistance to moisture. *European Journal of Wood and Wood Products*. in press.

Morin-Bernard, A., Blanchet, P., Dagenais, C. & Achim, A. (2020b). Strength grading of northern hardwood species for structural engineered wood products: Identification of the relevant indicating properties. in preparation.

MRNF. (2012). *Stratégie 2012-2017 pour transformer l'industrie québécoise des produits forestiers*. Récupéré de: https://mffp.gouv.qc.ca/publications/forets/entreprises/strategie-developpement-2012-2017.pdf.

Nabuurs, G.J., Andrasko, K., Benitez-Ponce, P., Boer, R., Dutschke, M., Elsiddig, E., Ford-Robertson, J., *et al*. (2007). Ch. 9 – Forestry, in *Clim. Change 2007 Mitig. Contrib. Work. Group III Fourth Assess. Rep. Intergov. Panel Clim. Change*, B Metz Davidson PR Bosch R Dave LA Meyer Eds. Cambridge University Press, Cambridge, United Kingdom and New York, NY, USA.

Natural Resources Canada. (2018). *Indicateur : Volume récolté par rapport à l'approvisionnement en bois durable*. Récupéré de: https://www.rncan.gc.ca/forets/rapport/recolte/16551.

NHLA. (2019). *Rules for the measurement and inspection of hardwood and cypress*. National Hardwood Lumber Association. Memphis. TN. 102 p.

Niemz, P., & Mannes, D. (2012). Non-destructive testing of wood and wood-based materials. *Journal of Cultural Heritage* 13S S26-S34.

NLGA. (2014a). *Special Products Standard for Fingerjoined Machine Graded Lumber SPS-4*. National Lumber Grades Authority. Vancouver, Canada.

NLGA. (2014b). *Special Products Standard for Fingerjoined Structural Lumber SPS-1*. National Lumber Grades Authority. Vancouver, Canada.

NLGA. (2017). *Standard Grading Rules for Canadian Lumber*. National Lumber Grades Authority. Vancouver, Canada.

Nocetti, M., Brunetti, M., & Bacher, M. (2016). Efficiency of the machine grading of chestnut structural timber: prediction of strength classes by dry and wet measurements, *Materials and Structures*, 49, 4439-4450. DOI: 10.1617/s11527-016-0799-3

Ohnesorge, D., Richter, K., & Becker, G. (2010). Influence of wood properties and bonding parameters on bond durability of European Beech (*Fagus sylvatica* L.) glulams. *Annals of Forest Sciences*, 67(6), 601–601.

Okkonen, E.A., & River, B.H. (1989). Factors affecting the strength of block-shear specimens. *Forest Products Journal*, 39(1), 43-50.

Olsson, A., Oscarsson, J., Serrano, E., Källsner, B., Johansson, M., & Enquist, B. (2013). Prediction of timber bending strength and in-member cross-sectional stiffness variation on the basis of local wood fibre orientation, *European Journal of Wood Products*, 71, 319-333. DOI: 10.1007/s00107-013-0684-5

Panshin, A.J., Zeeuw, C.D. (1970). *Textbook of Wood Technology. Volume I. Structure, Identification, Uses, and Properties of the Commercial Woods of the United States and Canada*. McGraw-Hill Book Company Inc.: New York, NY. 643 p.

Pedersen, M.U., Clorius, C.O., Damkilde, P., & Hoffmeyer, P. (2003). A simple size effect model for tension perpendicular to grain," *Wood Science and Technology*, 37(2), 125–140. DOI: 10.1007/s00226-003-0168-6

Pizzi, A., & Mittal, K. (2003). *Handbook of Adhesive Technology, Revised and Expanded*. CRC Press. Récupéré de: http://www.crcnetbase.com/doi/book/10.1201/9780203912225.

Rao, S., Gong, M., Chui, Y. H., & Mohammad, M. (2012). Effect of geometric parameters of finger joint profile on ultimate tensile strength of single finger-joined boards. *Wood and Fiber Science*, 44(3), 263-270.

Ravenshorst, G.J.P. (2015). Species independent strength grading of structural timber, PhD Thesis, Technische Universiteit Delft, Delft, The Netherlands.

Ravenshorst, G., Gard, W.F., & van de Kuilen, J.W.G. (2019). Influence of slope of grain on the mechanical properties of hardwoods and the consequences for grading, in: *Proceedings of the 7th International Scientific Conference on Hardwood Processing*, Delft, The Netherlands, pp. 169-175.

R Core Team. (2018). *R: A language and environment for statistical computing*. Récupéré de: http://www.R-project.org/.

R Core Team. (2019). *R: A language and environment for statistical computing*. Récupéré de: http://www.R-project.org/.

Ridley-Ellis, D., Stapel, P., & Baño, V. (2016). Strength grading of sawn timber in Europe: an explanation for engineers and researchers. *European Journal of Wood Products*, 74, 291-306. doi:10.1007/s00107-016-1034-1

Riesco-Muñoz, G., Remacha-Gete, A., & Pedras-Saavedra, F. (2011) Implications in the design of a method for visual grading and mechanical testing of hardwood structural timber for assignation within the European strength classes, *Forest Systems*, 20(2), 235-244. DOI: 10.5424/fs/2011202-9771

Riesco-Muñoz, G., & Remacha-Gete, A. (2012). Prediction of Bending Strength in Oak Beams on the Basis of Elasticity, Density, and Wood Defects, *Journal of Materials in Civil Engineering*, 24(6), 629-634. DOI: 10.1061/(ASCE)MT.1943-5533.0000428

Ritter, M.A., Williamson, T.G., & Moody, R.C. (1994). Innovations in Glulam Timber Bridge Design. *Proceedings of Structures Congress '94*, American Society of Civil Engineers, Atlanta, GA. New York, 1298-1303.

River, B.H., Vick, C.B., & Gillespie, R.H. (1991). *Wood as an adherend.* Treatise on adhesion and adhesives. Vol 7. Marcel Dekker Inc., New York. 230 p.

Ressources Naturelles Canada. (2018). *Indicateur : Volume récolté par rapport à l'approvisionnement en bois durable*. Récupéré de: https://www.rncan.gc.ca/forets/rapport/recolte/16551.

Ross, R.J. (2010). *Wood handbook: wood as an engineering material*, (Gen. Tech. Rep. FPL-GTR-190). U.S. Department of Agriculture, Forest Service, Forest Products Laboratory, Madison, WI. 508 p.

Ross, R.J., & Erickson, J.R. (2020). *Undervalued hardwoods for engineered materials and components: second edition*. (Gen. Tech. Rep. FPL-GTR-276). U.S. Department of Agriculture, Forest Service, Forest Products Laboratory, Madison, WI. 108 p.

Sarnaghi, A.K., Gard, W.F., & van de Kuilen, J.W.G. (2017). 3D FE-numerical modelling of growth defects in medium dense European hardwoods, in: *Proceedings of the 6th International Scientific Conference on Hardwood Processing*, Lahti, Finland, pp.116-122.

Schlesinger, R.C. (1990). *Fraxinus Americana* L. in: *Sylvics of North America, Volume 2, Hardwoods*. Agriculture handbook 654. U.S. Department of Agriculture, Forest Service. Washington D.C. pp. 333-338.

Schlotzhauer, P., Nelis, P.A., Bollmus, S., Gellerich, A., Militz, H., & Seim, W. (2017). Effect of size and geometry on strength values and MOE of selected hardwood species, *Wood Material Science and Engineering*, 12(3), 149-157. DOI: 10.1080/17480272.2015.1073175

Schlotzhauer, P., Kovryga, A., Emmerich, L., Bollmus, S., Van de Kuilen, J.W.G., & Militz, H. (2019). Analysis of Economic Feasibility of Ash and Maple Lamella Production for Glued Laminated Timber. *Forests*. 10, 529. doi:10.3390/f10070529

Selbo, M.L. (1963). Effect of joint geometry on tensile strength of finger-joints. *Forest Products Journal, 13*(9), 390-400.

Selbo, M.L. (1975). *Adhesive bonding of wood (Tech. Bull. No. 1512)*. U.S. Department of Agriculture, Forest Service, Washington D.C. 122 p.

Sellers, T., McSween, J.R., & Nearn, W.T. (1988). *Gluing of Eastern Hardwoods: A Review*. (Gen. Tech. Rep. SO-71). U.S. Department of Agriculture, Forest Service, Southern Forest Experiment Station. New Orleans, LA, 30 p.

Shedlauskas, J.P., Manbeck, H.B., Janowiak, J.J., Hernandez, R., Moody, R.C., Labosky, P., & Blankenhorn P.R. Jr. (1996). Efficient Use of Red Oak for Glued-laminated Beams. *Transactions of the ASAE*, 39(1), 203–209. doi:10.13031/2013.27499

Smulski, S.J. (1991). Relationship of stress wave-and static bending-determined properties of four northeastern hardwoods, *Wood and Fiber Science*, 23(1), 44-57.

Stapel, P., & van de Kuilen, J.W.G. (2014). Efficiency of visual strength grading of timber with respect to origin, species, cross-section, and grading rules: a critical evaluation of the common standards, *Holzforschung*, 68(2), 203-216. DOI: 10.1515/hf-2013-0042

Statistics Canada. (2019). *Report – Trade data online: Canadian trade balances – oak lumber* (HS 440791). Récupéré de: https://www.ic.gc.ca/eic/site/tdo-dcd.nsf/eng/Home.

Strøbech, C. (1990). Polyurethane adhesives. *International Journal of Adhesion and Adhesives,* 10(3), 225–228.

Steiger, R., Gehri, E., & Richter, K. (2010). Quality control of glulam: shear testing of bondlines. *European Journal of Wood and Wood Products,* 68(3): 243–256. doi:10.1007/s00107-010-0456-4

Stoeckel, F., Konnerth, J., & Gindl-Altmutter, W. (2013). Mechanical properties of adhesives for bonding wood—A review. *International Journal of Adhesion and Adhesives*, 45, 32–41. doi:10.1016/j.ijadhadh.2013.03.013

Strickler, M.D. (1980). Finger-jointed dimensioned lumber: past, present and future, *Forest Products Journal*, 30 (9) 51–56.

Tardif, J.C., Conciatori, F., Nantel, P., & Gagnon, D. (2006). Radial Growth and Climate Responses of White Oak (Quercus alba) and Northern Red Oak (Quercus rubra) at the Northern Distribution Limit of White Oak in Quebec, Canada. *Journal of Biogeography*, 33(9), 1657–1669. doi:10.1111/j.1365-2699.2006.01541.x

Thelandersson, S., & Larsen, H.J. (2003). *Timber engineering*. Chichester, UK: John Wiley and Sons Ltd. West Sussex, England. 456 p.

Thormark, C. (2006). The effect of material choice on the total energy need and recycling potential of a building. *Building and Environment*, 41(8), 1019–1026. doi:10.1016/j.buildenv.2005.04.026

Tran V.-D., Oudjene, M., & Méausoone, P.-J. (2014a). Experimental and numerical analyses of the structural response of adhesively reconstituted beech timber beams. *Composite Structures,* 119, 206–217. doi: doi.org/10.1016/j.compstruct.2014.08.013

Tran, V.-D., Oudjene, M., & Méausoone, P.-J. (2014b). FE analysis and geometrical optimization of timber beech finger-joint under bending test. *International Journal of Adhesion & Adhesives*, 52, 40-47. doi: doi.org/10.1016/j.ijadhadh.2014.03.007

Tran, V.-D., Oudjene, M., & Méausoone, P.-J. (2016). Experimental investigation on fullscale glued oak solid timber beams for structural bearing capacity, *Construction and Building Materials*, 123, 365–371. doi: doi.org/10.1016/j.conbuildmat.2016.07.002

UNECE/FAO. (2018). *Forest Products - Annual Market Review 2017-2018*. Récupéré de: https://www.unece.org/fileadmin/DAM/timber/publications/FPAMR2018.pdf.

Vega, A., Arriaga, F., Guaita, M., & Baño, V. (2013). Proposal for visual grading criteria of structural timber of sweet chestnut from Spain, *European Journal of Wood Products*, 71, 529-532. DOI: 10.1007/s00107-013-0705-4

Verreault, C. (2000). *Utilisation des cœurs de bois francs dans des bois d'ingénierie à usage structural*. Forintek Canada Corp.

Vick, C.B. (1995). Hydroxymethylated Resorcinol Coupling Agent for enhanced Adhesion of Epoxy and Other Thermosetting Adhesives. *Proceedings of the 1996 symposium sponsored by U.S. Department of Agriculture Forest Service, Forest Products Laboratory and the Forest Products society 1995*, Madison, WI, 47-55.

Vick, C.B., & Okkonen, E.A. (1998). Strength and Durability of One-Part Polyurethane Adhesive Bonds to Wood. *Forest Products Journal* 48(11), 71–76.

Vick, C.B., (1999). Adhesive Bonding of Wood Materials. in *Wood handbook—Wood as an engineering material*., U.S. Department of Agriculture, Forest Service, Forest Products Laboratory., Madison, WI. pp. 9.1 – 9.24.

Weibull, W. (1939). A statistical theory of the strength of material, in: *The Royal Swedish Institute for Engineering Research, Proceedings No. 151*, Stockholm, Sweeden, pp. 1–45.

Weidenhiller, A., Linsenmann, P., Lux, C., & Brüchert, F. (2019). Potential of microwave scanning for determining density and tension strength of four European hardwood species. *European Journal of Wood and Wood Products*, 77, 235-247. doi:10.1007/s00107-019-01387-x

Westermayr, M., Stapel, P., & van de Kuilen, J.W.G. (2018). Tensile strength and stiffness of low-quality beech (Fagus sylvatica) sawn timber, in: *Proceedings of WCTE 2018*, Seoul, South Korea.

Widmann, R., Beikircher, W., Cabo, J.L.F., & Steiger, R. (2014). Bending Strength and Stiffness of Glulam Beams Made of Thermally Modified Beech Timber. in *Materials and Joints in Timber Structures*, Aicher, S., H.-W. Reinhardt, and H. Garrecht (eds.). Springer Netherlands, Dordrecht. pp. 569–576. doi:10.1007/978-94-007-7811-5_52

Xiao, H., Wang, W., & Chui, Y. H. (2007). *Evaluation of Shear Strength and Percent Wood Failure Criteria for Qualifying New Structural Adhesives*. Rapport de l'Université du Nouveau Brunswick pour Ressources Naturelles Canada. Récupéré de : https://unb.ca/fredericton/forestry/wstc/_resources/pdf/unb50.pdf; last accessed October 30, 2018.

Zhang, S.Y. (1997). Wood specific gravity-mechanical property relationship at species level, *Wood Science and Technology*, 31, 181-191. DOI: 10.1007/BF00705884

Annexe A – Analyses relatives au chapitre 2.

A1. Analyse des données des essais de résistance au cisaillement

A1.1 Analyses de variance

A1.1.1 Essais à l'état sec

```
> lmer_dry <- lmer(Fv_Mpa ~ GROUP * (1|COLLAGE), data = Global_dry)
> Anova(lmer_dry)
Analysis of Deviance Table (Type II Wald chisquare tests)

Response: Fv_Mpa
      Chisq Df Pr(>Chisq)
GROUP  39.8  7  1.375e-06 ***
```

A1.1.2 Essais en conditions humides

```
> lmer_wet <- lmer(Fv_Mpa ~ GROUP * (1|COLLAGE), data = Global_wet)
> Anova(lmer_wet)
Analysis of Deviance Table (Type II Wald chisquare tests)

Response: Fv_Mpa
       Chisq Df Pr(>Chisq)
GROUP 58.634  7  2.827e-10 ***
---
Signif. codes:  0 '***' 0.001 '**' 0.01 '*' 0.05 '.' 0.1 ' ' 1
```

A1.2 Comparaisons multiples

A1.2.1 Essais à l'état sec

```
> HSD_lmer_dry<-emmeans(lmer_dry, "GROUP")
> pairs(HSD_lmer_dry)
 contrast                              estimate    SE   df t.ratio p.value
 MF-Paper birch - MF-White ash        -2.50358 0.756 39.6 -3.313  0.0376
 MF-Paper birch - MF-White oak        -4.05869 0.756 39.6 -5.372  0.0001
 MF-Paper birch - MF-Yellow birch     -1.87510 0.756 39.6 -2.482  0.2328
 MF-Paper birch - PUR2-Paper birch    -1.02678 0.756 39.6 -1.359  0.8699
 MF-Paper birch - PUR2-White ash      -2.25331 0.756 39.6 -2.982  0.0830
 MF-Paper birch - PUR2-White oak      -2.95189 0.756 39.6 -3.907  0.0078
 MF-Paper birch - PUR2-Yellow birch   -1.03157 0.756 39.6 -1.365  0.8672
 MF-White ash - MF-White oak          -1.55511 0.756 39.6 -2.058  0.4582
 MF-White ash - MF-Yellow birch        0.62848 0.756 39.6  0.832  0.9901
 MF-White ash - PUR2-Paper birch       1.47680 0.756 39.6  1.954  0.5238
 MF-White ash - PUR2-White ash         0.25028 0.756 39.6  0.331  1.0000
 MF-White ash - PUR2-White oak        -0.44831 0.756 39.6 -0.593  0.9988
 MF-White ash - PUR2-Yellow birch      1.47201 0.756 39.6  1.948  0.5279
 MF-White oak - MF-Yellow birch        2.18359 0.756 39.6  2.890  0.1021
 MF-White oak - PUR2-Paper birch       3.03191 0.756 39.6  4.013  0.0057
 MF-White oak - PUR2-White ash         1.80539 0.756 39.6  2.389  0.2744
 MF-White oak - PUR2-White oak         1.10680 0.756 39.6  1.465  0.8209
 MF-White oak - PUR2-Yellow birch      3.02712 0.756 39.6  4.006  0.0059
 MF-Yellow birch - PUR2-Paper birch    0.84832 0.756 39.6  1.123  0.9478
```

```
 MF-Yellow birch - PUR2-White ash     -0.37820 0.756 39.6 -0.501  0.9996
 MF-Yellow birch - PUR2-White oak     -1.07679 0.756 39.6 -1.425  0.8402
 MF-Yellow birch - PUR2-Yellow birch   0.84353 0.756 39.6  1.116  0.9493
 PUR2-Paper birch - PUR2-White ash    -1.22652 0.756 39.6 -1.623  0.7338
 PUR2-Paper birch - PUR2-White oak    -1.92511 0.756 39.6 -2.548  0.2059
 PUR2-Paper birch - PUR2-Yellow birch -0.00479 0.756 39.6 -0.006  1.0000
 PUR2-White ash - PUR2-White oak      -0.69859 0.756 39.6 -0.925  0.9818
 PUR2-White ash - PUR2-Yellow birch    1.22173 0.756 39.6  1.617  0.7375
 PUR2-White oak - PUR2-Yellow birch    1.92032 0.756 39.6  2.541  0.2083

P value adjustment: tukey method for comparing a family of 8 estimates
```

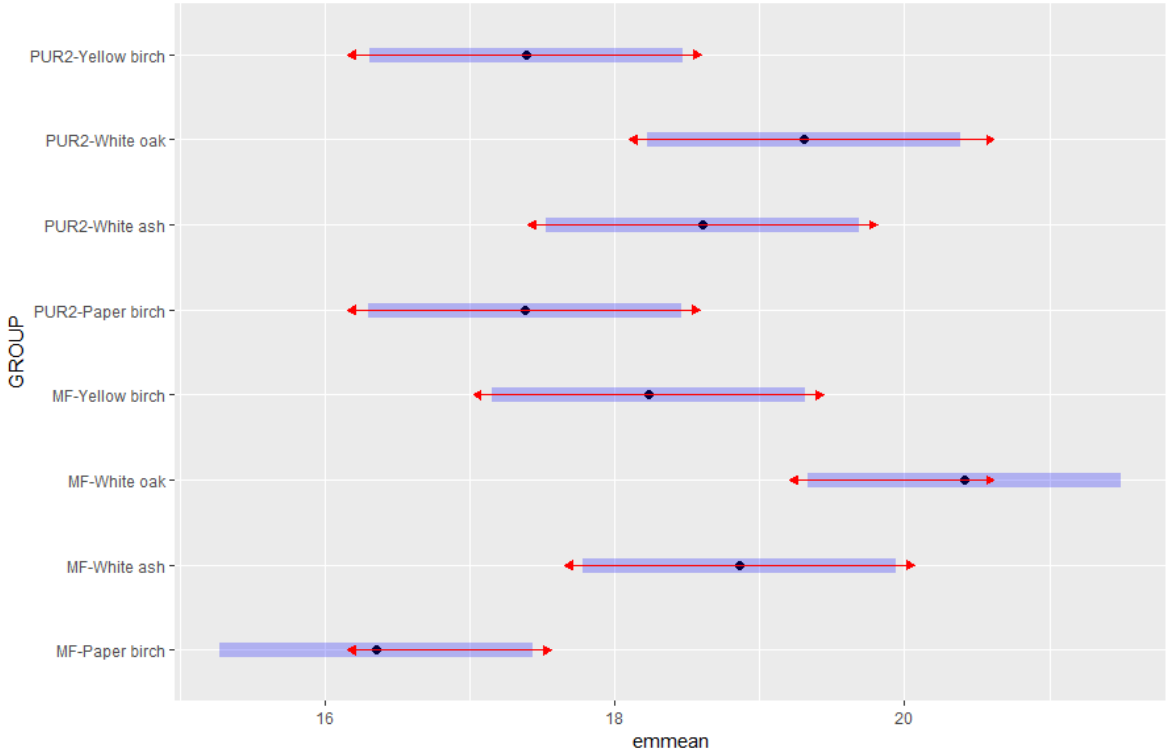

A1.2.2 Essais en conditions humides

```
> HSD_lmer_wet<-emmeans(lmer_wet, "GROUP")
> pairs(HSD_lmer_wet)
 contrast                          estimate    SE   df t.ratio p.value
 MF-Paper birch - MF-White ash      -2.5033 0.583 35.3 -4.293  0.0030
 MF-Paper birch - MF-White oak      -2.7432 0.583 35.3 -4.704  0.0009
 MF-Paper birch - MF-Yellow birch   -1.0786 0.596 32.6 -1.810  0.6179
 MF-Paper birch - PUR2-Paper birch  -0.0389 0.596 32.6 -0.065  1.0000
 MF-Paper birch - PUR2-White ash    -0.3159 0.583 35.3 -0.542  0.9993
 MF-Paper birch - PUR2-White oak     0.2531 0.583 35.3  0.434  0.9998
 MF-Paper birch - PUR2-Yellow birch -0.1977 0.596 32.6 -0.332  1.0000
 MF-White ash - MF-White oak        -0.2399 0.570 38.6 -0.421  0.9999
 MF-White ash - MF-Yellow birch      1.4247 0.583 35.3  2.443  0.2529
 MF-White ash - PUR2-Paper birch     2.4644 0.583 35.3  4.226  0.0036
 MF-White ash - PUR2-White ash       2.1874 0.570 38.6  3.836  0.0097
 MF-White ash - PUR2-White oak       2.7564 0.570 38.6  4.834  0.0005
 MF-White ash - PUR2-Yellow birch    2.3056 0.583 35.3  3.954  0.0076
 MF-White oak - MF-Yellow birch      1.6647 0.583 35.3  2.855  0.1136
 MF-White oak - PUR2-Paper birch     2.7043 0.583 35.3  4.637  0.0011
 MF-White oak - PUR2-White ash       2.4273 0.570 38.6  4.257  0.0029
 MF-White oak - PUR2-White oak       2.9963 0.570 38.6  5.255  0.0001
```

```
 MF-White oak - PUR2-Yellow birch       2.5455 0.583 35.3  4.365  0.0024
 MF-Yellow birch - PUR2-Paper birch     1.0396 0.596 32.6  1.745  0.6592
 MF-Yellow birch - PUR2-White ash       0.7626 0.583 35.3  1.308  0.8898
 MF-Yellow birch - PUR2-White oak       1.3317 0.583 35.3  2.284  0.3304
 MF-Yellow birch - PUR2-Yellow birch    0.8808 0.596 32.6  1.478  0.8129
 PUR2-Paper birch - PUR2-White ash     -0.2770 0.583 35.3 -0.475  0.9997
 PUR2-Paper birch - PUR2-White oak      0.2920 0.583 35.3  0.501  0.9996
 PUR2-Paper birch - PUR2-Yellow birch  -0.1588 0.596 32.6 -0.267  1.0000
 PUR2-White ash - PUR2-White oak        0.5690 0.570 38.6  0.998  0.9720
 PUR2-White ash - PUR2-Yellow birch     0.1182 0.583 35.3  0.203  1.0000
 PUR2-White oak - PUR2-Yellow birch    -0.4508 0.583 35.3 -0.773  0.9935

P value adjustment: tukey method for comparing a family of 8 estimates
```

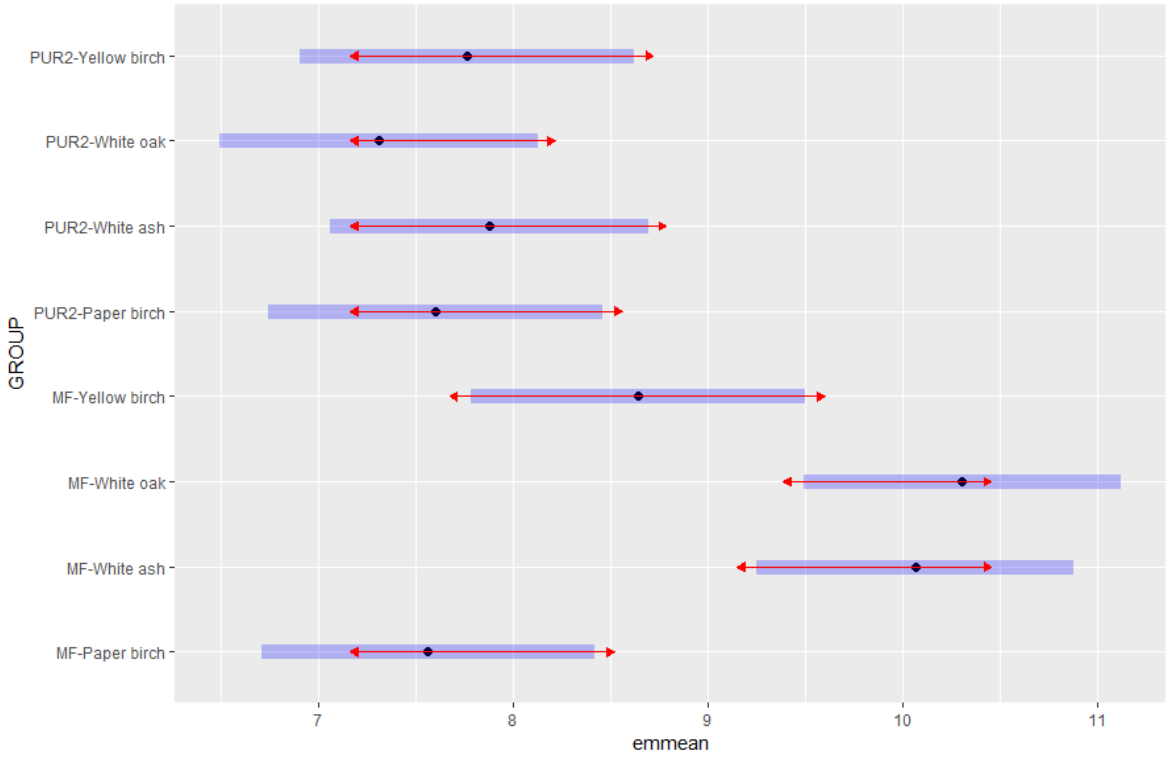

A1.3 Impact de la masse volumique sur le taux de rupture dans le bois

A1.3.1 Bouleau à papier

```
Call:
lm(formula = RUPT_BOIS ~ MV, data = BOP)

Residuals:
    Min      1Q  Median      3Q     Max
-19.822  -3.558   5.115   5.155   5.221

Coefficients:
             Estimate Std. Error t value Pr(>|t|)
(Intercept) 92.994008  71.345808   1.303    0.203
MV           0.002986   0.115796   0.026    0.980

Residual standard error: 7.732 on 28 degrees of freedom
Multiple R-squared:  2.375e-05,       Adjusted R-squared:  -0.03569
F-statistic: 0.0006649 on 1 and 28 DF,  p-value: 0.9796
```

A1.3.2 Bouleau jaune

```
Call:
lm(formula = RUPT_BOIS ~ MV, data = BOJ)

Residuals:
    Min      1Q  Median      3Q     Max
-70.448  -9.094   3.630  14.264  21.238

Coefficients:
            Estimate Std. Error t value Pr(>|t|)
(Intercept) 279.8768    90.1646   3.104  0.00434 **
MV           -0.3031     0.1380  -2.196  0.03651 *
---
Signif. codes:  0 ‘***’ 0.001 ‘**’ 0.01 ‘*’ 0.05 ‘.’ 0.1 ‘ ’ 1

Residual standard error: 20.04 on 28 degrees of freedom
Multiple R-squared:  0.147,    Adjusted R-squared:  0.1165
F-statistic: 4.824 on 1 and 28 DF,  p-value: 0.03651
```

A1.3.3 Frêne d’Amérique

```
Call:
lm(formula = RUPT_BOIS ~ MV, data = FRA)

Residuals:
    Min      1Q  Median      3Q     Max
-42.147 -13.452   1.724  18.161  46.241

Coefficients:
            Estimate Std. Error t value Pr(>|t|)
(Intercept) 571.0934   141.7840   4.028  0.00039 ***
MV           -0.6846     0.1934  -3.541  0.00142 **
---
Signif. codes:  0 ‘***’ 0.001 ‘**’ 0.01 ‘*’ 0.05 ‘.’ 0.1 ‘ ’ 1

Residual standard error: 24.07 on 28 degrees of freedom
Multiple R-squared:  0.3093,   Adjusted R-squared:  0.2846
F-statistic: 12.54 on 1 and 28 DF,  p-value: 0.001418
```

A1.3.4 Chêne blanc

```
Call:
lm(formula = RUPT_BOIS ~ MV, data = CHB)

Residuals:
    Min      1Q  Median      3Q     Max
-38.457 -12.253  -2.558  15.233  38.814

Coefficients:
            Estimate Std. Error t value Pr(>|t|)
(Intercept) 280.83095   33.60723   8.356 4.32e-09 ***
MV           -0.29344    0.04339  -6.763 2.41e-07 ***
---
Signif. codes:  0 ‘***’ 0.001 ‘**’ 0.01 ‘*’ 0.05 ‘.’ 0.1 ‘ ’ 1

Residual standard error: 20.78 on 28 degrees of freedom
Multiple R-squared:  0.6203,   Adjusted R-squared:  0.6067
F-statistic: 45.74 on 1 and 28 DF,  p-value: 2.411e-07
```

Annexe B – Analyses relatives au chapitre 3.

B1. Essais de lamelles jointées - Distributions Weibull et 5e percentile

Bouleau jaune – Joint de 22 mm, adhésif PUR

```
> WBULL_BOJ_PUR_22 <- fitdist(Results_BOJ_PUR_22$UTS_MPa, "weibull")
> summary(WBULL_BOJ_PUR_22)
Fitting of the distribution ' weibull ' by maximum likelihood
Parameters :
       estimate Std. Error
shape  9.104518  1.2526245
scale 38.158328  0.8562803
Loglikelihood:  -77.74689   AIC:  159.4938   BIC:  162.0855
Correlation matrix:
          shape     scale
shape 1.0000000 0.3358569
scale 0.3358569 1.0000000

> plot(WBULL_BOJ_PUR_22)
> quantile(WBULL_BOJ_PUR_22, probs = 0.05)
Estimated quantiles for each specified probability (non-censored data)
            p=0.05
estimate 27.53646
```

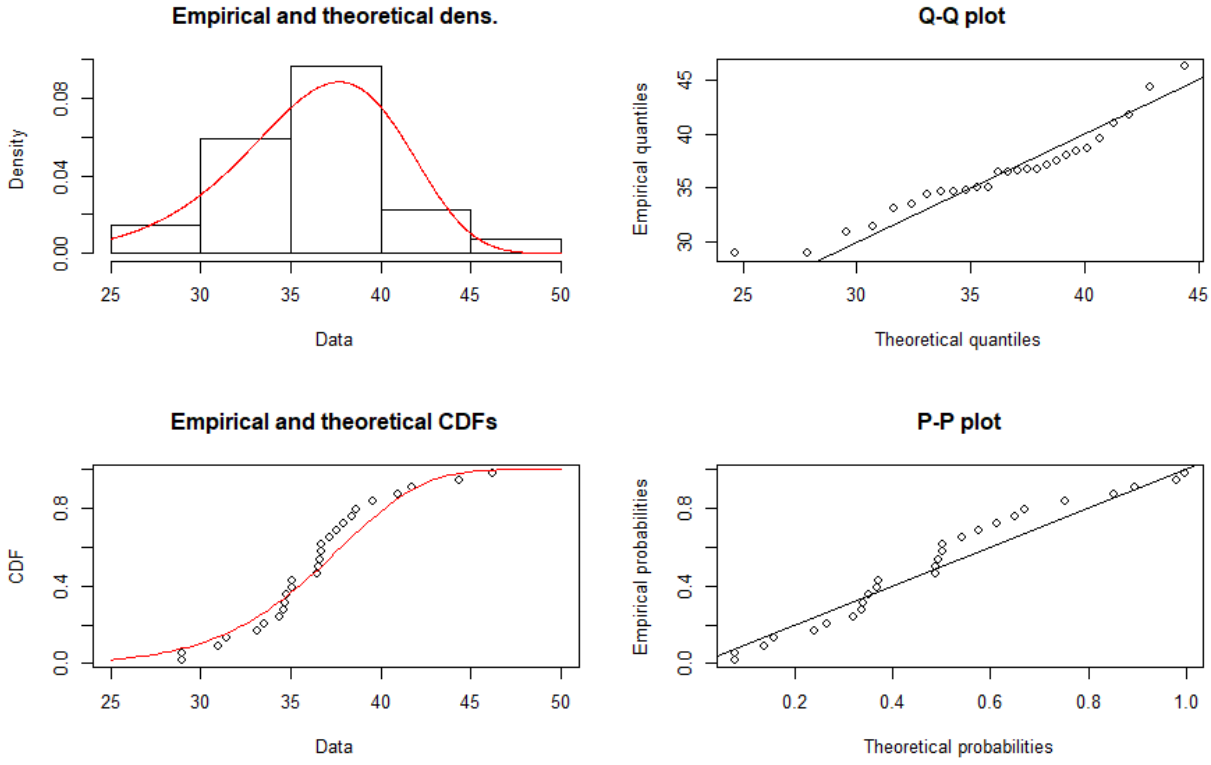

Bouleau jaune – Joint de 22 mm, adhésif MF

```
> WBULL_BOJ_MF_22 <- fitdist(Results_BOJ_MF_22$UTS_MPa, "weibull")
```

```
> summary(WBULL_BOJ_MF_22)
Fitting of the distribution ' weibull ' by maximum likelihood
Parameters :
       estimate Std. Error
shape  7.715645  1.1328396
scale 34.228787  0.8649068
Loglikelihood:  -87.23828   AIC:  178.4766   BIC:  181.2112
Correlation matrix:
          shape     scale
shape 1.0000000 0.3041785
scale 0.3041785 1.0000000

> plot(WBULL_BOJ_MF_22)
> quantile(WBULL_BOJ_MF_22, probs = 0.05)
Estimated quantiles for each specified probability (non-censored data)
           p=0.05
estimate 23.29199
```

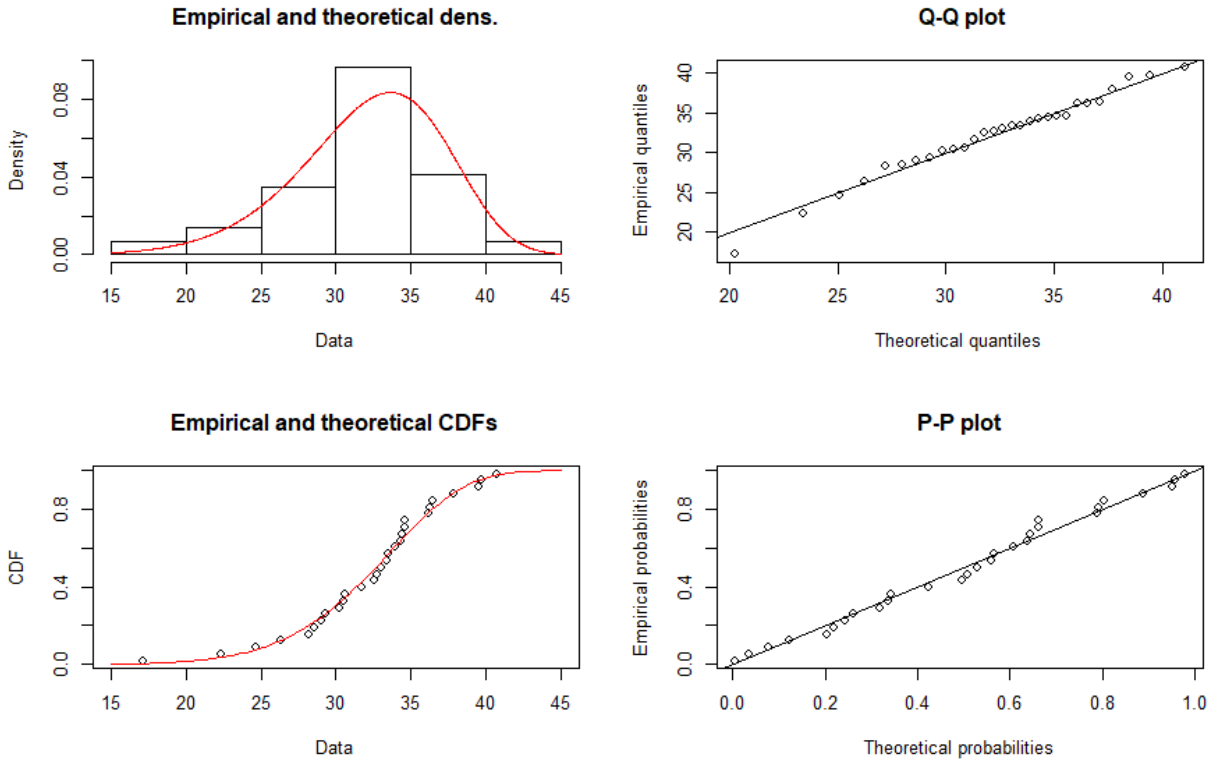

Bouleau jaune – Joint de 15 mm, adhésif PUR

```
> WBULL_BOJ_PUR_15 <- fitdist(Results_BOJ_PUR_15$UTS_MPa, "weibull")
> summary(WBULL_BOJ_PUR_15)
Fitting of the distribution ' weibull ' by maximum likelihood
Parameters :
      estimate Std. Error
shape 10.76389  1.4381185
scale 44.27960  0.7569037
Loglikelihood:  -96.26103   AIC:  196.5221   BIC:  199.5151
Correlation matrix:
          shape     scale
shape 1.0000000 0.3239293
scale 0.3239293 1.0000000
```

```
> plot(WBULL_BOJ_PUR_15)
> quantile(WBULL_BOJ_PUR_15, probs = 0.05)
Estimated quantiles for each specified probability (non-censored data)
          p=0.05
estimate 33.60193
```

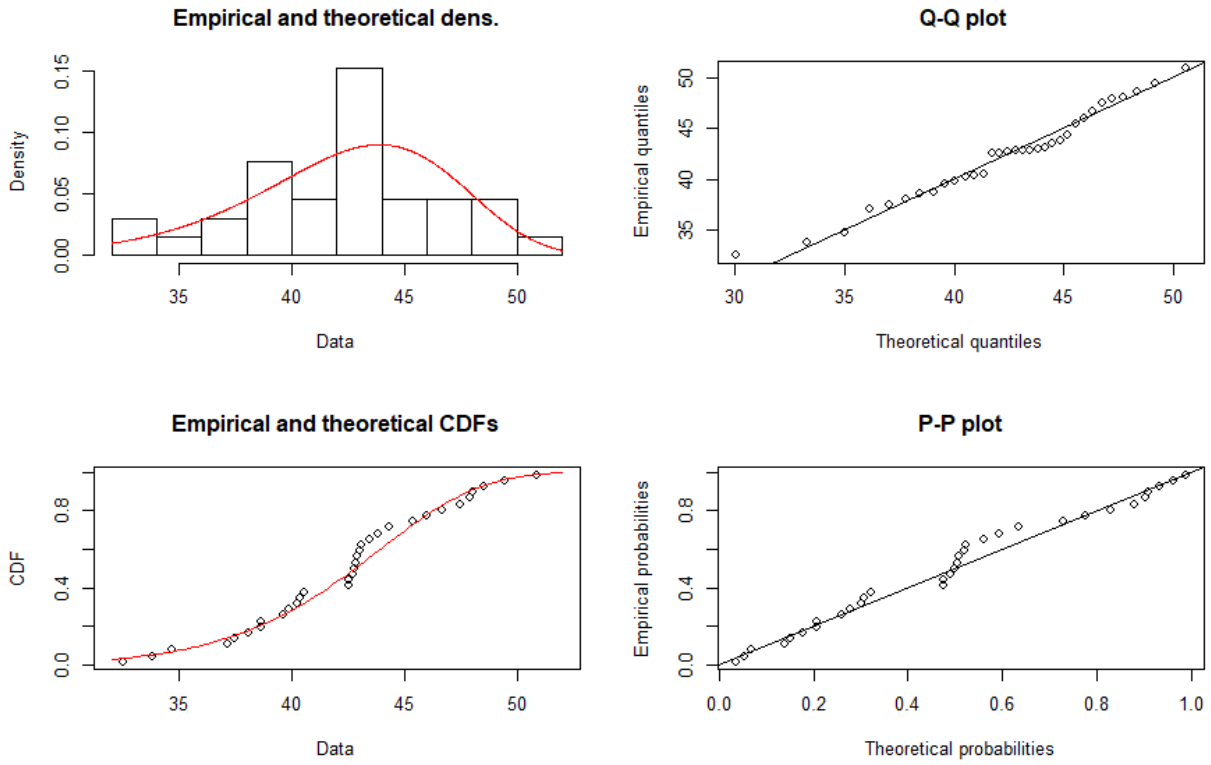

Bouleau jaune – Joint de 15 mm, adhésif MF

```
> # WEIBULL
> WBULL_BOJ_MF_15 <- fitdist(Results_BOJ_MF_15$UTS_MPa, "weibull")
> summary(WBULL_BOJ_MF_15)
Fitting of the distribution ' weibull ' by maximum likelihood
Parameters :
       estimate Std. Error
shape  8.273225   1.213785
scale 46.411844   1.142576
Loglikelihood:  -86.51566   AIC:  177.0313   BIC:  179.623
Correlation matrix:
          shape    scale
shape 1.000000 0.327544
scale 0.327544 1.000000

> plot(WBULL_BOJ_MF_15)
> quantile(WBULL_BOJ_MF_15, probs = 0.05)
Estimated quantiles for each specified probability (non-censored data)
          p=0.05
estimate 32.41242
```

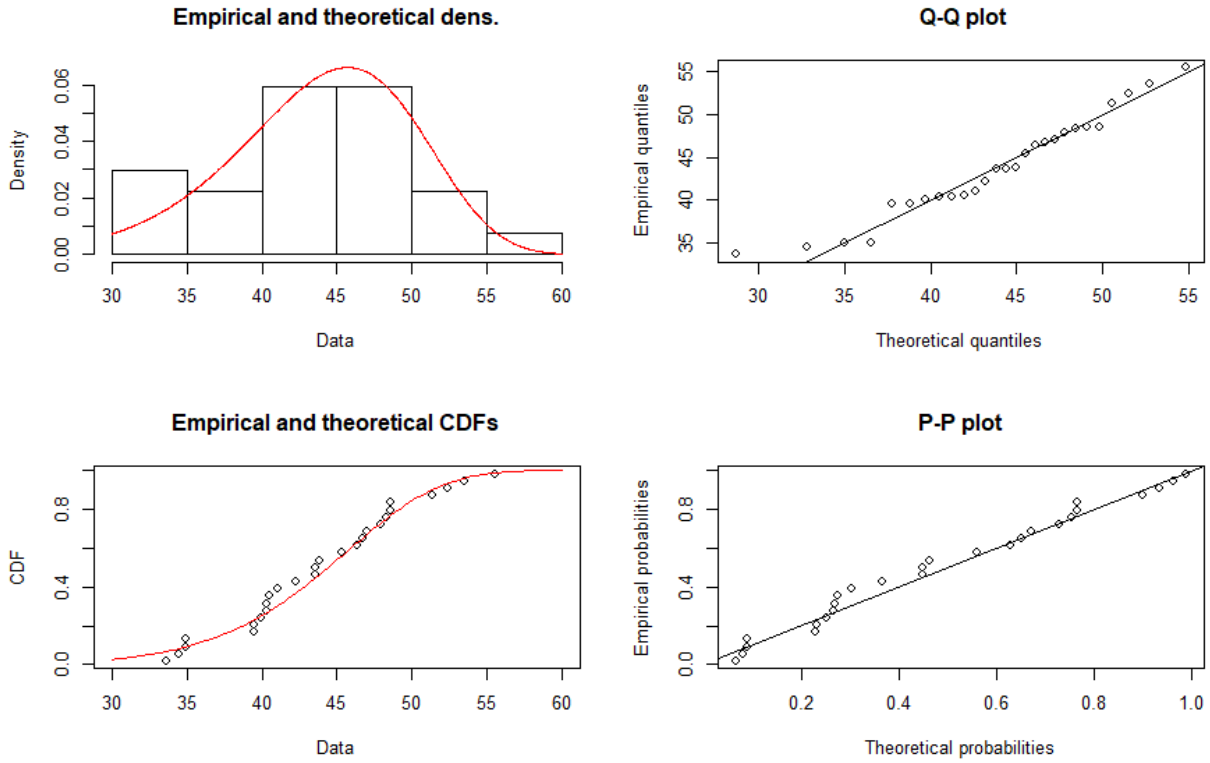

Frêne d'Amérique – Joint de 22 mm, adhésif PUR

```
> WBULL_FRA_PUR_22 <- fitdist(Results_FRA_PUR_22$UTS_MPa, "weibull")
> summary(WBULL_FRA_PUR_22)
Fitting of the distribution ' weibull ' by maximum likelihood
Parameters :
       estimate Std. Error
shape  6.359267  0.9127364
scale 39.111335  1.1562441
Loglikelihood:  -103.3251   AIC:  210.6501   BIC:  213.5181
Correlation matrix:
          shape     scale
shape 1.0000000 0.2952255
scale 0.2952255 1.0000000

> plot(WBULL_FRA_PUR_22)
> quantile(WBULL_FRA_PUR_22, probs = 0.05)
Estimated quantiles for each specified probability (non-censored data)
            p=0.05
estimate 24.51651
```

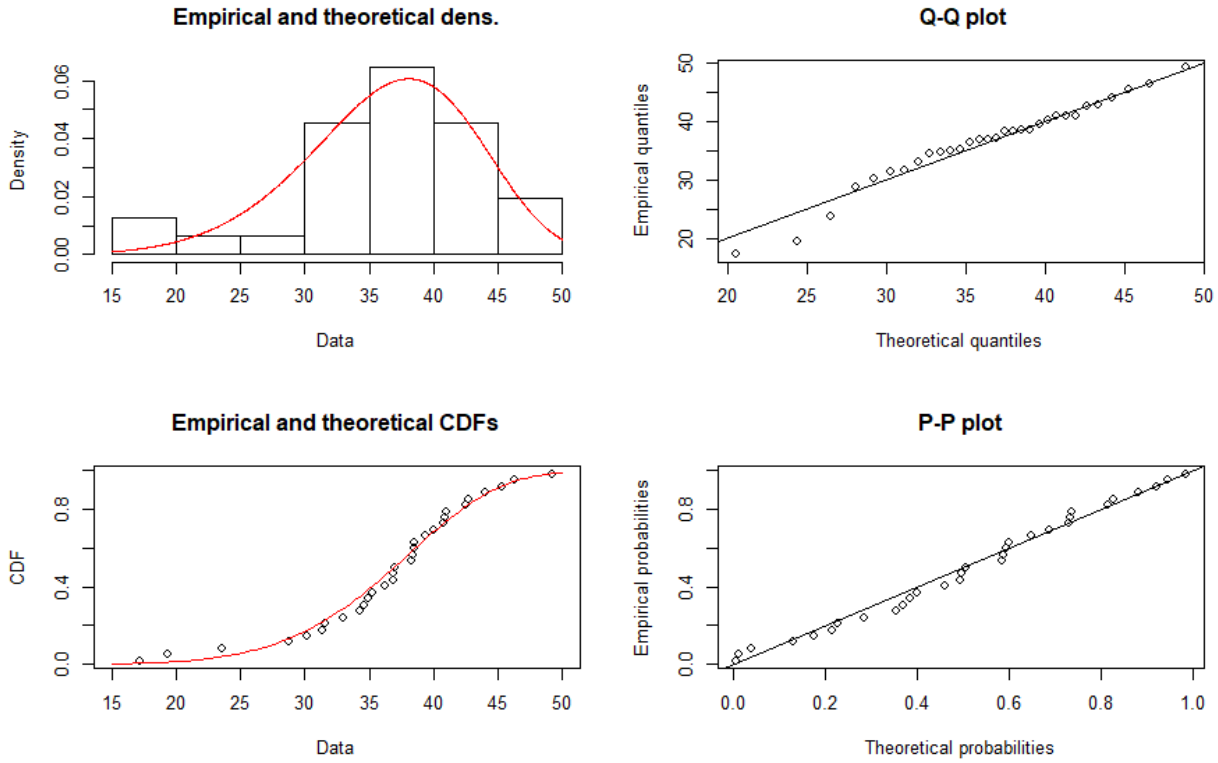

Frêne d'Amérique – Joint de 22 mm, adhésif MF

```
> WBULL_FRA_MF_22 <- fitdist(Results_FRA_MF_22$UTS_MPa, "weibull")
> summary(WBULL_FRA_MF_22)
Fitting of the distribution ' weibull ' by maximum likelihood
Parameters :
       estimate Std. Error
shape  7.960005  1.1221399
scale 38.152538  0.9255633
Loglikelihood:  -91.54375   AIC:  187.0875   BIC:  189.8899
Correlation matrix:
          shape     scale
shape 1.0000000 0.3257336
scale 0.3257336 1.0000000

> plot(WBULL_FRA_MF_22)
> quantile(WBULL_FRA_MF_22, probs = 0.05)
Estimated quantiles for each specified probability (non-censored data)
            p=0.05
estimate 26.27065
```

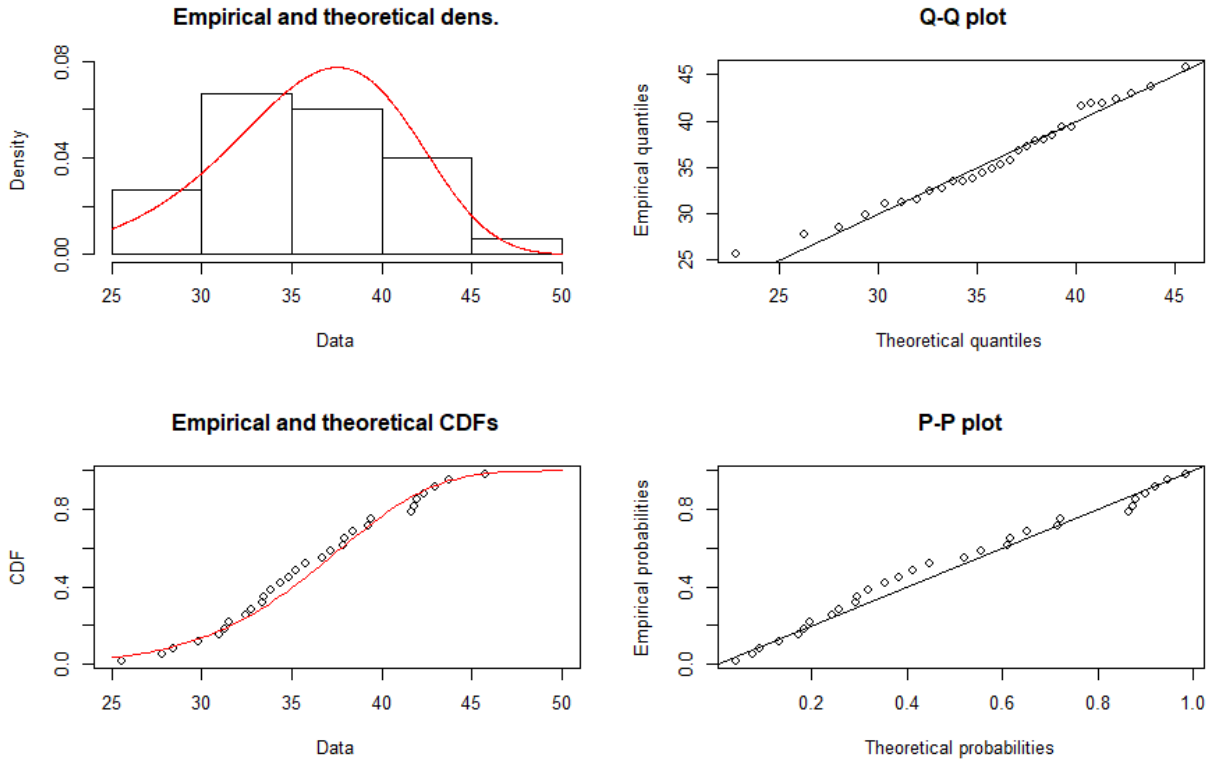

Frêne d'Amérique – Joint de 15 mm, adhésif PUR

```
> WBULL_FRA_PUR_15 <- fitdist(Results_FRA_PUR_15$UTS_MPa, "weibull")
> summary(WBULL_FRA_PUR_15)
Fitting of the distribution ' weibull ' by maximum likelihood
Parameters :
       estimate Std. Error
shape  8.826763   1.145015
scale 49.584981   1.051794
Loglikelihood:  -102.1066   AIC:  208.2133   BIC:  211.1447
Correlation matrix:
         shape    scale
shape 1.000000 0.329827
scale 0.329827 1.000000

> plot(WBULL_FRA_PUR_15)
> quantile(WBULL_FRA_PUR_15, probs = 0.05)
Estimated quantiles for each specified probability (non-censored data)
          p=0.05
estimate 35.4169
```

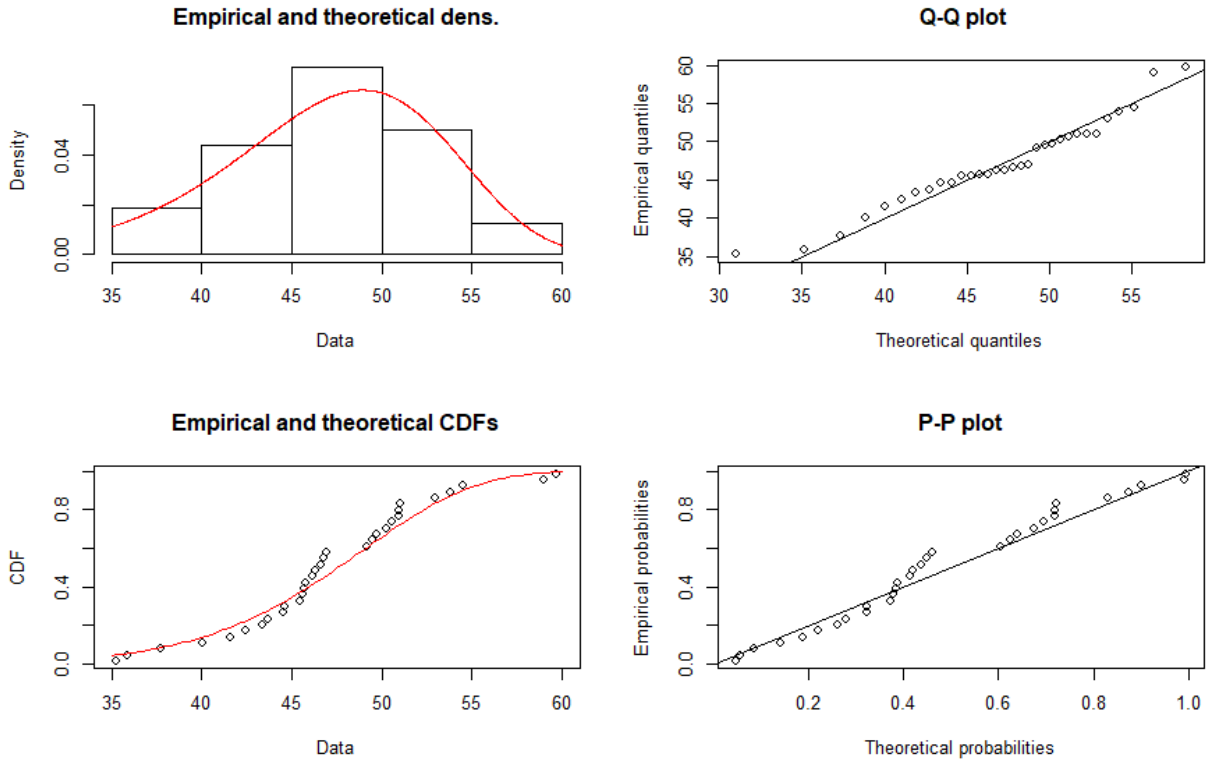

Frêne d'Amérique – Joint de 15 mm, adhésif MF

```
> WBULL_FRA_MF_15 <- fitdist(Results_FRA_MF_15$UTS_MPa, "weibull")
> summary(WBULL_FRA_MF_15)
Fitting of the distribution ' weibull ' by maximum likelihood
Parameters :
       estimate Std. Error
shape  8.617019   1.177354
scale 51.316383   1.111683
Loglikelihood:  -104.9651   AIC:  213.9303   BIC:  216.8617
Correlation matrix:
          shape     scale
shape 1.0000000 0.3213917
scale 0.3213917 1.0000000

> plot(WBULL_FRA_MF_15)
> quantile(WBULL_FRA_MF_15, probs = 0.05)
Estimated quantiles for each specified probability (non-censored data)
          p=0.05
estimate 36.3546
```

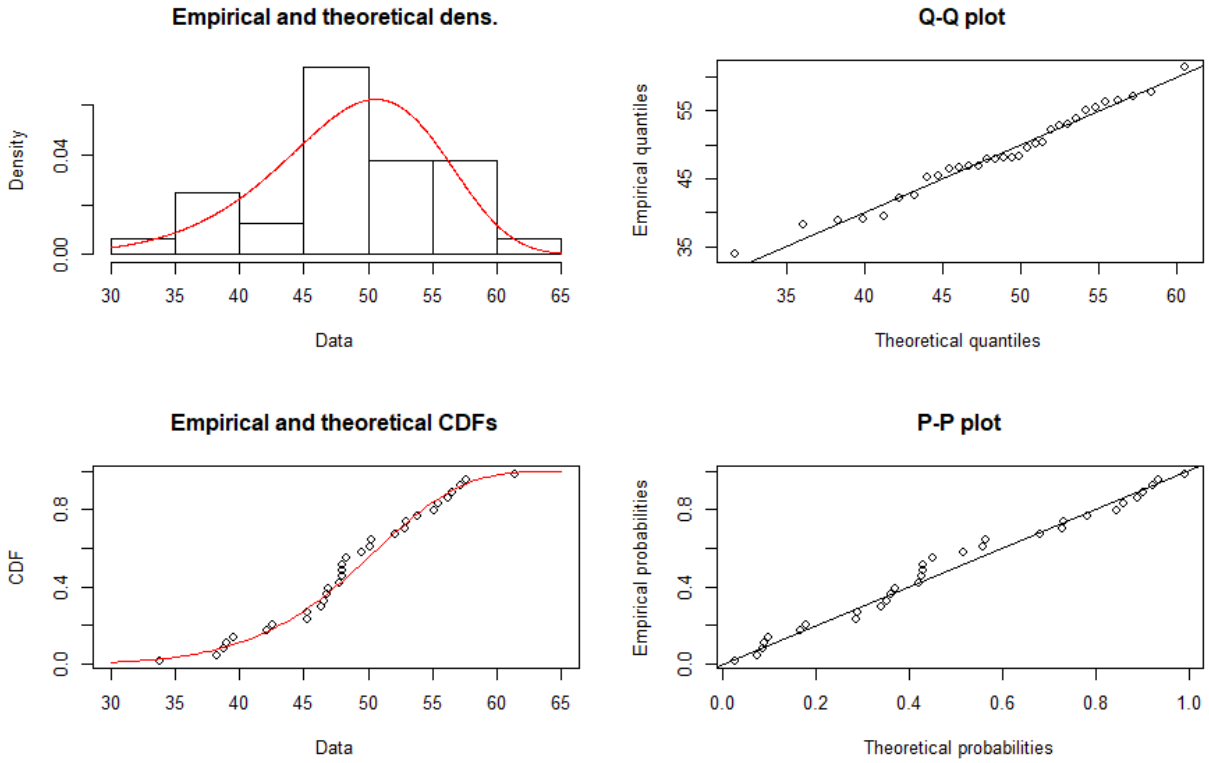

Chêne blanc – Joint de 22 mm, adhésif PUR

```
> WBULL_CHB_PUR_22 <- fitdist(Results_CHB_PUR_22$UTS_MPa, "weibull")
> summary(WBULL_CHB_PUR_22)
Fitting of the distribution ' weibull ' by maximum likelihood
Parameters :
      estimate Std. Error
shape 10.12956   2.425407
scale 42.23916   1.323608
Loglikelihood:  -32.51562   AIC:  69.03124   BIC:  69.82703
Correlation matrix:
          shape     scale
shape 1.0000000 0.3126642
scale 0.3126642 1.0000000

> plot(WBULL_CHB_PUR_22)
> quantile(WBULL_CHB_PUR_22, probs = 0.05)
Estimated quantiles for each specified probability (non-censored data)
         p=0.05
estimate 31.5044
```

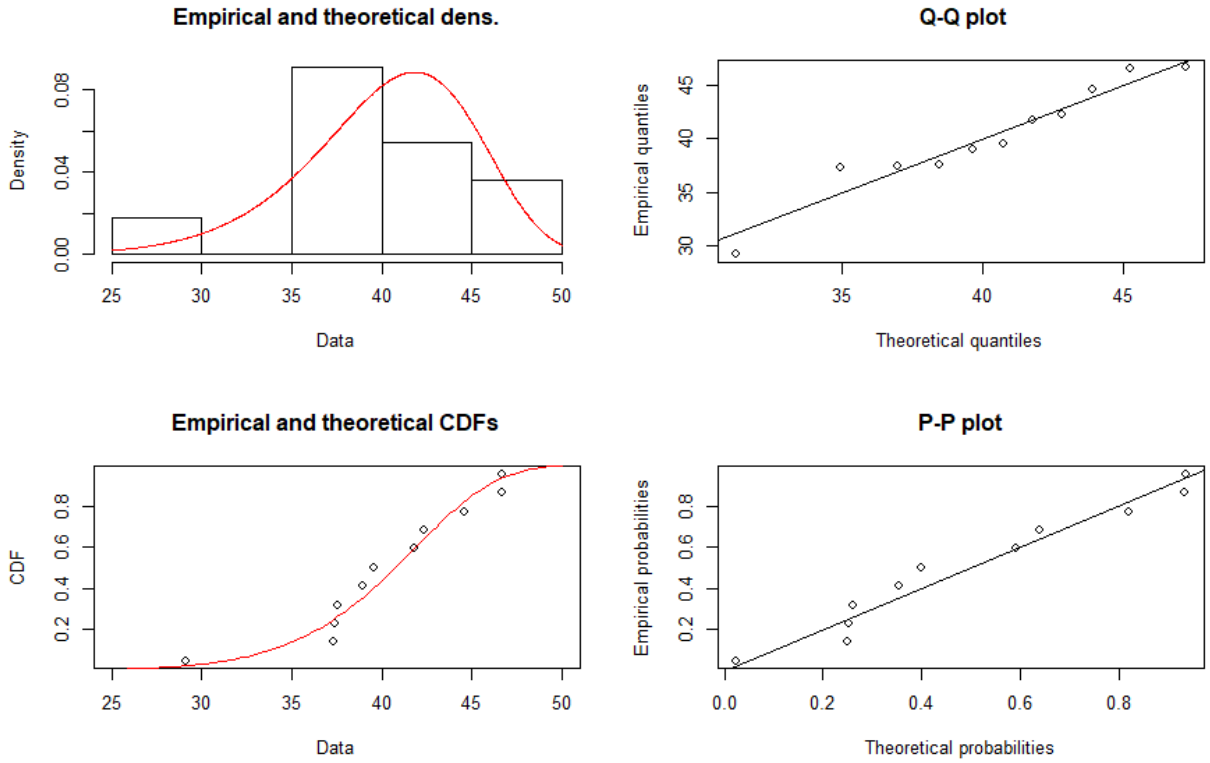

Chêne blanc – Joint de 22 mm, adhésif MF

```
> WBULL_CHB_MF_22 <- fitdist(Results_CHB_MF_22$UTS_MPa, "weibull")
> summary(WBULL_CHB_MF_22)
Fitting of the distribution ' weibull ' by maximum likelihood
Parameters :
       estimate Std. Error
shape  7.556558   1.816108
scale 36.795801   1.631653
Loglikelihood:  -30.50924   AIC:  65.01848   BIC:  65.62365
Correlation matrix:
          shape     scale
shape 1.0000000 0.3308528
scale 0.3308528 1.0000000

> plot(WBULL_CHB_MF_22)
> quantile(WBULL_CHB_MF_22, probs = 0.05)
Estimated quantiles for each specified probability (non-censored data)
            p=0.05
estimate 24.83668
```

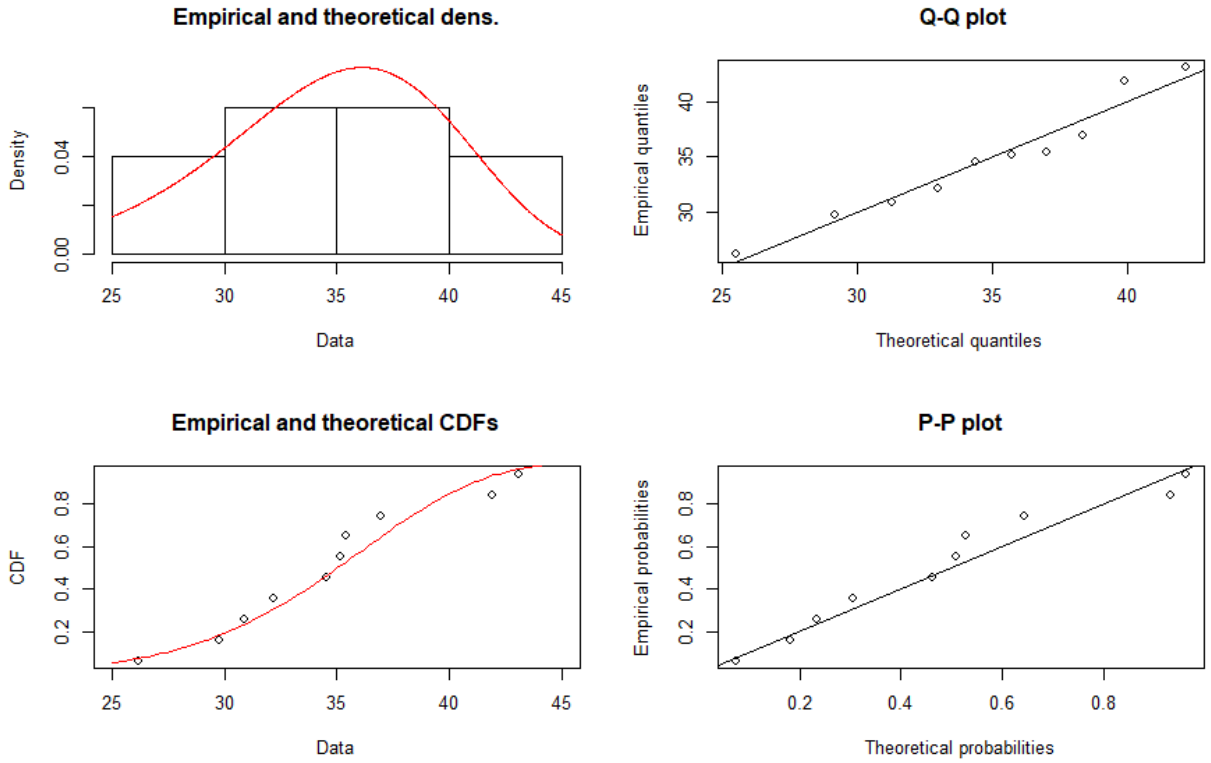

Chêne blanc – Joint de 15 mm, adhésif PUR

```
> WBULL_CHB_PUR_15 <- fitdist(Results_CHB_PUR_15$UTS_MPa, "weibull")
> summary(WBULL_CHB_PUR_15)
Fitting of the distribution ' weibull ' by maximum likelihood
Parameters :
      estimate Std. Error
shape 11.24938   2.578348
scale 49.04834   1.319698
Loglikelihood:  -36.2605   AIC:  76.52099   BIC:  77.49081
Correlation matrix:
          shape     scale
shape 1.0000000 0.3010815
scale 0.3010815 1.0000000

> plot(WBULL_CHB_PUR_15)
> quantile(WBULL_CHB_PUR_15, probs = 0.05)
Estimated quantiles for each specified probability (non-censored data)
            p=0.05
estimate 37.66663
```

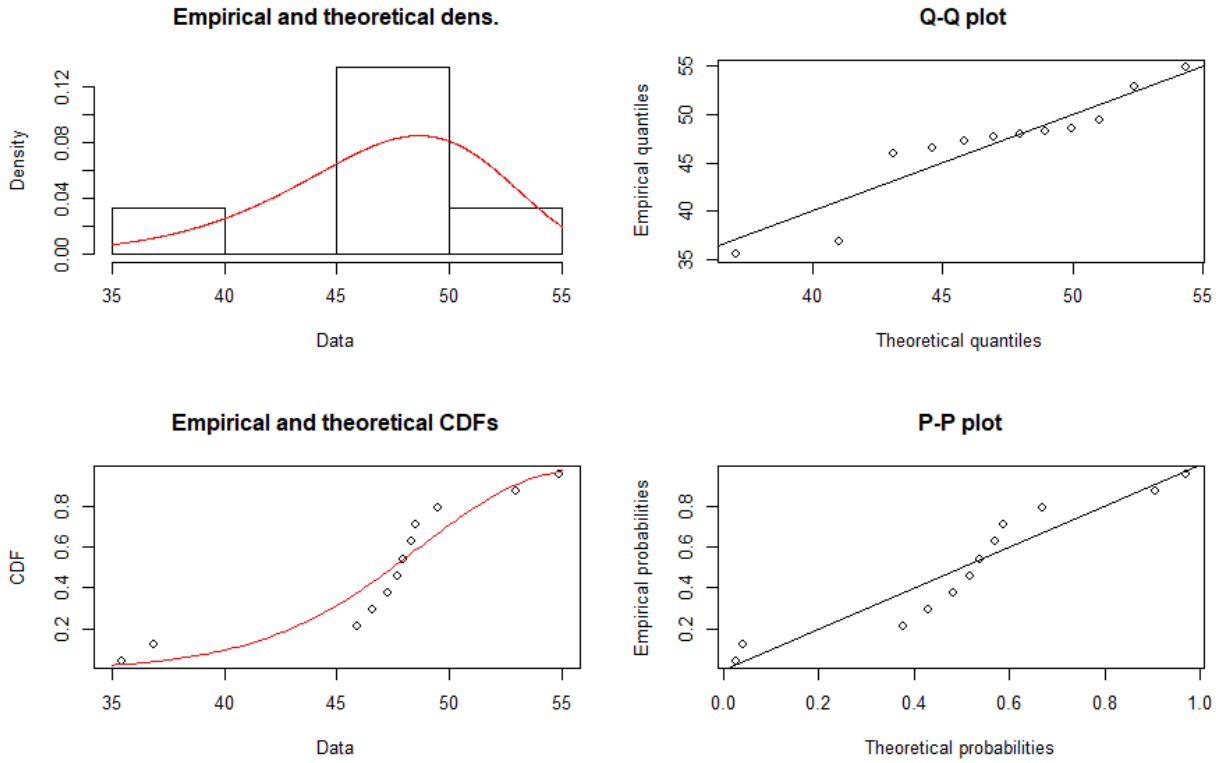

Chêne blanc – Joint de 15 mm, adhésif MF

```
> WBULL_CHB_MF_15 <- fitdist(Results_CHB_MF_15$UTS_MPa, "weibull")
> summary(WBULL_CHB_MF_15)
Fitting of the distribution ' weibull ' by maximum likelihood
Parameters :
      estimate Std. Error
shape 15.74148   4.027674
scale 51.44792   1.022276
Loglikelihood:  -30.97813   AIC:  65.95626   BIC:  66.75205
Correlation matrix:
          shape     scale
shape 1.0000000 0.2658262
scale 0.2658262 1.0000000

> plot(WBULL_CHB_MF_15)
> quantile(WBULL_CHB_MF_15, probs = 0.05)
Estimated quantiles for each specified probability (non-censored data)
            p=0.05
estimate 42.60127
```

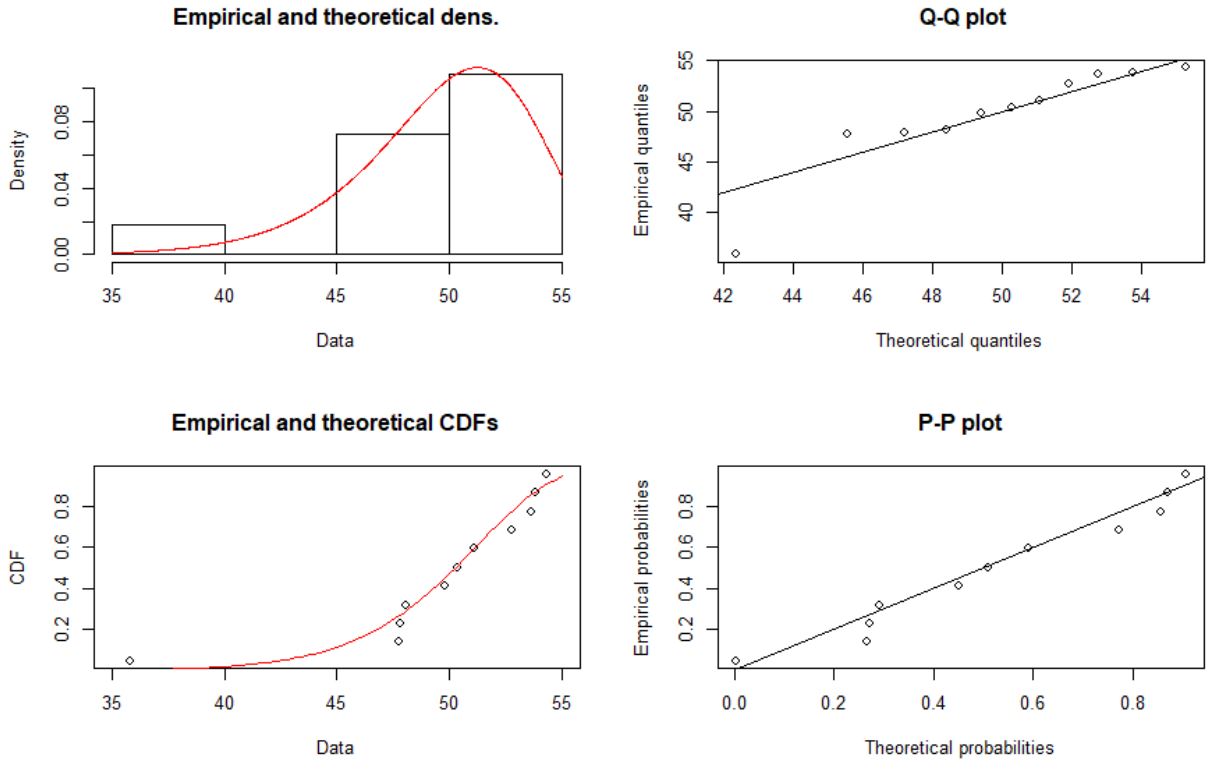

Résineux – Joint de 28 mm, adhésif PUR

```
> WBULL_SPF_28 <- fitdist(Results_SPF_28$UTS_MPa, "weibull")
> summary(WBULL_SPF_28)
Fitting of the distribution ' weibull ' by maximum likelihood
Parameters :
       estimate Std. Error
shape  6.213827  0.7864125
scale 39.040094  1.0925867
Loglikelihood:  -122.1343   AIC:  248.2687   BIC:  251.4905
Correlation matrix:
          shape     scale
shape 1.0000000 0.3258193
scale 0.3258193 1.0000000

> plot(WBULL_SPF_28)
> quantile(WBULL_SPF_28, probs = 0.05)
Estimated quantiles for each specified probability (non-censored data)
            p=0.05
estimate 24.20578
```

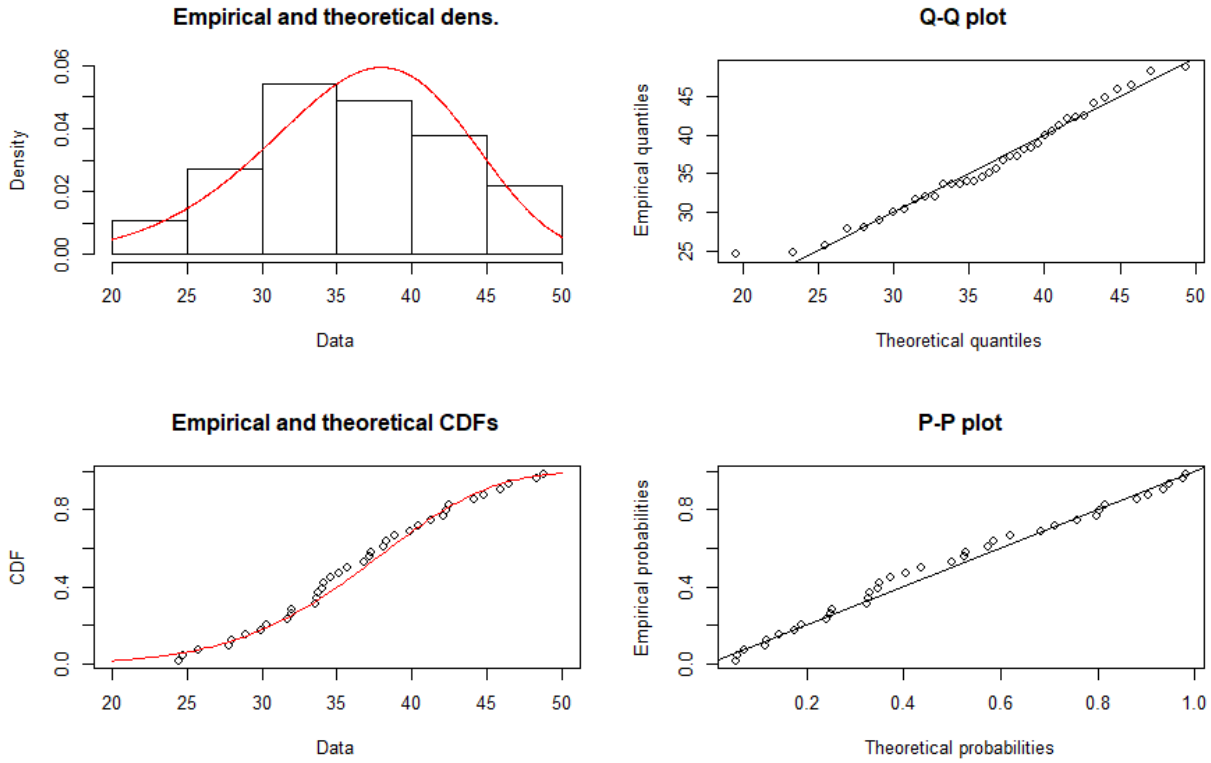

Résineux – Joint de 22 mm, adhésif PUR

```
> WBULL_SPF_22 <- fitdist(Results_SPF_22$UTS_MPa, "weibull")
> summary(WBULL_SPF_22)
Fitting of the distribution ' weibull ' by maximum likelihood
Parameters :
       estimate Std. Error
shape  5.756847  0.7825686
scale 39.892970  1.2334366
Loglikelihood:  -119.8118   AIC:  243.6237   BIC:  246.7344
Correlation matrix:
          shape     scale
shape 1.0000000 0.3129846
scale 0.3129846 1.0000000

> plot(WBULL_SPF_22)
> quantile(WBULL_SPF_22, probs = 0.05)
Estimated quantiles for each specified probability (non-censored data)
            p=0.05
estimate 23.81365
```

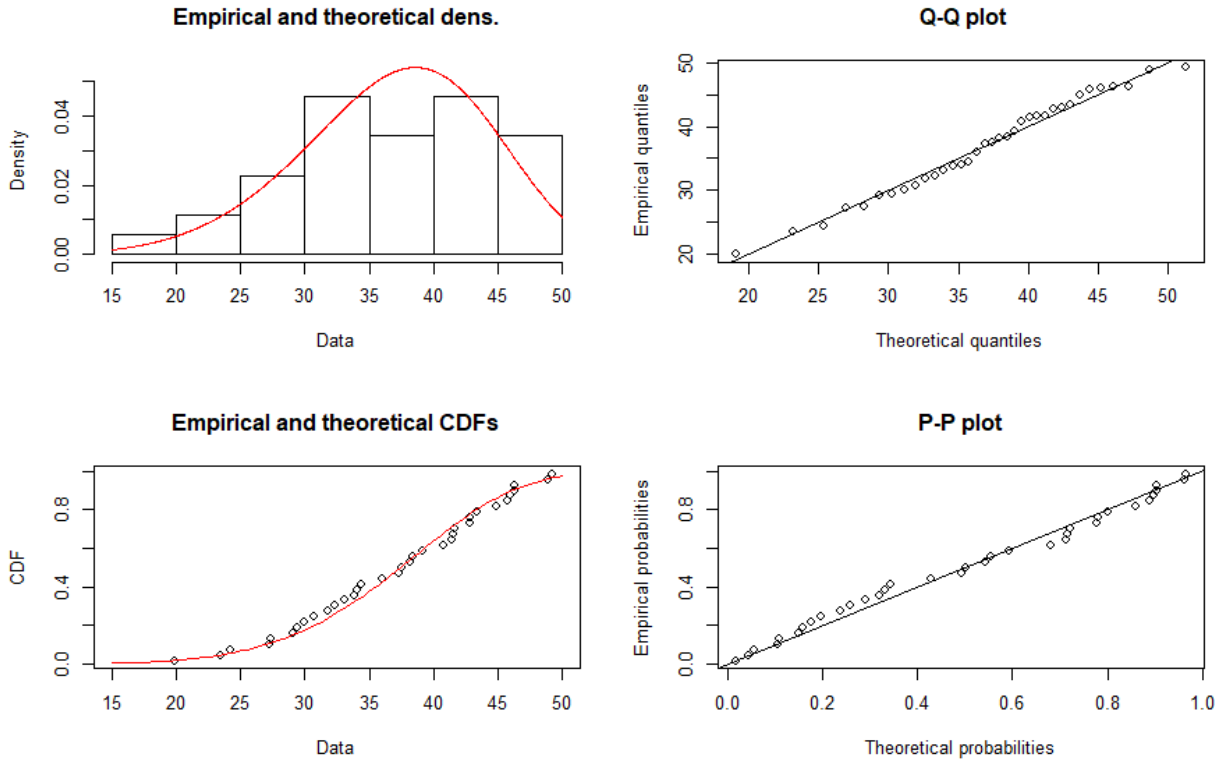

Résineux – Joint de 15 mm, adhésif PUR

```
> WBULL_SPF_15 <- fitdist(Results_SPF_15$UTS_MPa, "weibull")
> summary(WBULL_SPF_15)
Fitting of the distribution ' weibull ' by maximum likelihood
Parameters :
       estimate Std. Error
shape  6.039349  0.6977395
scale 40.948724  1.1061112
Loglikelihood:  -141.3635   AIC:  286.7271   BIC:  290.2024
Correlation matrix:
          shape     scale
shape 1.0000000 0.3248063
scale 0.3248063 1.0000000

> plot(WBULL_SPF_15)
> quantile(WBULL_SPF_15, probs = 0.05)
Estimated quantiles for each specified probability (non-censored data)
            p=0.05
estimate 25.04097
```

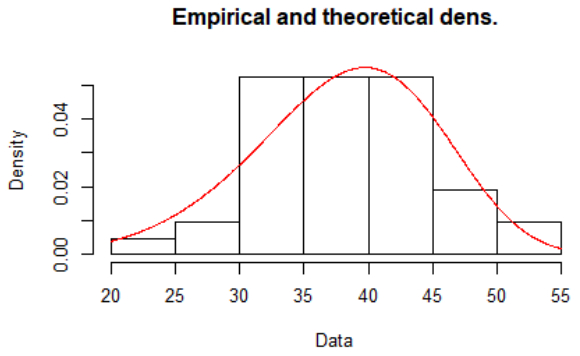
Empirical and theoretical dens.
Density
0.00
0.02
0.04
20
25
30
35
40
45
50
55
Data

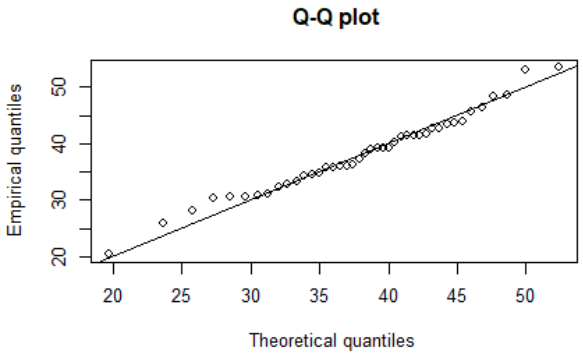
Q-Q plot
Empirical quantiles
20
30
40
50
20
25
30
35
40
45
50
Theoretical quantiles

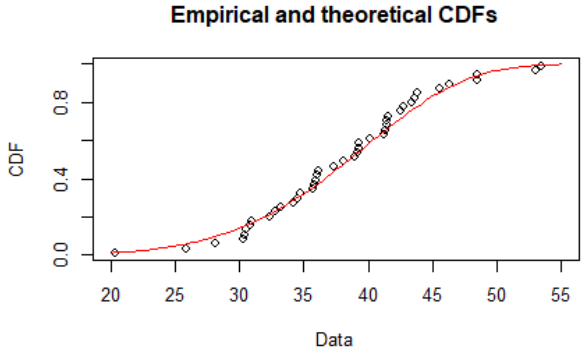
Empirical and theoretical CDFs
CDF
0.0
0.4
0.8
20
25
30
35
40
45
50
55
Data

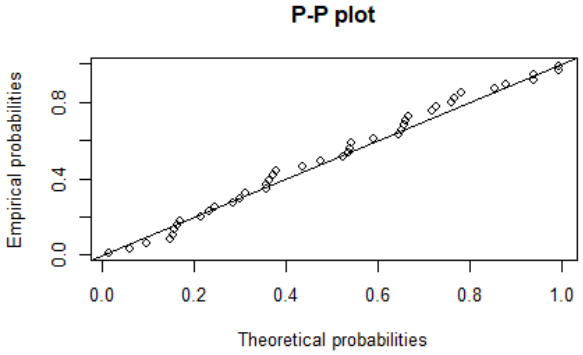
P-P plot
Empirical probabilities
0.0
0.4
0.8
0.0
0.2
0.4
0.6
0.8
1.0
Theoretical probabilities

Annexe C – Stage au Centre for Offsite Construction and Innovative Structures à l'Edinburgh Napier University

Calcul de la rigidité flexionnelle et de la résistance en flexion de poutres en bois lamellé-collé.

1. Introduction

BS EN 14080 (2013) standard provides requirements for the manufacture and testing of homogeneous and combined glued-laminated timber. Homogeneous glued-laminated timber can be considered as fulfilling the requirements of a given strength class if it is manufactured in accordance with one of the lay-up combinations proposed in BS EN 14080 (2013), provided it is also fulfilling the requirements of initial type testing and factory production control. The standard also provides the equations required to derive the bending strength and other mechanical properties from the properties of the laminations.

Combined glued-laminated timber manufactured accordingly to the lay-up combinations from BS EN 14080 Table 2 cans also be considered as fulfilling the requirements of the corresponding strength class. However, many other lay-up combinations have the potential of providing comparable in-service performance, despite not being formally proposed in the standard. In this case, according to BS EN 14080, the mechanical properties of a custom lay-up of combined glued-laminated timber can either be determined from full-scale tests or from calculations.

Considering the high costs and the time required to conduct a full-scale test campaign, a manufacturer interested in developing its own product may prefer to rely as much as possible on the calculation method. For this purpose, BS EN 14080 provides detailed instructions at section 5.1.5. The properties of a beam with a custom lay-up combination, including the characteristic bending strength, characteristic tensile and compression strength parallel to the grain, the mean modulus of elasticity and the characteristic density "shall be determined from the respective values of the different lamination zones considered as homogeneous glued-laminated timber by means of the elastic composite beam theory".

The objective of this study was to identify a calculation method conforming to the provisions of BS EN 14080 appropriate to assess the mechanical properties of combined glued-laminated timber and to apply it to custom lay-up combinations, designed by taking into account the grading yield of UK grown timber.

2. Calculation method

2.1 Calculation of mean modulus of elasticity

The method for the calculation of the modulus of elasticity is derived from Eurocode 5 (BS EN 1995-1-1:2004+A2:2014) Annex B, which provides the equation to calculate the effective bending stiffness of mechanically jointed beams.

$$(EI)_{ef} = \sum_{i=1}^{n} (E_i I_i + \gamma_i E_i A_i a_i^2) \quad \text{Eurocode 5 equation B.}$$

Where: E_i: Mean E of the boards used in the lamination zone

$$I_i = \frac{b_i {h_i}^3}{12}$$

$$A_i = b_i h_i$$

$$\gamma_2 = 1$$

$$\gamma_i = 1 + \left[\frac{\pi^2 E_i A_i s_i}{(K_i l^2)}\right]^{-1} for\ i = 1\ and\ i = 3$$

$$a_2 = \frac{\gamma_1 E_1 A_1 (h_1 + h_2) - \gamma_3 E_3 A_3 (h_2 + h_3)}{2 \sum_{i=1}^{3} \gamma_i E_i A_i}$$

s: Spacing between fasteners

K= Slip modulus

l= Span of the simply supported beam

Since no fasteners are used in glued laminated timber, no slip is occurring between the lamellae. Consequently, the equation was simplified and the γ variable removed because its value could be set to 1 for all lamination zones. For the same reason, the value of variable a, was assumed to be equal to the distance between the neutral axis and the center of the lamination zone. In order to isolate E, the effective bending stiffness $(EI)_{ef}$ was divided by I, the beam second moment of area. The resulting value was multiplied by 1.05, according to the formulae given in BS EN 14080 Table 6. The resulting formula for mean modulus of elasticity of combined glued-laminated timber is therefore:

$$E_{0,g,mean} = 1.05\ \frac{\sum_{i=1}^{n} (E_i I_i + E_i A_i a_i^2)}{I_{beam}}$$

2.2 Calculation of the characteristic bending strength

BS EN 14080 table 6 provides the equation required to calculate the characteristic bending strength of homogeneous glued-laminated timber.

$$f_{m,g,k} = -2.2 + 2.5 f_{t,0,l,k}^{0.75} + 1.5 \left(\frac{f_{m,j,k}}{1.4} - f_{t,0,l,k} + 6\right)^{0.65}$$

It was assumed that the elastic beam theory was applicable not only to the beam stiffness, but also to its bending strength. The calculation of the beam bending strength was therefore realized using the equation for the effective bending stiffness, in which E values were replaced with the values of the bending strength of the different lamination zones, considered as homogeneous glued-laminated timber. For the bending strength calculation of custom lay-up combinations, the finger joint bending strength $f_{m,j,k}$ was taken from BS EN 14080 Table 3 for the corresponding lamination strength class.

$$f_{m,g,k} = \frac{\sum_{i=1}^{n} (f_i I_i + f_i A_i a_i^2)}{I_{beam}}$$

3. Validation of results

In order to validate the methods for the calculation of the mean modulus of elasticity and bending strength, the equations were first used to calculate the properties of several combined glued-laminated timber lay-up combinations presented in BS EN 14080 Table 2. Table 1 presents the results of these calculations as the corresponding value for each strength class, as presented in BS EN 14080. An example of the calculation of the bending strength, modulus of elasticity and mean density is shown in Annex A.

Table 1. Standard and calculated properties of combined glued-laminated timber from BS EN 14080.

	Values from BS EN 14080 Table 4			Calculated values		
Lay-up	$f_{m,j,k}$	$E_{0,g,mean}$	$\rho_{g,mean}$	$f_{m,j,k}$	$E_{0,g,mean}$	$\rho_{g,mean}$
GL20c	20.00	10 400	390.0	21.58	10 383	389.6
GL22c	22.00	10 400	390.0	22.08	10 383	389.6
GL24c	24.00	11 000	400.0	24.04	11 414	400.0
GL26c	26.00	12 000	420.0	26.01	11 978	420.0
GL28c*	28.00	12 500	420.0	27.56	12 469	440.0
GL30c*	30.00	13 000	430.0	28.98	13 197	443.6

*First lay-up displayed in BS EN 14080 Table 2 for the corresponding strength class.

4. Calculation example 1 - Calculation of beam *E* for combined GLT - GL22c

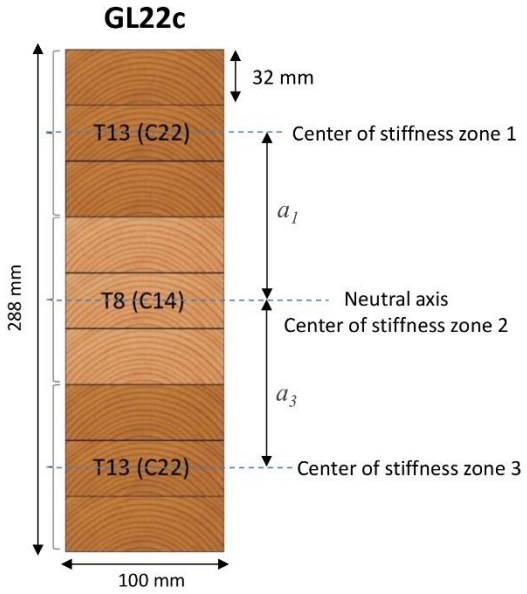

4.1 Calculation of the lamination zones second moment of area I_i:

$$I_1 = I_2 = I_3 = \frac{bh^3}{12} = \frac{100 \cdot (3 \cdot 32)^3}{12} = 7\,372\,800\ mm^4$$

4.2 Calculation of the beam second moment of area I_{beam}:

$$I_{beam} = \frac{bh^3}{12} = \frac{100 \cdot (9 \cdot 32)^3}{12} = 199\,065\,600\ mm^4$$

4.3 Calculation of lamination zones area A:

$$A_1 = A_2 = A_3 = b \cdot h = 100 \cdot (3 \cdot 32) = 600\ mm^2$$

4.4 Calculation of the distance between center of lamination zones and neutral axis, a:

$$a_1 = a_3 = 96\ mm$$

$$a_2 = 0\ mm$$

4.5 Calculation of the effective bending stiffness EI_{ef}:

$$(EI)_{ef} = (E_1\,I_1 + E_1\,A_1\,a_1^2) + (E_2\,I_2 + E_2\,A_2\,a_2^2) + (E_3\,I_3 + E_3\,A_3\,a_3^2)$$

$$(EI)_{ef} = (10\,000 \cdot 7\,372\,800 + 10\,000 \cdot 9\,600 \cdot 96^2) + (7\,000 \cdot 7\,372\,800 + 7\,000 \cdot 9\,600 \cdot 0^2) + (10\,000 \cdot 7\,372\,800 + 10\,000 \cdot 9\,600 \cdot 96^2)$$

$$(EI)_{ef} = 1\,968\,537\,600\,000\ Nmm^2$$

4.6 Calculation of the beam modulus of elasticity E:

$$E_{0,g,mean} = 1.05\ \frac{1\,968\,537\,600\,000\ Nmm^2}{199\,065\,600\ mm^4} = 10\,383.33\ \frac{N}{mm^2}$$

5 Calculation example 2 - Calculation of beam bending strength $f_{m,g,k}$ for combined GLT - GL22c

5.1 Calculation of the bending strength f_i of each lamination zone:

$$f_{zone\,1} = f_{zone\,3} = -2.2 + 2.5 \cdot 13^{0.75} + 1.5\left(\frac{26}{1.4} - 13 + 6\right)^{0.65} = 22.28\ \frac{N}{mm^2}$$

$$f_{zone\,2} = -2.2 + 2.5 \cdot 8^{0.75} + 1.5\left(\frac{18}{1.4} - 8 + 6\right)^{0.65} = 16.76\ \frac{N}{mm^2}$$

5.2 Calculation of $(fI)_{ef}$

$$(fI)_{ef} = (f_1\ I_1 + f_1\ A_1\ a_1^2) + (f_2\ I_2 + f_2\ A_2\ a_2^2) + (f_3\ I_3 + f_3\ A_3\ a_3^2)$$

$$(fI)_{ef} = (22.28 \cdot 7\,372\,800 + 22.28 \cdot 9\,600 \cdot 96^2) + (16.76 \cdot 7\,372\,800 + 16.76 \cdot 9\,600 \cdot 0^2) + (22.28 \cdot 7\,372\,800 + 22.28 \cdot 9\,600 \cdot 96^2) = 4\,395\,031\,483\ Nmm^2$$

5.3 Calculation of the beam bending strength:

$$f_{m,g,k} = \frac{4\,395\,031\,483}{199\,065\,600}\frac{Nmm^2}{mm^4} = 22.08\ \frac{N}{mm^2}$$

Annexe D – Affiches scientifiques présentées dans le cadre de colloques et conférences

1. Journée de la recherche étudiante – Semaine des sciences forestières 2019

2. Colloque facultaire FFGG 2019 - Carrefour Forêts 2019

CHAIRE INDUSTRIELLE DE RECHERCHE SUR LA CONSTRUCTION ÉCORESPONSABLE EN BOIS

CONSTRUIRE MATÉRIAUX

Utilisation d'espèces feuillues dans la fabrication de bois lamellé-collé

Alexandre MORIN-BERNARD, Pierre BLANCHET, Christian DAGENAIS et Alexis ACHIM

Mise en contexte

28 %

Au Québec, l'utilisation du bois pour la construction de bâtiments commerciaux, industriels et multifamiliaux a presque doublé entre 2007 et 2017, passant de 15% à 28%[1]. En remplaçant des matériaux à l'empreinte écologique plus importante comme l'acier ou le béton, les produits de bois d'ingénierie comme le bois lamellé-collé permettent de diminuer l'empreinte écologique des bâtiments. En plus d'utiliser rationnellement une matière renouvelable, ces produits à forte valeur ajoutée se distinguent par leurs propriétés mécaniques compétitives.

À ce jour, ces produits sont presque exclusivement composés de bois d'espèces résineuses. Les espèces feuillues génèrent toutefois un intérêt grandissant en raison de leur résistance mécanique supérieure, de leur apparence distinctive et de leur disponibilité. Chaque année au Québec, la moitié de la possibilité forestière en feuillus, soit environ 5 millions de m³, n'est pas attribuée et les volumes récoltés ne sont pas toujours pleinement valorisés[2].

5 millions m³

Utiliser le bois d'espèces feuillues pour la fabrication de produits d'ingénierie structuraux permettrait d'accroître les débouchés à forte valeur ajoutée pour ces espèces en plus d'élargir l'offre de produits destinés à la construction.

Méthodologie

Essais de résistance au cisaillement

- À l'état sec et après cycle vide-pression, norme CSA O112.9[3]

Sélection de 4 espèces et 2 adhésifs

Caractérisation de la matière première

- Mesure du module d'élasticité (MOE) par onde acoustique
- Évaluation de l'impact des défauts sur la résistance en traction, norme ASTM D4761[4]
- Vérification de la relation MOE/UTS

Proposition de seuils de défauts admissibles

Sélection des paramètres d'aboutage

- Mise à l'essai de 2 géométries de joints à entures multiples
- Essais de résistance en traction, norme ASTM D7469[5]

Sélection de la géométrie la plus performante

Assemblage et mise à l'essai de poutres pleine grandeur

- Définition du plan d'assemblage et fabrication de poutres pleine grandeur
- Essais de contrôle qualité selon la norme CSA O122[6]
- Essais de résistance en flexion selon la norme ASTM D198[7]

Estimation des classes de résistance potentielles

Objectif

Évaluer la faisabilité technique d'un bois lamellé-collé composé d'espèces feuillues du nord-est de l'Amérique du Nord

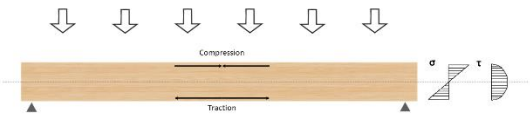

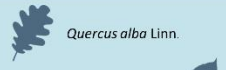

Quercus alba Linn.

Fraxinus americana Linn.

Betula alleghaniensis Britt.

Betula papyrifera Marsh.

Résultats préliminaires

Résistance au cisaillement

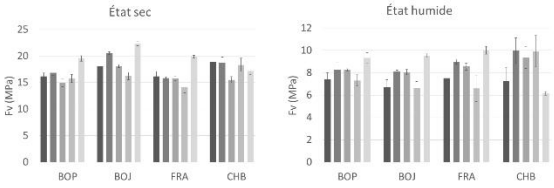

Taux médian de défaillance dans le bois

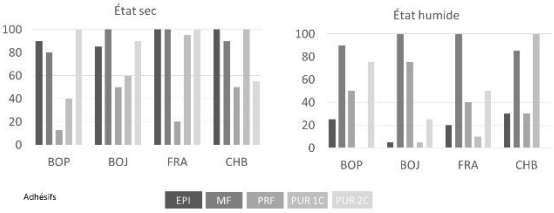

Références

1. Cecobois. 2017. *Étude sur les parts de marché du matériau bois dans la construction non résidentielle de 4 étages ou moins au Québec.* Rapport réalisé par FEA pour Cecobois.
2. MFFP. 2017. Ressources et industries forestières du Québec - Portrait statistique 2017. Disponible en ligne à : https://mffp.gouv.qc.ca/wp-content/uploads/portrait-statistique-2017.pdf.
3. CSA. 2010. *Evaluation of adhesives for structural wood products (exterior exposure) CAN/CSA O112.9-10.* Association Canadienne de Normalisation, Etobicoke, Ontario.
4. ASTM. 2018. *Standard Test Methods for Mechanical Properties of Lumber and Wood-Based Structural Materials.* American Society for Testing and Materials, West Conshohocken, PA.
5. ASTM. 2016. *Standard Test Methods for End-Joints in Structural Wood Products.* American Society for Testing and Materials, West Conshohocken, PA.
6. CSA. 2016. *Éléments de charpente en bois lamellé-collé CAN/CSA O122-16.* Association Canadienne de Normalisation, Etobicoke, Ontario.
7. ASTM. 2015. *Standard Test Methods of Static Tests of Lumber in Struc* [illegible] and Ma

ART MASSIF STRUCTURE DE BOIS

FPInnovations

CRSNG NSERC

UNIVERSITÉ LAVAL

3. Colloque CRMR – Congrès ACFAS 2019

CHAIRE INDUSTRIELLE DE RECHERCHE SUR LA CONSTRUCTION ÉCORESPONSABLE EN BOIS

CONSTRUIRE MATÉRIAUX

Utilisation d'espèces feuillues dans la fabrication de bois lamellé-collé

Alexandre MORIN-BERNARD, Pierre BLANCHET, Christian DAGENAIS et Alexis ACHIM

Mise en contexte

28 %

Au Québec, l'utilisation du bois pour la construction de bâtiments commerciaux, industriels et multifamiliaux a presque doublé entre 2007 et 2017, passant de 15% à 28%[1]. En remplaçant des matériaux à l'empreinte écologique plus importante comme l'acier ou le béton, les produits de bois d'ingénierie comme le bois lamellé-collé permettent de diminuer l'empreinte écologique des bâtiments. En plus d'utiliser rationnellement une matière renouvelable, ces produits à forte valeur ajoutée se distinguent par leurs propriétés mécaniques compétitives.

À ce jour, ces produits sont presque exclusivement composés de bois d'espèces résineuses. Les espèces feuillues génèrent toutefois un intérêt grandissant en raison de leur résistance mécanique supérieure, de leur apparence distinctive et de leur disponibilité. Chaque année au Québec, la moitié de la possibilité forestière en feuillus, soit environ 5 millions de m³, n'est pas attribuée et les volumes récoltés ne sont pas toujours pleinement valorisés[2].

5 millions m³

Utiliser le bois d'espèces feuillues pour la fabrication de produits d'ingénierie structuraux permettrait d'accroître les débouchés à forte valeur ajoutée pour ces espèces en plus d'élargir l'offre de produits destinés à la construction.

Méthodologie

Essais de résistance au cisaillement

- À l'état sec et après cycle vide-pression, norme CSA O112.9[3]

Sélection de 4 espèces et 2 adhésifs

Caractérisation de la matière première

- Mesure du module d'élasticité (MOE) par onde acoustique
- Évaluation de l'impact des défauts sur la résistance en traction, norme ASTM D4761[4]
- Vérification de la relation MOE/UTS

Proposition de seuils de défauts admissibles

Sélection des paramètres d'aboutage

- Mise à l'essai de 2 géométries de joints à entures multiples
- Essais de résistance en traction, norme ASTM D7469[5]

Sélection de la géométrie la plus performante

Assemblage et mise à l'essai de poutres pleine grandeur

- Définition du plan d'assemblage et fabrication de poutres pleine grandeur
- Essais de contrôle qualité selon la norme CSA O122[6]
- Essais de résistance en flexion selon la norme ASTM D198[7]

Estimation des classes de résistance potentielles

Objectif

Évaluer la faisabilité technique d'un bois lamellé-collé composé d'espèces feuillues du nord-est de l'Amérique du Nord

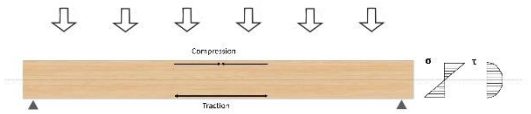

Résultats préliminaires

Résistance au cisaillement

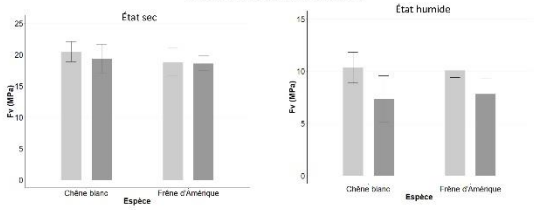

Taux médian de défaillance dans le bois

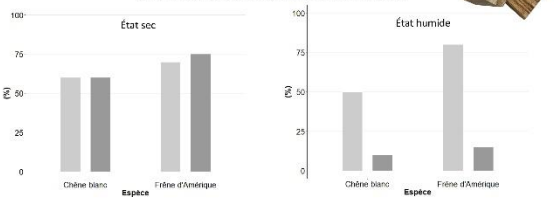

Références

1. Cecobois. 2017. *Étude sur les parts de marché du matériau bois dans la construction non résidentielle de 4 étages ou moins au Québec.* Rapport inédit par FTA pour Cecobois.
2. MFFP. 2017. Ressources et industries forestières du Québec - Portrait statistique 2017. Disponible en ligne à : https://mffp.gouv.qc.ca/wp-content/uploads/portrait-statistique-2017.pdf.
3. CSA. 2010. *Evaluation of adhesives for structural wood products (exterior exposure) CAN/CSA O112.9-10.* Association Canadienne de Normalisation, Etobicoke, Ontario.
4. ASTM. 2018. *Standard Test Methods for Mechanical Properties of Lumber and Wood-Based Structural Materials.* American Society for Testing and Materials, West Conshohocken, PA.
5. ASTM. 2018. *Standard Test Methods for End-Joints in Structural Wood Products.* American Society for Testing and Materials, West Conshohocken, PA.
6. CSA. 2016. *Éléments de charpente en bois lamellé-collé CAN/CSA O122.16.* Association Canadienne de Normalisation, Etobicoke, Ontario.
7. ASTM. 2015. *Standard Test Methods of Static Tests of Lumber in Structural Sizes.* American Society for Testing and Materials, West Conshohocken, PA.

ART MASSIF STRUCTURE DE BOIS — FPInnovations — CRSNG NSERC — UNIVERSITÉ LAVAL

Annexe E – Avis de recherche forestière publié à la suite du Carrefour Forêts 2019

AVIS DE RECHERCHE FORESTIÈRE
JUILLET 2019 n° 131

gagnant 2e cycle
Carrefour Forêts 2019
concours

Construire des bâtiments à partir du bois d'essences feuillues du Québec?

Par Alexandre Morin-Bernard, ing.f., étudiant à la maîtrise en sciences du bois,
Pierre Blanchet, ing.f., Ph. D., Christian Dagenais, ing., Ph. D., et Alexis Achim, ing.f., Ph. D.

Territoires où les résultats s'appliquent.

Cet Avis de recherche forestière présente le sujet de l'affiche gagnante du 1er prix catégorie 2e cycle au concours d'affiches universitaires Gustave-Clodomir-Piché dans le cadre du Carrefour Forêts 2019.

L'utilisation du bois pour la construction de bâtiments est en forte hausse au Québec. En remplaçant des matériaux comme l'acier ou le béton, les produits de bois d'ingénierie, dont le bois lamellé-collé, permettent de diminuer l'empreinte écologique des bâtiments (Thormark 2006). À ce jour au Québec, ces produits sont exclusivement composés de bois d'espèces résineuses, mais les espèces feuillues génèrent un intérêt grandissant.

Un bois lamellé-collé composé d'espèces feuillues du Québec

Le bois lamellé-collé est composé d'un empilement de lamelles de longueurs variables, aboutées puis collées les unes aux autres à l'aide d'un adhésif à haute résistance. Il est utilisé en tant que poutres, colonnes ou arches dans les bâtiments à structure de bois. La demande croissante pour ce produit, motivée par ses avantages écologiques et son attrait esthétique, rend possible une diversification de l'offre. Les produits de bois à usage structural sont traditionnellement fabriqués à partir d'espèces résineuses. Pourtant, la structure anatomique des feuillus leur confère une densité généralement plus élevée et une résistance mécanique impressionnante. De plus, l'apparence distinctive des feuillus constitue un atout de taille.

L'objectif de ce projet est d'évaluer la faisabilité technique d'un bois lamellé-collé composé d'espèces feuillues du nord-est de l'Amérique du Nord, soit le chêne blanc (*Quercus alba*), le frêne d'Amérique (*Fraxinus americana*), le bouleau jaune (*Betula alleghaniensis*) et le bouleau à papier (*Betula papyrifera*). Ces espèces ont été sélectionnées selon des critères variables qui comprennent notamment la résistance mécanique, l'apparence et la disponibilité.

Le développement d'un nouveau produit de bois d'ingénierie structural

L'utilisation de nouvelles espèces dans un produit d'ingénierie structural introduit une certaine incertitude. Par exemple, la densité élevée des bois d'espèces feuillues, qui leur confère leur résistance, est d'autre part susceptible de limiter la pénétration de l'adhésif dans les cellules du bois, compromettant ainsi la résistance des assemblages. Cette densité provoque également des changements dimensionnels majeurs lors de variations du taux d'humidité, ce qui exerce une contrainte importante sur la ligne de colle (Frihart et Hunt 2010).

Lorsqu'elle est soumise à une charge, une poutre en bois lamellé-collé tend à fléchir, ce qui génère un effort de compression sur la face supérieure et un effort de traction sur la partie inférieure (σ) (figure 1). La poutre étant composée de plusieurs lamelles, il s'exerce également une contrainte de cisaillement (τ) entre chacune d'entre elles, cette contrainte étant maximale au centre de la poutre. La résistance dépend donc des caractéristiques de la matière première, mais également de la résistance des lamelles une fois aboutées ainsi que de la qualité du collage entre celles-ci (Dietsch et Tannert 2015). Le projet est divisé en quatre phases d'essais, soit 1) la sélection des paramètres de collage, 2) la sélection des paramètres d'aboutage, 3) la caractérisation de la matière première et 4) l'assemblage et la mise à l'essai de poutres pleine grandeur. Le projet permettra de déterminer la résistance de poutres composées des essences étudiées, fabriquées selon les paramètres identifiés comme les plus performants lors des trois premières phases d'essais.

Figure 1. Contraintes subies par une poutre soumise à une charge uniforme.

Le défi du collage des bois d'espèces feuillues : résultats des premiers essais

Très peu de travaux ont été réalisés jusqu'ici sur le collage des espèces feuillues disponibles au Québec et les études réalisées sur des espèces apparentées ont montré que les résultats peuvent fortement varier d'une espèce à l'autre et en fonction de l'adhésif utilisé (Aicher, Ahmad et Hirsch 2018). La première phase expérimentale du projet a permis d'évaluer la capacité de différents adhésifs à former un lien résistant et durable avec les essences de bois étudiées. Des échantillons prélevés sur des assemblages réalisés avec les quatre espèces et cinq adhésifs ont été soumis à des essais de résistance au cisaillement. Certains échantillons ont été testés dans des conditions sèches et les autres après qu'ils eurent été complètement saturés d'eau, atteignant ainsi leur gonflement maximal. Deux paramètres étaient mesurés, soit la force maximale exercée avant rupture (f_v) et le taux de défaillance dans le bois. Une défaillance à 100 % dans le bois (figure 2b) indique que le lien adhésif est plus résistant que le bois lui-même et donc que l'assemblage permet de tirer pleinement profit de la résistance de la matière première. Une défaillance à l'interface de deux lamelles (figure 2a), dans la ligne de colle, indique que le lien adhésif était l'élément limitant dans l'assemblage.

Les résultats obtenus (figure 3) ont permis de constater que la force à laquelle se produisait la rupture était relativement semblable pour chacun des adhésifs, tant dans des conditions sèches qu'humides. La résistance en conditions humides était toutefois de loin inférieure à celle en conditions sèches (figure 3, a et b). Les taux de défaillance dans le bois étaient fortement variables (figure 3, c et d). Dans des conditions sèches, plusieurs adhésifs (EPI, MF, PUR 2C) ont fourni des résultats équivalents, avec une rupture se produisant le plus souvent entièrement dans la fibre du bois. Ces adhésifs conviennent à un produit structural utilisé dans des conditions sèches. Toutefois, seul un adhésif (MF) a conservé un taux de défaillance dans le bois comparable après le test dans des conditions humides. Dans le cas des autres adhésifs, la présence d'humidité ainsi que le gonflement du bois ont occasionné un grand nombre de défaillances dans la ligne de colle. Ces adhésifs ne sont donc pas appropriés pour le collage structural des espèces étudiées dans le contexte d'une utilisation extérieure ou en présence de fortes variations du taux d'humidité.

Figure 2. Taux de défaillance dans le bois de 0 % (a) et 100 % (b).

Les implications pour la construction en bois au Québec

À terme, les résultats de ce projet pourraient permettre une plus grande utilisation des espèces feuillues dans la fabrication de produits d'ingénierie structuraux. Cette offre élargie encouragera le choix du matériau bois dans une plus grande variété de projets de construction en plus de fournir de nouveaux débouchés pour des espèces non valorisées à leur plein potentiel.

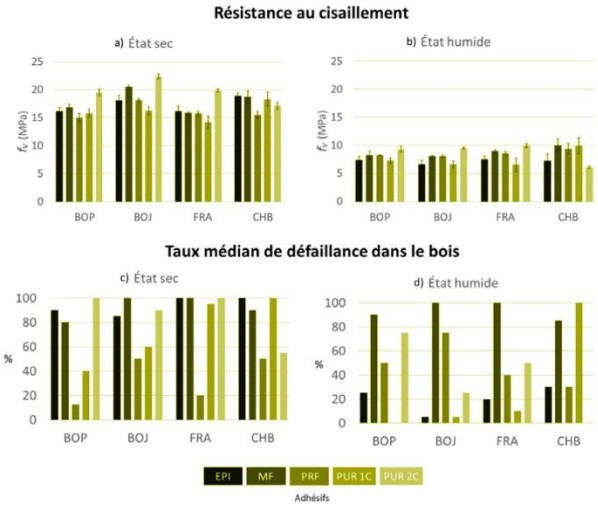

*Figure 3. Résultats des essais de résistance au cisaillement. *EPI = Émulsion isocyanate et polymère, MF = Mélamine-formaldéhyde, PRF = Phénol-résorcinol formaldéhyde, PUR 1C = Polyuréthane mono-composante, PUR 2C = Polyuréthane bi-composante.*

Pour en savoir plus

Aicher, S., Z. Ahmad et M. Hirsch, 2018. *Bondline shear strength and wood failure of European and tropical hardwood glulams.* European Journal of Wood and Wood Products 76(4): 1205-1222.

Dietsch, P., et T. Tannert, 2015. *Assessing the integrity of glued-laminated timber elements.* Construction and Building Materials 101: 1259-1270.

Frihart, C.R., et C.G. Hunt, 2010. *Wood Handbook, Chapter 10: Adhesives with Wood Materials- Bond Formation and Performance.*General Technical Report FPL-GTR-190. Madison, WI: U.S. Department of Agriculture, Forest Service, Forest Products Laboratory: 10-1 - 10-24.

Thormark, C., 2006. *The effect of material choice on the total energy need and recycling potential of a building.* Building and Environment 41(8): 1019-1026.

Les liens Internet de ce document étaient fonctionnels au moment de son édition.

Pour plus de renseignements, veuillez communiquer avec :

ISSN: 1715-0795

Direction de la recherche forestière
Ministère des Forêts, de la Faune et des Parcs
2700, rue Einstein, Québec (Québec) G1P 3W8

Téléphone : 418 643-7994
Télécopieur : 418 643-2165
Courriel : recherche.forestiere@mffp.gouv.qc.ca
Internet : www.mffp.gouv.qc.ca/forets/connaissances/recherche

Forêts, Faune et Parcs Québec